Abu Dhabi Crude Oil Characterization and Evaluation for Gas Turbine Applications

By

Akinola Anthony Olanrewaju

A Thesis Presented to the Masdar Institute of Science and Technology

in Partial Fulfillment of the Requirements for the Degree of

Master of Science

In

Chemical Engineering

Abu Dhabi Crude Oil Characterization and Evaluation for Gas Turbine Applications

By Akinola Anthony Olanrewaju

A Thesis Presented to the Masdar Institute of Science and Technology in Partial Fulfillment of the Requirements for the Degree of

Master of Science in Chemical Engineering

May 2015

AUTHOR'S DECLARATION

I understand that copyright in my thesis is transferred to Masdar Institute of Science and Technology.

Author _____

RESEARCH SUPERVISORY COMMITTEE MEMBERS

Dr. Mohammad Abu Zahra, Chair, _____
Masdar Institute of Science and Technology

Dr. Shadi Wajih Hasan, _____
Masdar Institute of Science and Technology

Dr. Mohammed Ibrahim Ali, _____
Masdar Institute of Science and Technology

Abstract

This study focused on the rheological and physiochemical characterization of three samples of light crude oil and a fuel oil obtained from oil-fields in the United Arab Emirates to determine the feasibility of using any of these liquid fuels from the Abu-dhabi Emirate as substitute or additive fuel for powering conventional gas turbines. Rheological and physicochemical properties such as n-heptane insoluble asphaltenes, apparent pH values, pour point, percentage moisture content, viscosity and density were measured according to the standard methods (American Society of Testing and Materials; ASTM). The dependence of density on temperature ranging from 20^{o}C to 200 ^{o}C was determined using Anton Paar DMA 5000 density meter at atmospheric pressure. Also, the impact of temperature on viscosity, shear stress τ, shear rate $\dot{\gamma}$, yield shear stress τ_o and thixotropic behavior was investigated and characterized by Haake RheoStress 6000. The exponential decrease of viscosity over temperature range was modeled using Arrhenius equation. Results showed that the activation energy for flow initiation for crude oil A, B, C and the fuel oil is 1246.1, 1201.3, 1309.5 and 4809.8 mPa.s.K, respectively. The shear stress–viscosity data revealed that crude oil A solely exhibited Newtonian behavior while crude oil B, C and fuel oil followed Herschel-Bulkley model over specific range of temperatures. This study also encapsulates the feasibility of powering a simple conventional gas turbine with liquid fuel using the modelling software IPSEpro^{TM}, this was done based on the variation of the elemental component of the sample. Variation of each component helped to determine its effect on power generation, quality and quantity of the exhaust of the turbine.

This research was supported by the Government of Abu Dhabi to help fulfill the vision of the late President Sheikh Zayed Bin Sultan Al Nahyan for sustainable development and empowerment of the UAE and humankind.

Acknowledgments

My sincere appreciation goes to my parents, Late (Mr.) S.K Olanrewaju and Mrs. C.R. Olanrewaju through whom I came to this world to fulfill my earthly ambitions. Also, to my Advisor, Dr. M.R.M Abu Zahra, for taking his time to mentor me, go through and make necessary corrections in this thesis project, I am highly grateful, sir. My heartfelt appreciation also goes to my Co-advisor, Dr. Shadi W. Hasan for his unflinching assistance in the course of my study. May God Almighty preserve and bless your live. Gratitude to my Research Supervisory Committee member, Dr. Mohamed Ibrahim Ali for his support and training on the use of IPSEpro™ software for the completion of my thesis.

To my laboratory group colleagues; Dr. Aravind V. Rayer, Dr. Dang Viet Quang, Dr. Nabil El Hajri, Abdullah Dindi and Abdurahim Abdulkadir, may God reward you for every portion of your time you dedicated towards the achievement of this degree.

To my lovely friends and well-wishers Miss Adetola Adeleye, Miss Oluwadetan Oyedele, Miss Damilola Aderemi, Kunle Adepitan, Wole Ajumobi, Tayo Aluko, Sodiq Ahmed, Yusuf Ahmed, Adetunji Alabi, Saad Asad, Femi Sofela, Adewale Giwa, Joyner Ekeh, Elham Abdulkareem, Adesola Ajayi, Oghare Ogidiama and Musbaudeen Bamgbopa just to mention a few, thank you all for your encouragement.

To my wonderful sisters; Abimbola Olanrewaju and Abiola Olanrewaju, thanks for your support.

Table of Content

List of Tables

List of Figures

CHAPTER 1

Introduction

1.1. Problem Statement

The Middle East and North Africa (MENA) region's Total Primary Energy Supply (TPES) reached about 800 million tonnes of oil equivalent (Mtoe) in 2010. This was an increase of 14.9% compared to 2007 (15.3% in the Net Oil-Exporting Countries (NOEC) and 10.5% in the Net Oil-Importing Countries (NOIC), respectively), or an average annual growth of 4.7% over the period. Increased energy consumption in the region is largely due to population growth, with related increases in demand for liquid fuels and electricity for domestic use and devices, heating, cooling, and desalination of water [1].

Sustainable infrastructure expansion is therefore a priority for the countries on the Arabian Gulf in order to meet their needs for better energy efficiency and sustainable power generation. Increased power generation capacity is an important concern for the Gulf Cooperation Council (GCC) countries (Bahrain, Saudi Arabia, UAE, Oman, Qatar and Kuwait), since they are amongst the region's highest electricity consuming countries[2]. Moreover, Electricity demand in the UAE is growing by 9% per year and is expected to require 40,000MW of electricity by 2020 [3].

As at the year 2012, 98% of the UAE power plants are fired by natural gas and the remaining 2% are run by liquid fuels. Since, the country's gas consumption has outpaced production, it imports natural gas from Qatar through the dolphin gas pipeline. The contribution of natural gas as fuel in the power sector is just 49% in Saudi Arabia and 29% in Kuwait [4].

The importation of high amount of natural gas can be reduced by modifying the already operating conventional gas turbine to utilize the ubiquitous crude oil or possibly mixture of both, so as to rationalize expenses on power generation. The operational flexibility of the fuel utilized in the gas turbine would not be possible without full and crucial characterization of the available crude oil in the UAE. Crude oil from different exploration sites have different properties (density, rheological properties, pour point and pH) and constituents (asphaltene, and moisture content), which would have changed with time as the reservoir ages. These reasons makes it imperative to conduct this research by measuring the aforementioned characteristics.

1.2. Research Objectives

This objective of this study is to determine the feasibility of using these liquid fuels from the Abu-dhabi Emirate as substitute or additive fuel for powering conventional gas turbines. The tasks required to achieve this objective will comprise the determination of physicochemical characteristics of a fuel oil and three crude oil. In addition, the properties characterized will be evaluated against the operational window and properties of the conventional gas turbines by modelling software.

The characterized physicochemical properties will include;

- Measurement of density of the liquid fuels at different temperature and modelling the relationship between density and temperature for each liquid fuel.

- Determination of dynamic viscosity of the liquid fuels at different temperature and developing the Arrhenius relationship between dynamic viscosity and temperature, in order to obtain the activation energy required to cause flow in each liquid fuel.
- Measurement of the rheological properties of the liquid fuel such as yield shear stress, steady flow behaviour, thixotropy and verification of rheological models such as Newton, Herschel-Bulkley and Casson.
- Determination of the liquid fuels' Pour point
- Determination of the liquid fuels' Asphaltene content
- Determination of the liquid fuels' Moisture content and apparent pH
- Investigating the feasibility of powering a simple conventional gas turbine with liquid fuel using the modelling software IPSEpro^{TM}

1.3. Organization of the Thesis

Chapter 2 discusses the literature review. Chapter 3 discusses the measurement standards, methodology and experimental set up. Chapter 4 entails the results gotten from the experiments, simulation and experimental results modelling. Chapter 5 summarizes the conclusion drawn from this study. Detailed results obtained from the experiments are in the Appendix

CHAPTER 2

Literature Review

2.1. Crude oil in United Arab Emirates

Crude oil, a critical fuel can be categorized in the upper class of the highly traded products on the planet. Its price changes daily as a result of fluctuating conditions geared by factors of demand and supply. The annual world demand for crude oil is ever increasing and this has grown immensely over the past 30 years. Global consumption of crude oil has increased from 90.49 million barrels per day in 2013 to 91.39 million barrels per day in 2014, an annual increment of about 0.8 million barrels per day, the largest increment since 2008 [5]. The UAE is regarded as one of the largest producers of crude oil in the world, having the world's seventh largest proved reserves of both oil and natural gas, estimated at 97.8 million barrels and 215 trillion cubic feet respectively. The UAE is the world's eighth biggest oil producer and the fourth largest net oil exporter, with only Russia, Saudi Arabia and Iraq exporting substantially more [6].

They are many crude oil field distributed throughout the UAE. For example, the Emirates of Abu Dhabi has; Abu al-Bukhoosh, Asab, Bab, Bu Hasa, Bunduq, Mubarraz, Sahil, Satah, Umm al-Dalkh, Umm Shaif, Lower Zakum and Upper Zakum. The emirates of Dubai has; Falah, Fateh,

Rashid and Margham. The emirates of Sharjah has; Kahaif, Saja'a/Moyeid, and Mubarak. The emirates of Ras al khaimah has; Saleh [7].

2.2. Crude Oil Characteristics and Compositions

Crude oil are complex mixtures containing tens of thousands of chemically distinct organic compositions within a dynamic range of 10^4-10^5 in relative abundance. Current technical and industrial applications of petroleum crude oil and its products demand fast and accurate chemical fingerprinting of hydrocarbons, specifically, non-covalent multimers and distributions of heteroatoms, rings, and double bonds. That information can potentially determine the characteristics of the refining process and the production efficiency to convert the full mass balance into useful energy. It can also help determine the economic value of the crude oil and the level of environmental pollution upon combustion [8].

So it is more important to know which fuel is more suitable to specific application. In order for the decision to be made, it is necessary to;

- Determine each fuel's characteristics
- Compare one fuel's characteristics directly with another fuel's.

It is understandable from literature that in order to achieve tangible results in analyzing crudes oil and it's derivate, it is imperative to separate crude oil sample into fractions and analyze them in details. The results from the analyses of each fraction in a consistent manner are combined to arrive at composition of the original sample [9].

Fuel characterization is an important consideration for effective spark ignition, compression ignition, and turbine engine fuel utilization [10]. The use of assays serve this purpose by listing

physical and chemical fuel properties provided with maximum and/or minimum data value requirements which a fuel must meet.

Determining the constituents and characteristics of crude oil is very crucial to the growth and development of the petroleum industry. Due to their formation process, crude oils are highly complex mixture. The major group of compounds found in petroleum are saturated hydrocarbons, including straight chained, branched and cyclic hydrocarbons, simple aromatic hydrocarbons, resins, very large aromatic asphaltene compounds and metals. Varieties in the constituents of crude oil has led to the prevalence of unique and diverse systems of crude oil characterization. Each of these characterization systems play important roles in decision-making stages of exploration, production, refining, transportation and utilization [11]. The systems of characterization can be generally grouped as stated below.

- Assay properties
- Whole crude properties
- Geochemical parameters

2.2.1. Crude Assays

Basic crude oil assay contains majorly two types of data for an oil sample, which are [12]:

- Bulk properties
- Fractional properties

Bulk properties addresses the primary information of the type of the crude oil sample such as sweetness or sourness, light or heavy nature of the crude oil, etc. This property class also include specific gravity, nitrogen content, organometallic content, Carbon-Hydrogen ratio, sulfur content, flash point, refractive index, smoke point, light hydrocarbon yields, aniline point, cloud point, pour

point, asphaltene content, viscosity, carbon residue, freeze point, acid number and boiling point curve [12]. These mentioned properties are defined as follow;

Sulfur Content is measured as the percentage weight of sulfur in the crude oil sample, which can vary from values less than 0.1% to values greater than 5%. Crude oils categorized as sweet crude or low-sulfur are those with less than 0.5 wt. % sulfur, and those high-sulfur content crude oil with more than 0.5 wt. % sulfur are referred to as sour crude.

Pour Point is the measure of ease or difficulty to pump crude oil, especially at lower temperature conditions. Precisely, pour point can be referred to as the lowest temperature at which a crude oil will pour or flow when it is cooled without perturbation under controlled conditions.

Conradson Carbon Residue is the measure of coke-forming propensities of crude oil. It is determined by the destructive distillation of crude oil sample in the absence of air, whereby the sample is reduced to elemental carbon (residual coke), which is expressed in weight percent of the initial sample.

Flash Point of any liquid hydrocarbon signifies its explosion and fire tendencies, which is the lowest temperature at which sufficient amount of vapor above the liquid mixes with air, such that it can spontaneously be ignited in the presence of any spark.

Freeze Point indicates temperature whereby liquid hydrocarbon solidifies under atmospheric pressure.

Aniline Point depicts minimum temperature for even miscibility of equal amount (volume) of aniline and crude oil.

Smoke Point is determined by measuring the height of the smokeless flame from a burning liquid fuel in millimeters after which smoking occurs. It shows the burning qualities of kerosene and jet fuels.

Cloud Point is defined as the temperature at which the wax present in the crude oil sample initiates crystallization or start to separate from the solution under cooling conditions.

Acid Number which is stipulated by ASTM test method D3339, which is the determination of the organic acidity of a crude oil sample.

Fractional properties In order to appropriately refine crude oil into diverse end products such as diesel, gasoline and other raw materials for different chemical process, these properties of crude oil samples should be determined as it indicate the characteristics and constituents for specific boiling point range. Fractional properties mostly comprise of sulfur content, nitrogen content for each boiling-point range, paraffins, naphthenes and aromatics (PNA) contents, freezing point, octane number for gasoline, etc. [12]. These properties are mostly based on the components or fractions of crude oil and not crude oil itself.

2.2.2. Crude Oil Components

Crude oil are liquid fossil fuels which ranges from thick to light colored oils, black oil with similar appearance to melted tar. Crude oil are generally made up of hydrogen, carbon, sulfur, oxygen, nitrogen, salts and minerals in varying quantities which is dependent on their reservoir properties [13]. The elemental composition of Crude oil is less variable when compared with that of coal and can be in the range of; 83-87% carbon, 11-16% hydrogen, 0-4% oxygen plus nitrogen, and 0-4% sulfur.

Owing to the complex nature of crude oils, characterization by the individual molecular types is not possible. This complexity makes the use of elemental analysis inappropriate and ineffective as it only gives incomplete data about the component of crude oil because of the non-varying nature shown by elemental composition [14-19]. So, one of the practice of separating crude oils into its constituents is using the SARA-separation technique. This technique is a typical group type analysis, where the crude oils are separated into four main chemical classes based on the variation in their solubility and polarity. Instead of molecules or atoms classifications, certain chemical structures are considered the components of crude oil. The SARA-separation technique tend to give characteristic information, which can be classed as on one that lie amid information gotten from analysis for individual molecules and those from elemental analysis. The SARA-separation scheme that illustrates the fractions in crude oil is displayed in Fig. 1 [20]. Chemical constituents of crude oil based on the SARA-fractions will be discussed in the following.

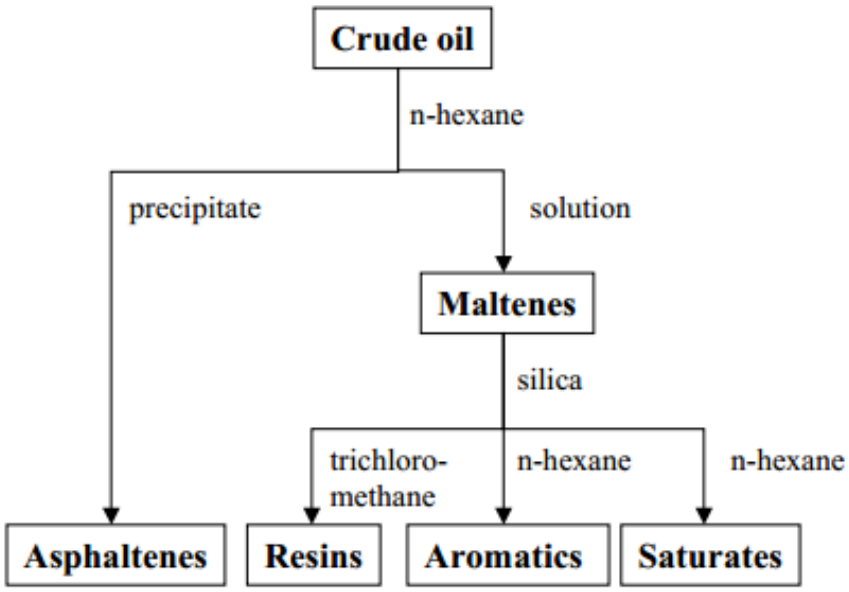

Fig. 1. SARA separation scheme [21]

Saturates: There are single bond non-polar hydrocarbons, which can be branched or straight-chain alkanes, and sometimes cycloalkanes (naphtenes) with low molecular weight. Cycloalkanes are made up of one or more rings, which can be attached to numerous alkyl-side chains. As the molecular weight of crude oil increases, the fraction of saturates present in the crude oil decreases, this indicates that saturates are the lightest fraction in crude oil [22-24].

Aromatics: These category is about benzene and its derivate. Aromatics can be found in all crude oil, and a large number of aromatics contain aromatic rings, cycloalkane rings and alkyl chains. Aromatic hydrocarbons can be monocyclic (MAH) or polycyclic (PAH) aromatics, this depending on the number of aromatic rings present in the molecule. Aromatics that are of higher molecular weight and polar, can fall in the asphaltene or resin fraction.

Resins: are made up of polar molecules which contains heteroatoms which are; sulphur, nitrogen or oxygen. This fraction is soluble in light alkanes like heptane and pentane, but they are not soluble in liquid butane or propane [20, 25]. Since they are defined by their solubility, it is expected that an overlap between the asphaltene and aromatic fraction will exist. Though, this fraction is very important fraction that affect properties of the crude oil as they also play an important role in the stabilization of petroleum and prevents the separation of asphaltenes constituents as a separate phase[25]. Little research has been reported on the characteristics of the resins, when compared with asphaltenes. On the contrary, some common features can be known, resins possess higher Hydrogen-Carbon ratio when compared with asphaltenes, 1.2-1.7 for resins and 0.9-1.2 for asphaltenes [16]. Resins and asphaltenes are structurally alike, but have lesser molecular weight.

Asphaltenes: This fraction are also defined by their polarity and solubility like the resins, they are precipitated in light alkanes like heptane, pentane or hexane as illustrated in Fig. 2[25] . This

precipitate dissolves in toluene and benzene, which are aromatic solvents. This fraction comprises of the major amount of heteroatoms (N, O and S) and porphyrine with organometallic constituents such as Nickel, Vanadium and Iron in the crude oil. Although, asphaltenes are hydrocarbons that present an extremely complex molecular structure. Chemical and spectroscopic evidence have led to the proposal of an average structure in which relatively small hydrocarbon units are linked together by sulphur bridges. However, the structure and composition of asphaltene may vary considerably with the origin and mode of formation of the source reservoir [26, 27]. The structure has always been contested by various investigations, though it is understood to be made up of polycyclic aromatic clusters, with its alkyl-side chains replaced [15]. Fig. 3 expresses an illustration of an asphaltene structure as well as other component of the SARA fraction.

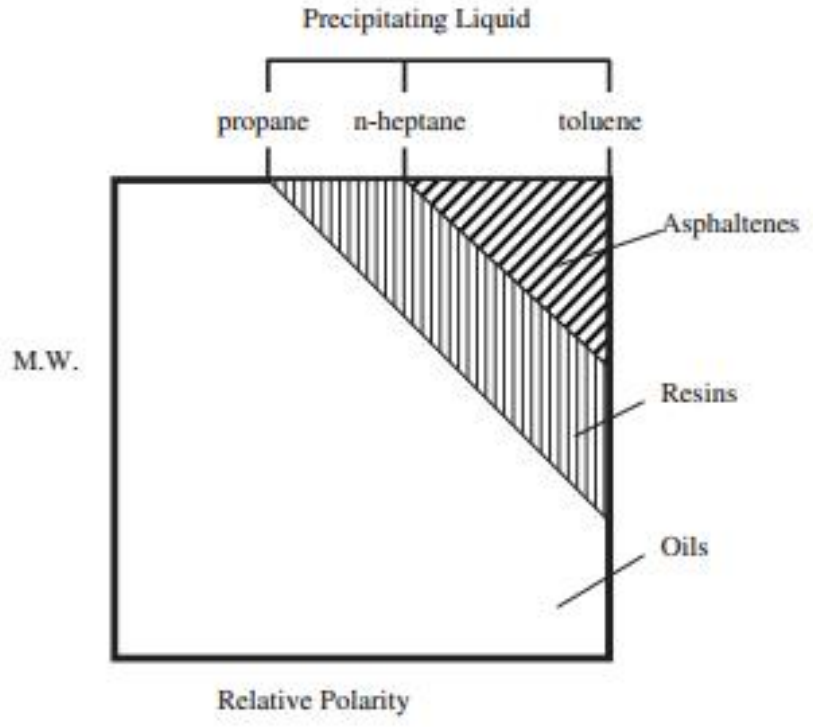

Fig. 2. Asphaltenes and resin definition according to the polarity-molecular weight map [25]

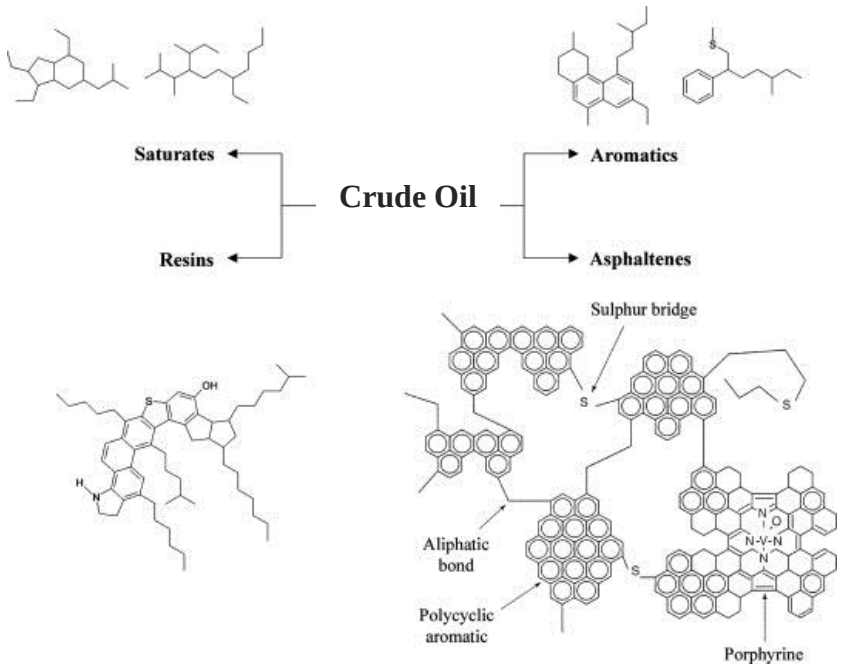

Fig. 3. SARA composition of Crude oil (saturates, aromatics, resins, asphaltenes) [28]

2.3. Crude Oil Classification

Crude oil contains different amount of hydrocarbons in different phases (gases, liquids or solids), bearing this in mind, it will be difficult to classify it in a uni-dimensional manner. So the petroleum industry in its entirety has defined ways by which the crudes can be classified, which can be by the geographical location it was produced, its API gravity (measure of its density/Specific Gravity), sulphur content and its predominant fraction (paraffinic, naphthenic or aromatic). This classification are discussed as follows.

2.3.1. Specific Gravity

The generally accepted petroleum industry method for specifying the specific gravity of the liquid petroleum products is the API gravity, which was devised jointly by the American Petroleum Institute (API) and the National Institute of Standards and Technology (NIST). This method works on an inverted scale that denotes the lightness or heaviness of crude oils and

other liquid hydrocarbons. It can be calculated by expressing the ratio of weights of equal volumes of oil and pure water at a temperature of 60°F and atmospheric pressure as shown in Eq. 1.

$$\text{API gravity} = \frac{141.5}{\text{Specific Gravity at } 60^{\circ}\text{F}} - 131.5 \quad (1)$$

From Eq. 1 it shows that the lower the specific gravity or density, the higher the API gravity. Crude oils with have higher API gravity value, often contain high amount of naphtha which are mostly volatile hydrocarbons that are paraffinic in nature. This kind of crude oil can be easily processed and they are called light crude. The heavy crude oils are considered more viscous, highly dense and higher boiling ranges, and this translates to lower API gravity. They have high content of aromatics and they contain more residual substances such as; heterocyclics, asphaltenes, nitrogen, sulfur, etc. [5]. So, according to the accepted method of classification based on density, crude oil can be characterized as the following [29]:

- Extra heavy crude: Crude oil which have their API gravity below 10°.
- Heavy crude: Crude oil which have their API gravity below 22.3°.
- Medium crude: Crude oil which have their API gravity between 22.3° and 31.1°.
- Light crude: Crude oil which have their API gravity above 31.1°.

2.3.2. Sulphur Content

This classification scheme is centered on the qualitative analysis of crude oil, where the amount of sulphur present in a sample of the crude oil is determined. The quantity of the sulphur contaminant is then use to characterize the oil. The two main classes are sour and sweet crude oil, they are discussed as follow [30];

- Sour crude oil: It is sour if its sulphur content is greater than 0.5% and some of this will be in the form of hydrogen sulphide. It also contains more carbon dioxide. Most sulphur in

crude oil is actually bonded to carbon atoms. Nevertheless, high quantities of hydrogen sulphide in sour crude poses serious health problems that could be fatal. This impurities need to be removed before this lower-quality crude can be refined, thereby increasing the cost of processing.

- Sweet crude oil: It is considered sweet if it contains less than 0.5% sulphur. Sweet crude is easier to refine and safer to extract and transport than sour crude. Because sulphur is corrosive, sweet crude oil poses less damage to refineries and thus results in lower maintenance costs over time.

2.3.3. Predominant Crude Oil Fractions

Crude oils contain different classes of hydrocarbon which are aromatic, naphthenic and paraffinic hydrocarbons, they can be categorized as naphthenic or paraffinic-based depending on the most of the prevalent proportion of hydrocarbon type present[31]. Aromatic crude are characterized by the presence of ring hydrocarbons that are unsaturated such as the benzene ring, while naphthenic crude comprises majorly saturated-ring, cycloparaffinic hydrocarbons and Paraffinic crude are rich in straight chain and branched saturated hydrocarbons [5].

2.4. Crude Oil Property Measurement Standards

Different crude oil types have their unique molecular, physical and chemical characteristics. Therefore, it is essential to obtain their individual crude oil assay, which is a chemical evaluation of the crude oil feedstock by petroleum testing laboratories. The result from this evaluation provides extensive and detailed hydrocarbon analysis data for oil traders, refiners and producers. The information obtained shows the present conditions of the oil in its reservoir and how the properties of crude oil changed as the oil field age. The use of accepted standards like those stipulated by International Standard Organization (ISO), American Society for Testing and

Materials (ASTM), American National Standards Institute, etc. ensures reproducibility and precision of results and makes it easier for the industry to accepts result from different laboratories.

The following sections will be discussing standards of measurements of crude oil properties that are crucial to its utilization, refining and transportation such as; Viscosity, Density, Pour point, moisture and asphaltenes content.

2.4.1. Density, Specific Gravity and API Gravity

The density, specific gravity and API gravity are parameters that indicates the heaviness or lightness of crude oil and its derivatives. These aforementioned properties cannot be measured independently because they are closely related to each other and the value one depends on the other. There is no need to measure all these properties separately; only a density or a specific gravity is needed to be measured. If a specific gravity is known for a particular crude oil fraction, then it is possible to calculate the density as well as the API gravity. In petroleum industry, specific gravity and API gravity measure at reference temperature of 60°F (15.56℃). There are variety of test methods and techniques available for measuring density, specific gravity and API gravity of crude oil which are described below.

ASTM D1298- 12B

This standard method discusses the use of glass hydrometer in laboratory determination of the relative density, density, or API gravity of crude oil, petroleum derivate, or blends of non-petroleum and petroleum products which are in liquid state. The measured sample should not have their Reid vapor pressure greater than 101.325 kPa (14.696 psi). This measurement is followed by some calculations for corrections. This values can be determined under uncontrolled or controlled temperatures and adjusted to 15°C or 60°F using international standard tables and correction

calculations. These Readings are corrected for thermal glass expansion effect, meniscus effect, and alternate calibration temperature effects and corrected to the reference temperature by means of the Petroleum Measurement Tables.

This procedure is most suitable for determining the density, relative density (specific gravity), or API gravity of low viscosity transparent liquids. In order for this test method to be used for viscous liquids, it is crucial to allow ample time for the hydrometer to attain equilibrium temperature with the liquid. In the case of opaque liquids measurement, it is important to carry out meniscus correction. In general, opaque and transparent liquids should have their readings corrected for effects of alternate calibration temperature prior to correction of reference temperature and thermal glass expansion effect [32].

The hydrometer, made of glass and consists of a cylindrical stem and a bulb weighted with mercury or lead shot to make it float upright when placed in a liquid as shown in Fig. 4 but without the thermometer, operates based on Archimedes' principle, which states that when a body is immersed in a fluid it loses weight equal to the liquid weight displaced. The hydrometer element is a constant weight body (constant buoyant force), which will displace different volumes of fluid for different fluid densities. Since they are accurate, frictionless, direct indicating without need for mechanical linkages or external energy sources, and are compatible with most corrosive fluids, therefore, the amount of stem submersion is an indication of fluid density [32]. The specific gravity at 60/60 which means that both the density of the crude oil and the water are measured at 60^{o}F can be computed using Eq. 2 below. From this the API gravity can be obtained using Eq. 1.

$$\text{Specific Gravity} = \frac{\rho_{oil}}{\rho_{water}} \tag{2}$$

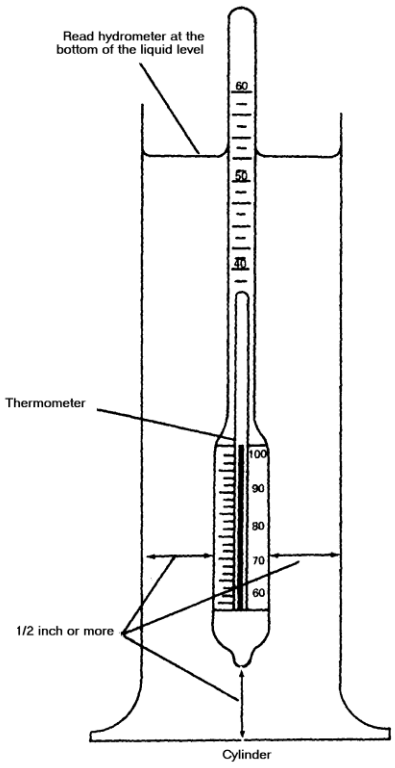

Fig. 4. Thermohydrometer in use[33]

ASTM D4052- 11

This test standard covers the determination of the density, relative density, and API Gravity of petroleum distillates and viscous oils that can be handled as liquids at the temperature of test, utilizing either manual or automated sample injection equipment, where the automated option shown in Fig. 5. Its application is restricted to liquids with total vapor pressures typically below 100 kPa and viscosities typically below about 15000 mm^2/s at the temperature of test. The total vapor pressure limitation can be extended to pressures greater than 100 kPa provided that it is first ascertained that no bubble forms in the U-shaped oscillating tube. Some examples of products that may be tested by this procedure include: gasoline and gasoline-oxygenate blends, diesel, jet, basestocks, waxes, and lubricating oils.

This test method should not be applied to samples so dark in color that the absence of air bubbles in the sample cell cannot be observed with certainty. Waxy samples require a temperature cell operated at elevated temperatures necessary to ensure that the sample to be analysed is in liquid form[34].

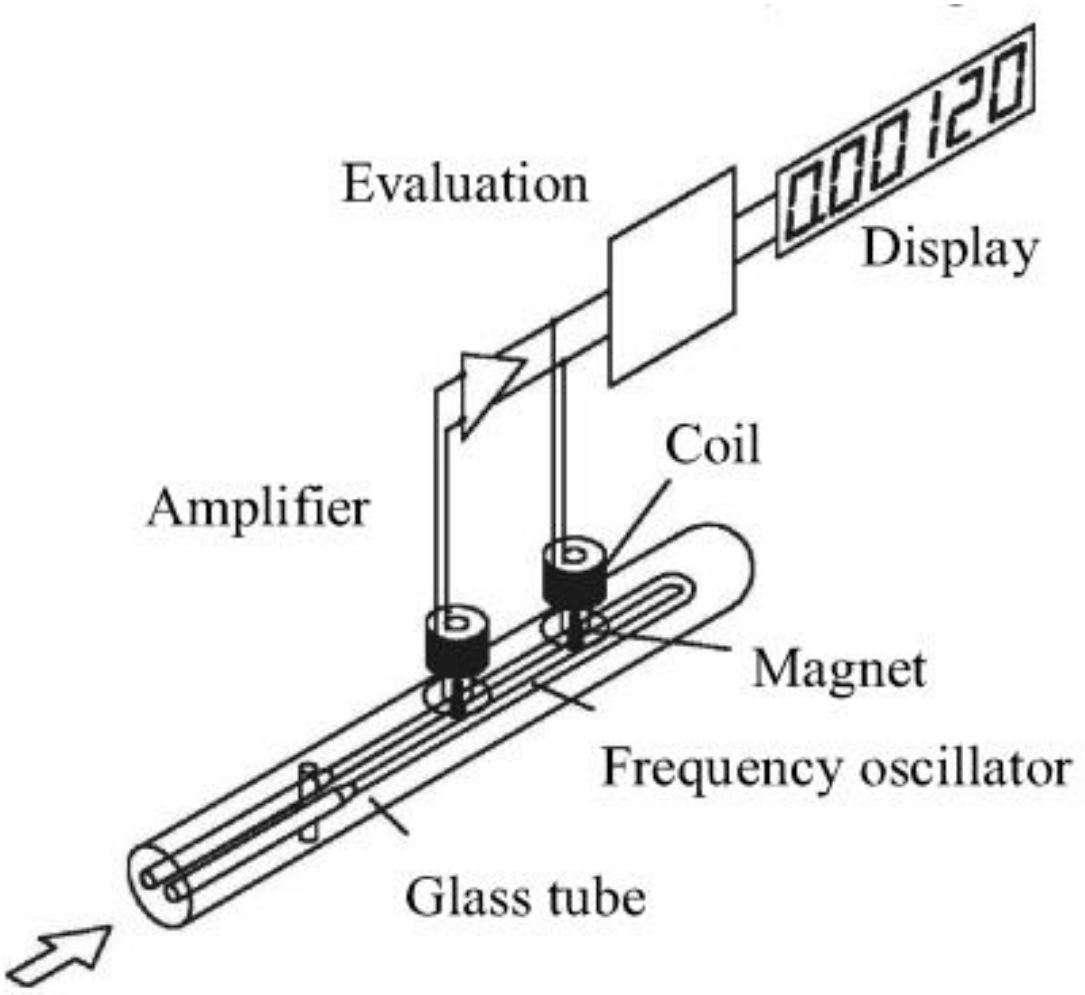

Fig. 5. Measurement cell of an oscillation-type density meter[35]

ASTM D1480-12

This test method covers two procedures for the measurement of the density of materials which are fluid at the desired test temperature with the aid of the Bingham Pycnometer. Its application is restricted to liquids of vapor pressures below 600 mm Hg (80 kPa) and viscosities below 40000

cSt (mm^2/s) at the test temperature. This method is designed for use at any temperature between 20 and 100°C. Although, it can be used at higher temperatures. The determination of densities at the elevated temperatures between 40 and 100°C is particularly useful in providing the data needed for the conversion of kinematic viscosities in centistokes (mm^2/s) to the corresponding dynamic viscosities in centipoises (mPa.s) [35].

The Bingham Pycnometer shown in Fig. 6 is used when the density or specific gravity is to be determined to five decimal places. Prior to measurement the instrument is calibrated by determining the weight of freshly boiled and cooled distilled water, the sample is introduced into the tarred, dry and clean pycnometer, equilibrated to the desired temperature and weighed. The density and specific gravity is then calculated from this weight and the previously determined weight of water required to fill the pycnometer at the same temperature, with both weights being corrected for the buoyancy of air[36].

ASTM D1481-12

This test method covers the determination of the density, using the Lipkin Bicapillary Pycnometer (see Fig. 7) for oils that are more viscous than 15 cSt at 20°C (mm^2/s), and of viscous oils and melted waxes at elevated temperatures, but not at temperatures at which the sample would have a vapor pressure of 100 mm Hg (13 kPa) or above [37].

The Lipkin Bicapillary Pycnometer works by drawing the liquid sample into the instrument and weighed. Then, it is equilibrated to the test temperature and the position of the liquid levels in the capillary is observed and recorded. The density and specific gravity is then computed from its weight, a calibration factor that is proportional to an equal volume of water and a term that corrects the buoyancy of air[36].

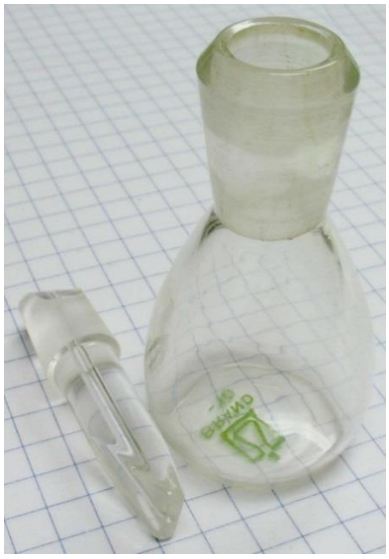

Fig. 6. Bingham Pycnometer[38]

Fig. 7. Lipkin Bicapillary Pycnometer [39]

2.4.2. Viscosity (Kinematic and Dynamic)

Viscosity of a fluid can be defined as the parameter that indicates fluid's resistance to deformation by tensile stress or shear stress. It can also be termed as the resistance of fluid to flow. The shear resistance in a fluid is caused by intermolecular friction exerted when layers of fluid try to slide by one another. The viscosity is an important fluid property when analyzing liquid behavior and

fluid motion near solid boundaries. The viscosity of the fluid plays a critical role in the design of fuel injector, pumps, mass transfer equipment, storage, transport facilities and utility such as selecting the appropriate lubricants for process equipment.

It can be expressed in two forms, which are dynamic (or absolute) viscosity and kinematic viscosity. The dynamic viscosity, μ is the tangential force per unit area required to move one horizontal plane of a fluid with respect to another plane at a unit velocity when maintaining a unit distance apart in the fluid as expressed in Eq.3, while Kinematic viscosity, υ can be obtained by dividing the dynamic viscosity of a fluid with the fluid mass density, ρ as shown in Eq.4.

$$\tau = -\mu \frac{dc}{dy} \tag{3}$$

$$\upsilon = \frac{\mu}{\rho} \tag{4}$$

Dynamic and kinematic viscosity properties is dependent on the measuring temperature of the analyzed fluid. This is especially true for petroleum products as their rate of viscosity change per unit temperature, this effect is significantly greater in petroleum crude than in other products. Thus, a slight variation in temperature can have a very large effect on the viscosity of the fluid. Although it sounds very simple and direct to obtain the values for this parameter, achieving the high accuracy and precision required by the industry is an extremely formidable task [40]. Therefore, it is imperative to commence the investigation of these properties following the standards applicable to crude oil stated below.

ASTM D7042-14

This test standard stipulates the technique for simultaneous measurement of the dynamic viscosity, η, and density, ρ, of crude oils and its derivate using the Stabinger viscometer. It is applicable to

transparent and opaque liquids. Dividing the dynamic viscosity (η) by the density (ρ) obtained from the device yields the kinematic viscosity (ν) at the same test temperature. Results gotten following this standard depends on the nature of the sample and it is intended to be used for liquids in which shear stress is directly proportional to the shear rate i.e. liquids that exhibit Newtonian flow behavior.

The Stabinger viscometer, patented in 2001 is a technology that makes the measurement of viscosity easy. The viscometer is constructed using two coaxial cylinders, where the outermost cylinder produces the driving power. This can be seen as a modification of the Couette rotational viscometer. The outermost cylinder rotates in a temperature-controlled copper housing at a steady speed. The internal cylinder which is molded like a conical rotor weighs less than the filled samples, thus it floats within the liquid and the outer cylinder. The inner cylinder is centered by centrifugal forces as shown in Fig. 8. This is done to avoid any bearing friction. The rotor is driven by the shear force of the rotating fluid, where the magnet in the rotor creates eddy current brake with the surrounding copper casing. Equilibrium speed in the rotor is established between the accelerating and decelerating forces. This dynamic viscosity is unambiguously measured by this forces interactions [41].

Viscosity can be defined as the parameter that is inversely proportional to the difference of the speed between the inner rotor and the outer tube. This implies that the lesser the viscosity of the sample, the higher the difference of the speed. This is so because a less viscous sample transmits less of the outer tube's speed to the floating rotor. Torque and speed measurement is effected without direct contact using a Hall-effect sensor which counts the frequency of the rotation of the magnetic field. This permits the determination of precise torque resolution up to 50 pNm with a wide measurement ranging from 0.2 to 20,000 mPa.s using a single measuring method. In order to

calculate the kinematic viscosity from the measured dynamic viscosity, the built-in density measuring device is used, this device works based on the oscillating U-tube principle[42].

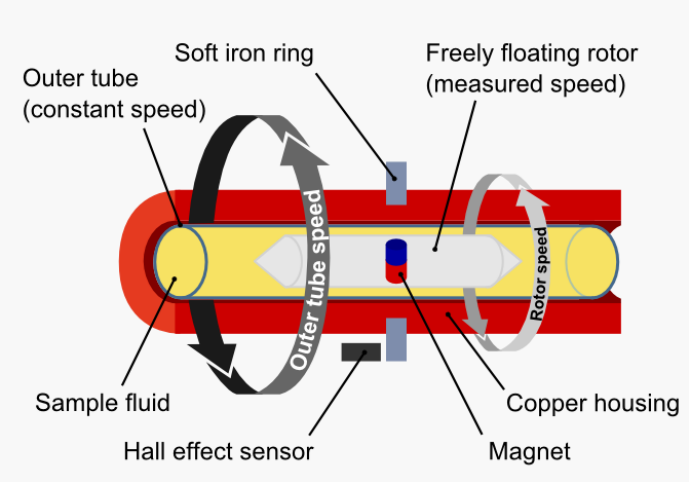

Fig. 8. Stabinger viscometer working principle [38]

ASTM D445-14a

This standard procedure specifies a method for the determination of the kinematic viscosity (v) of liquid petroleum products, both transparent and opaque, by measuring the time for a volume of liquid to flow under gravity through a calibrated glass capillary viscometer shown in Fig. 9. The dynamic viscosity (μ) can be obtained by multiplying the kinematic viscosity (v) by the density, (ρ) of the liquid.

The result obtained from this test method is dependent upon the behavior of the sample and is intended for application to liquids for which primarily the shear stress and shear rates are proportional (Newtonian flow behavior). If, however, the viscosity varies significantly with the rate of shear, different results may be obtained from viscometers of different capillary diameters. The range of kinematic viscosities covered by this test method is from 0.2 mm^2/s to 300 000 mm^2/s at all temperatures [43].

Fig. 9. Glass capillary viscometer [44]

ASTM D2893-09

This standard procedure involves the determination viscosity of lubricants at low-shear rate using Brookfield viscometers. This method is applicable to fluid with viscosity ranging from 500 to 900 000 mPa.s but with a limited temperature range which depends on the capability of the viscometer head[45].

The viscometer shown in Fig. 10 works on the Brookfield' operating principle. It operates with the aid of a motor that rotates a spindle at a defined speed or shear rate and the viscometer measures the resistance to rotation and reports a viscosity value. Various spindle designs can be employed, depending on the nature of the sample and the requirements. The spindle design are categorized as follow: Dip-in LV and RV spindles, Small sample Adapter, Ultra low Adapter, T-Bar and Helipath [46].

Fig. 10. Brookfield viscometer

2.4.3. Pour Point

Prior to burning of a fuel in an engine or any other form of utility, it must first be pumped from the fuel or source tank. Therefore, it is important to measure the temperature below which crude oil becomes plastic and will not flow. The knowledge of pour point of crude oil and its derivate is crucial especially during transportation. A fluid solidifying can clog pipelines and pumps broken by reduction in feed rate which leads to overstressing of the equipment [47].

There are variety of test methods and techniques available for measuring pour point of crude oil, some of which are described below.

ASTM D7346-14

This test standard dictates the method of determining the pour point of crude oil and its derivate using an automatic instrument. The measuring range of the apparatus is from –95 °C to 45 °C. Results from pour point measurement using this test method are reported at intervals of 3 °C or 1 °C [48].

This standard has several advantages over conventional cold flow analysis systems. It runs analysis three times faster than conventional systems. It also requires little operator training since it is easy to use; operators simply fill the test tube with the sample and push the start button. It increases laboratory productivity by running up to 10 samples with minimal attendance due to the built-in sample changer. It reduces product waste since it uses a smaller amount of sample, about 0.5 ml per sample[49].

ASTM D97

This test method can be used for on any petroleum product. This procedure is suitable for black specimens, cylinder stock, and non-distillate fuel oil. It is also suitable for testing the fluidity of residual fuel oil at specified temperature.

The test recommends preliminary heating of the sample, then the sample is cooled in baths at a specified rate and examined at intervals of 3°C for flow characteristics, as illustrated in Fig. 11. The lowest temperature at which movement of the specimen is observed is recorded as the pour point. If flow is observed at the upper limit of cooling of a particular bath, the sample is transferred to another one as specified by the standard, the freezing mixtures and schedule of transfer is stated as follows:

	For Temperature Downwards
Ice and water	9°C
Crushed ice and sodium chloride crystals	−12°C
Crushed ice and calcium chloride crystals	−27°C
Acetone or petroleum naphtha chilled in a covered metal beaker with an ice-salt mixture to −12°C, then with enough solid carbon dioxide to give the desired temperature.	−57°C

The refrigerator option for this standard was used, this apparatus has four baths with target temperature of 0, -18, -33 and -51^{o}C as illustrated in Fig. 25.

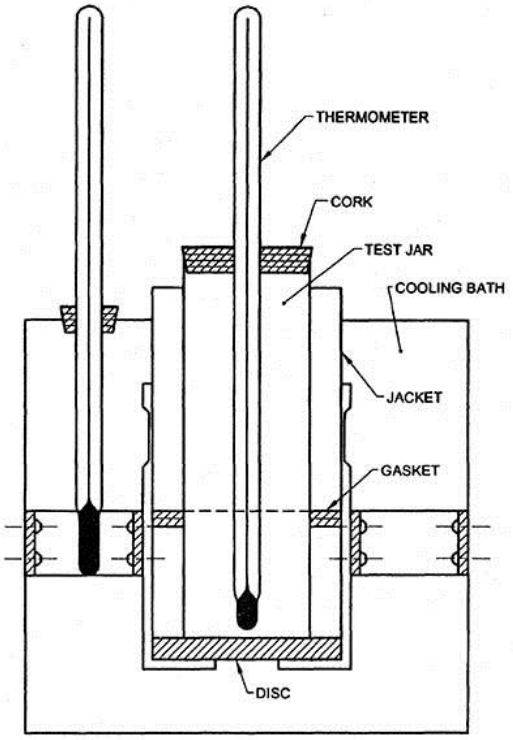

Fig. 11. Schematics of pour point Apparatus [50]

ASTM D5985

This test standard stipulates the measurement of pour point of petroleum derivate using instrument that rotates the test sample continuously in the presence of a detection device during chilling of the test sample. This method is created to cover temperatures ranging between −57 and +51°C.

In order to measure the pour point using the rotational method as stipulated by this standard, the sample is poured into the sample cup, the sample cup is rotated at 0.1 revolutions per minute. The, tiltable, coaxial temperature sensor is inserted into the sample. As soon as the pour point is attained, its viscosity increases after which the temperature sensor moves out of position and the light barrier is triggered as illustrated in Fig. 12 [51].

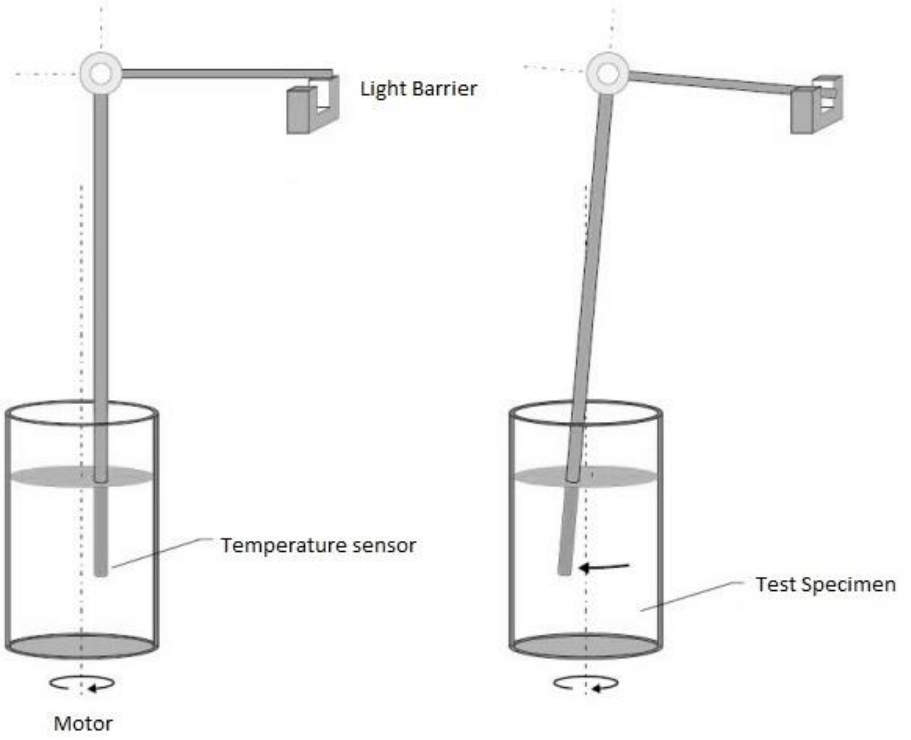

Fig. 12. Schematics of pour point measurement using ASTM 5985 [51]

ASTM D5853-11

This test standard discusses about two-stage process for determination of the pour point of crude oils to temperature as low as −36°C. The first stage measures the maximum pour point and the second stage measures the minimum pour point. These two pour point values helps create a temperature window where the crude oil might appear as solid as well as liquid, depending on its thermal history [52].

ASTM D6892

This test method which is also known as the Robotic tilt method. It determines the pour point of petroleum products using an automatic device that inclines the test jar and using an optical device to detect any motion in the surface of the test sample as illustrated by the schematics in Fig. 13, after being removed from a regulated, stepped-bath cooling jacket. This method is also designed to cover the range of temperatures from −57 to +51°C; results from this test method can be determined at either 1 or 3°C temperature intervals. This standard provides unparalleled precision and accuracy as it carries out pour point analysis with microprocessor precision [53].

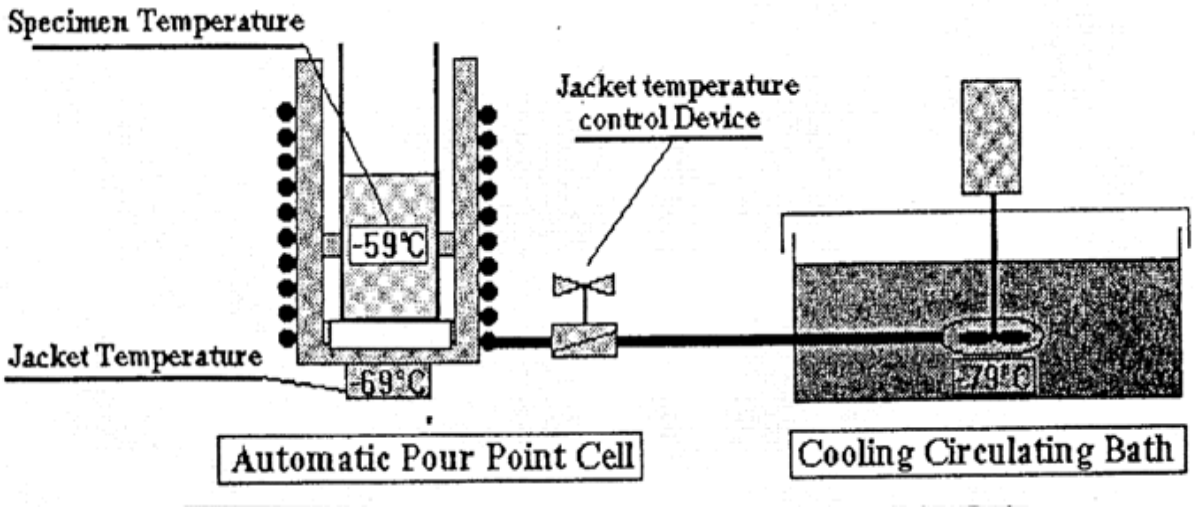

Fig. 13. Schematics of pour point measurement using ASTM 6892 [53]

2.4.4. Asphaltenes Content

Asphaltenes, which prove problematic in the course of handling and storing when the suspension of its molecules are stressed through incompatibility or application of excessive stress. They are organic molecules with the highest carbon-hydrogen ratio and molecular mass naturally occurring fraction in crude oil. Change in fluid property such as pressure, temperature and composition can cause the precipitation of asphaltenes during the production, transportation, use, etc. Due to their

polar and complex nature, it is proven that the elemental compositions of asphaltenes precipitated by different solvents from various sources are different[47, 54].

Therefore, it is vital to determine the asphaltenes content in crude oil this knowledge will alert buyers, seller, refiners, drillers, etc. of the impending problem that may stem from its precipitation during production, transportation, storage and utility. In order to obtain the percentage content by mass in crude oil; two methods have been proposed to precipitate asphaltenes. Stated below are the standard set by ASTM for quantitative analysis of asphaltenes in crude oil and derivate.

ASTM D3279-12

This test standard discusses about the determination of mass percent content of asphaltenes which are insoluble in n-heptane solvent. This test method can be applied gas oils, semi-solid and solid petroleum asphalts, heavy fuel oils, and crude oil that has a cut-point of 343°C or above.

In this method, the sample (which was weighed before sample introduction) and solvent are poured in a flask and weighed, then it is heated under reflux. After 20 minutes of heating, the sample is allowed to cool for 1hour. Upon cooling, the sample is filtered using a filter paper in a gooch crucible under gentle vacuum. The precipitate, filter and crucible is placed in the oven for 30 minutes at a temperature of 110 ± 5^{o}C. The mass percent of n-heptane insoluble (NHI, %) asphaltenes is computed using Eq.5 .

$$\text{NHI}, \% = \frac{\text{C} - \text{A}}{\text{B}} \times 100 \tag{5}$$

Where, A is the mass of crucible and filter, B is the sample mass and C is the addition of the crucible, filter, and insoluble material mass[55]

ASTM D6560 - 12

This test method is similar to ASTM D3279, as it also covers the procedure for the determination of the heptane insoluble asphaltene content of gas oil, diesel fuel, residual fuel oils, lubricating oil, bitumen, and crude petroleum but differ in the topped cut-off which is 260°C in this method. The accuracy of this method can detect asphaltene content ranging from 0.50 to 30.0 % m/m. Although, the values not within this range can be valid yet they lack similar precision as values within the range. It is recommended that oils containing additives may give erroneous results using this method [56].

2.4.5. Moisture Content

The accurate measurement of moisture content in crude oil, which is a crucial quality determining parameter constitutes an important role in the extraction, processing and utility of crude oil and its derivatives. During storage, the presence of water in crude oil can promote microbial activity if the growth mechanism is anaerobic and this may lead to the production of corrosive acid and hydrogen sulphide. Like salts, water contaminant in crude oil can cause fouling in heaters, exchangers and stills; these can contribute to corrosion of process equipment and piping. The knowledge of water content is valuable in determining the net volume of crude oil in sales, taxation, custody transfer and exchanges, the quantity of water in crude oil has a huge impact on its economic value [47, 57].

They are different standard methods by which the amount of water in crude oil can be determined, there are listed and explained as follows:

ASTM D4006-11

This test standard discusses the determination of water content in the range from 0 to 25 % volume in Crude oil by the distillation method. The material to be tested is heated under reflux with a

water-immiscible solvent, which co-distills with the water in the sample. Condensed solvent and water are continuously separated in a trap, the water settling in the graduated section of the trap and the solvent returning to the still. This standard may not be applicable to crude oils containing water-soluble alcohols and yet it is the most preferred and accurate method in determining water content in crude oil.

The solvent blank which is the water content of the solvent shall be determined by distilling an equivalent amount of the same solvent used for the test sample in the distillation apparatus. The blank shall be determined to the nearest scale division and used to correct the volume of water in the trap. Then the amount of water present in the crude oil is determined using Eq.6. [58]

$$\text{Water, \% } ({}^{v}/_{v}) = \frac{\text{volume in water trap, mL} - \text{water in solvent blank, mL}}{\text{volume in test sample, mL}} \times 100 \qquad (6)$$

ASTM D4377-00

This test standards explains the determination of water content in the range from 0.02 to 2 % in crude oils using the potentiometric Karl Fischer titration shown in Fig. 27. Pyridine-free Karl Fischer reagents or Karl Fischer reagent are used in this test method. Measurement interference can be caused by the presence of mercaptan and sulphide (S^- or H_2S) when using this test method [59].

In this test method, a definite current is passed between two platinum electrodes, and the change in potential (mV) is measured during dropping water determination test solution (Potentiometric titration at constant current). With the progress of titration, the value indicated by the potentiometer in the circuit decreases suddenly from a polarization state of hundreds (mV) to the non-polarization state, but it returns to the original state within several seconds. At the end of titration, the non-

polarization state persists for a certain time. As shown in Fig. 14, the end point of titration is determined by the detection unit, when this electric state attained. Finally, the water content in the crude oil is determined by measuring the quantity of electricity which is required for the electrolysis, based on the quantitative reaction of the used reagent with water [59].

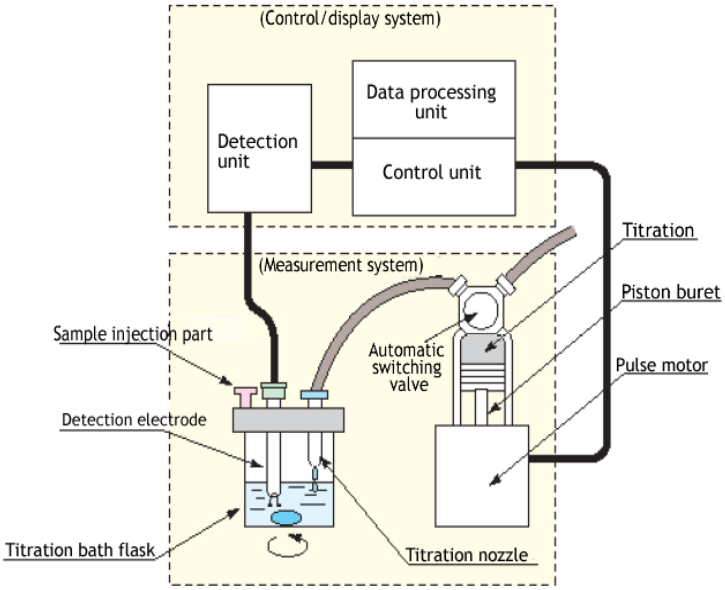

Fig. 14. Schematic of potentiometric Karl-Fischer moisture meter[60]

ASTM D4928-12

This test method stipulates the determination of water content in crude oil, with detection range between 0.02 and 5.00 volume or mass percent using the Coulometric Karl Fischer titration. As stated above in ASTM 4377, Mercaptan (RSH) and sulphide (S^- or H_2S) as sulfur are known to interfere with this test method, at concentrations which are less than 500 µg/g, the level of interference observed are insignificant. Though, the accuracy range of measurement for this test method is 0.005 to 0.02 mass % water content, the level of interference of mercaptan and sulphide have not been well determined[61].

The reagent and solvent are combined in the titration cell, as seen in Fig. 15. When a sample is introduced into the titration cell and dissolved, reagent is released by the induction of an electrical current, the water present in the sample is coulometrically titrated to a predefined end point at which there is a minute excess of free iodine present. Stoichiometrically, 1 mole of water will react

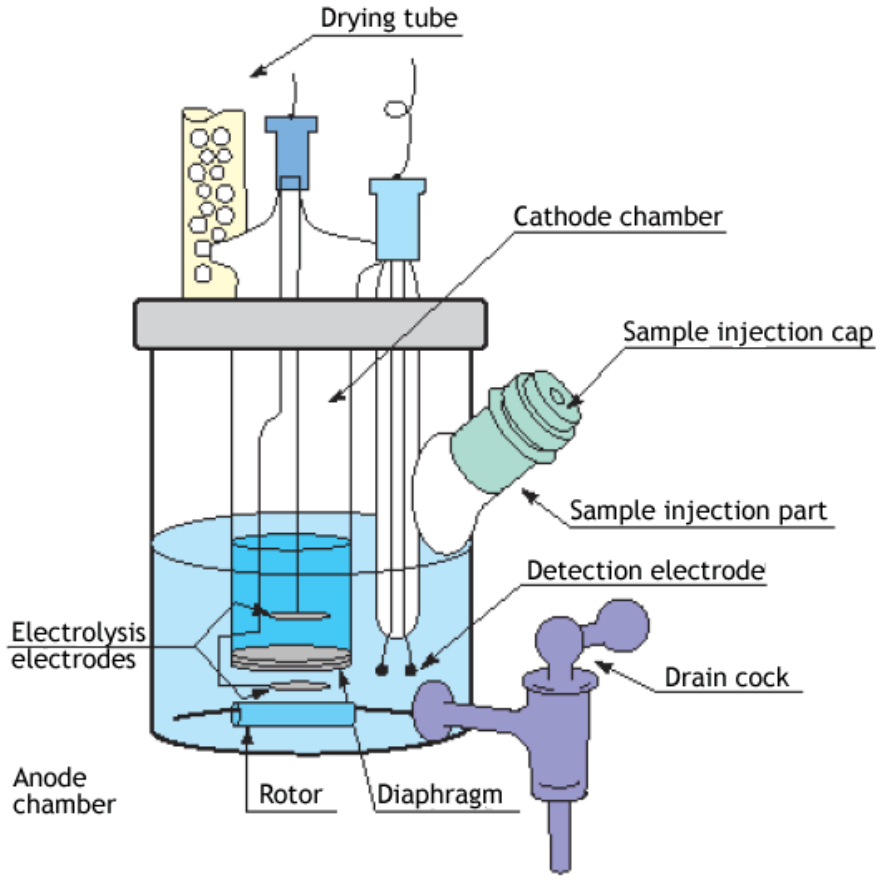

Fig. 15. Schematic of Coulometric Karl-Fischer moisture meter [60]

with 1 mole of iodine, so that 1 milligram of water is equivalent to 10.71 coulombs of electricity. The amount of current required to convert the water is the determinant of the amount of moisture i.e. the product of time and current is directly proportional to the amount of iodine generated and therefore to the amount of water determined. The advantage of the Coulometric Karl

Fischer method over the potentiometric method is the capability to accurately measure small amounts of moisture[62-64].

ASTM D4007-12

This test method describes the laboratory determination of water and tentatively sediment present in crude oils by means of the centrifuge procedure. This centrifuge method for determining water and sediment in crude oils is not totally reliable. As, the amount of water detected is mostly lower than the actual water content. When a highly accurate value is required, the revised procedures for water by distillation which is clearly described by ASTM D4006 above is to be used [65].

2.5. Crude Oil Impurities

Crude oil comes from the earth, which makes it contains variety of substances like gases, water, dissolved and insoluble minerals, etc. Pretreatment of the crude oil is important if the crude oil is to be transported, processed without causing fouling and corrosion in unit operations from distillation, catalytic reforming and secondary conversion processes and for the purpose of this study, used effectively[66].

Crude oils have been used effectively as fuel in E-class gas turbines for power generation applications for a good number of years. Using crude oil as a fuel introduces additional complexity when compared with other refined liquid fuels, especially when considering using these oils in other classes of gas turbines. Crude oils naturally contains impurities that affect its utility as fuel in gas turbines, they can be classified into two types; Oleophobic and Oleophilic impurities, and they are explained as follow[67, 68];

- Oleophobic impurities: are mostly inorganic substances that include chloride salt of Sodium , Calcium, Magnesium and Potassium, sediments such as sand, mud, iron oxide, iron sulphide etc. and water which are either finely dispersed and/or soluble emulsified.
- Oleophilic impurities: are soluble and largely organic impurities such as sulphur compounds, organometallic compounds which are Vanadium (V), Nickel (Ni), Iron (Fe) and Arsenic (As), etc., nitrogen compounds and organic acids (naphthenic acids, phenols and mercaptan).

2.5.1. Effects of Impurities

The Oleophilic and Oleophobic impurities in crude oil affects the operability of the conventional gas turbines when it is used as fuel in different ways, some attack the materials of construction directly, and some are activated upon combustion or change of state. The impurities and their effects are explained as follows:

Salts and oxides of Sodium and Potassium: The alkali metal impurities in the fuel react with the sulphur present in the fuel in the combustion chamber resulting in accelerated deposit formation of sodium and potassium sulphates, these condense on the surfaces of the turbine and hot gas path. The alkali sulphates on the turbine are molten and react with the metal, causing the hot corrosion which is also referred to as sulphidation at temperatures between 700°C - 900°C. Oxides of sodium and potassium reacts with sulphur and vanadium oxides which are combustion products to form molten ash deposits which are corrosive to the material of construction of the turbine nozzle and rotor blades by one or more mechanisms [67-70].

Sediments and water: The presence of this contaminant in crude oil encourages the formation of corrosive elements, bacterial growth which consequently leads to fuel degradation and may cause filter clogging. Water which can exist in free, emulsified or dissolve state also increases the level

of water-soluble contaminants such as alkali metals, this leads to poor turbine operation (fuel system and engine damage) and increased maintenance[69, 70].

Organometallic Complex: These are compounds formed mainly by trace metals such as Vanadium, Nickel and Iron which are porphyrin-forming agent in asphaltene molecules. Vanadium reacts with oxygen during combustion to form at least four oxides VO, V_2O_3, V_2O_4 (VO_2) and V_2O_5. Whereas the first three can be considered as refractory oxides (melting points in excess of 1500^oC), and the last with melting point of about 670^oC for V_2O_5. Therefore, vanadium pentoxide is a liquid at gas turbine operating temperatures. This vanadium compound react with water and alkali contaminants to induce vanadium hot corrosion and vanadium-sodium hot corrosion in the gas turbine hot gas path [71].

Nitrogen: It is sometimes found in lighter fractions of crude oil as basic compounds and in heavier fractions of crude oil as non-basic compounds. Nitrogen oxides are formed during combustion process. The decomposition of nitrogen compounds may lead to the formation of ammonia and cyanides that can cause corrosion because of the high temperature in the gas turbine [72].

Organic contaminants: Such as Tars and Asphaltenes are small solid particles found in crude oil. They combine to form a more homogenous mass affecting the filtration system or collect at the bottom of storage tanks forming a sludge like substance. Crude oils with high levels of carbon residue potentially creates coke deposits on fuel nozzles, which may affect liquid fuel injection[68, 70].

2.5.2. Crude Oil Pretreatment

For crude oil to be a substitute or permanent fuel for powering gas turbines, proper characterization before selection and pretreatment of the crude oil should be carried out prior to use. The characterization should involve investigating the quantitative properties of the impurities listed

above, then the appropriate measure for reducing, eliminating or inhibiting the contaminants should be initiated to ensure the reliable protection of the turbines, accessories and controls. The various methods for treating the crude oil prior to use are stated as follow.

Alkali metals such as Potassium and Sodium in form oxides and salts are generally water soluble and are found in the water phase of the fuel. Separation (centrifuges or electrostatic desalters) and water washing must be used to reduce alkali and other water soluble metals in the crude oil. Crude oil with high density reduces the efficiency of the centrifugal separators. Therefore, heating of the crude oil prior to separation helps in density reduction of the fuel, this is effective because the fuel density changes faster than the water density as temperature increases. However, the presence of volatile components in the crude oil might establish an upper limit for heating.

In order to remove water and sediments from liquid fuels, filtration and centrifugation process are employed. Demulsifiers are added to break up difficult to separate emulsified water. Sediments, which are impurities found in different amounts in liquid fuels frequently depending on transport and storage circumstances. The sediments can either be organic (asphaltene deposits, sludge, etc.) and inorganic (rust, sand, etc.) and may result in plugging and abrasive wear of the fuel system and engine components such as clog fuel pumps, flow dividers, and fuel nozzles.

Vanadium, which is a naturally occurring constituent of crude oil, is soluble in oil. Therefore, it cannot be removed by means of washing and separation. Its corrosive effect is mitigated by the use of chemical inhibitors. The most important element in these additives is magnesium, which reacts with vanadium to form compounds that melt at high temperatures, thus inhibiting the effect of vanadium pentoxide which has a low melting point. An optimum ratio of three parts of magnesium by weight to each part of vanadium will result in the formation of magnesium

orthovanadate ($3MgO \cdot V_2O_5$) that has a higher melting point above 1200°C compared to the 670°C melting point of V_2O_5. This form of treatment inhibits the corrosive characteristics of vanadium by forming high melting-temperature ash composed of magnesium vanadates, magnesium oxide, and magnesium sulphates. The deposition rate in the turbine will increase due to the additive treatment and therefore regular washing of turbine will be essential for application with high ash contents in order to minimize losses in turbine power output and efficiency [73, 74].

2.6. Rheology

2.6.1. Theory

The word rheology is gotten from the Greek word rheo which means "flow" and logia which mean "study of". It means the study of deformation and flow of matter, mainly in a liquid state, but also as semi solids or solids under conditions in which they respond with plastic flow rather than deforming elastically in response to an applied force. The forces applied can be either as compressional, tensional, shearing forces or some combination of the force types. The basic rheological parameter can be expressed by sample confined between two parallel plates. The plates are separated by a distance, h that is small compared to the linear dimensions of the plates. The force, F applied parallel to the top plate of area, A in the x direction while the bottom plate is held stationary is the shear force as shown in Fig. 16. The portion of fluid in contact with the top plate moves at velocity v while the portion of fluid in contact with the bottom plate does not move, this motion relative to the fluid creates a velocity gradient because of the difference in the fluid's velocity throughout the bulk media.

Rheology is used to characterize the flow properties of matter and also its structural features such as the inter-particle interactions when the material is in motion or at rest, this understanding of the inter-particle relationship helps to predict the stability or behaviour of the material with change in

temperature, handling and age. Fluid rheology is studied by the variations in intensive properties, which are: viscosity and elasticity, these intensive properties are affected by stress and strain [75-77].

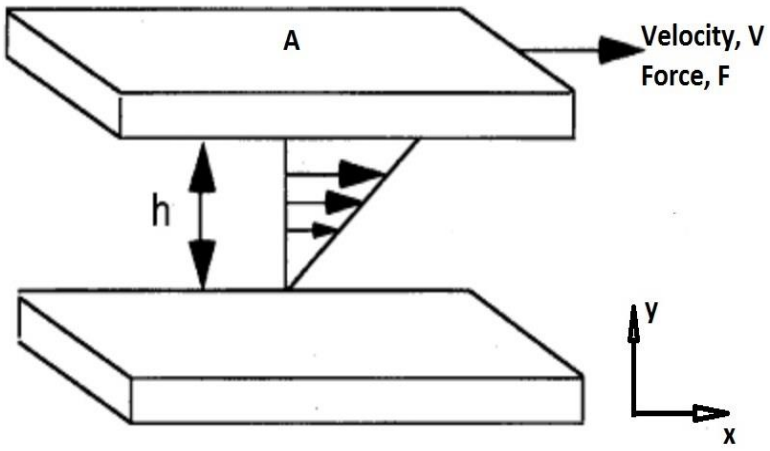

Fig. 16. Liquid deformation under applied shear force [75]

Shear stress, τ is the component of stress that is coplanar to the material cross section. It differs from tensile and compressive stresses, which are initiated by forces perpendicular to the area they act on, shear stress are propagated by forces which are tangential or parallel to the cross section of the material [21]. The can be expressed mathematically as the shear force acting per unit area as shown in Eq.7.

$$\tau = \frac{\text{Force Applied, F}}{\text{Area parallel to force applied, A}} \tag{7}$$

Shear rate, $\dot{\gamma}$ is the speed at which a progressive shearing deformation is applied to material, it can also be defined as the rate of change of velocity at which one layer of fluid passes over an adjacent layer in time, it can be represented mathematically by Eq. 8 [78, 79].

$$\dot{\gamma} = \frac{\text{Fluid Velocity, v}}{\text{Distance between plates, h}} \tag{8}$$

Shear strain, γ is a dimensionless parameter that indicates the force initiating deformation when there is a displacement of any plane relative to a second plane as seen in Fig. 17, this displacement is divided by the perpendicular distance between planes as shown in Eq.9 [80].

$$\gamma = \tan\alpha = \frac{\text{Displacement, } S}{\text{Distance between plates, h}} \tag{9}$$

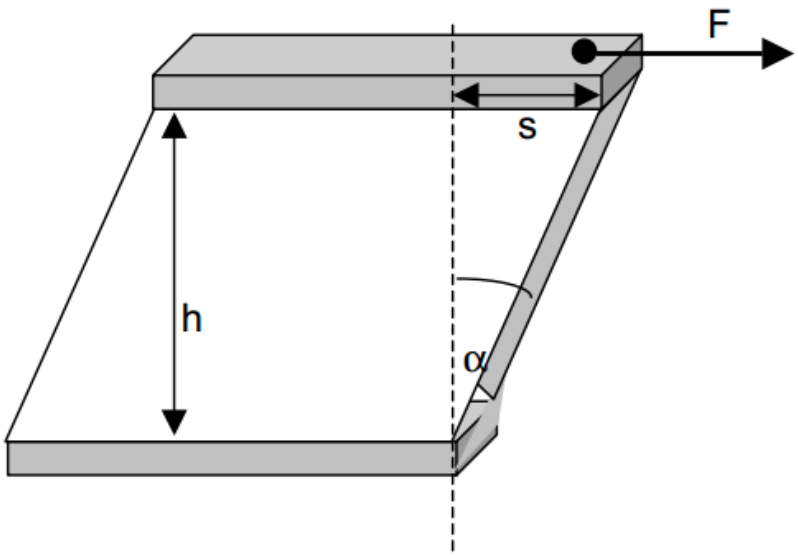

Fig. 17. Shear strain illustration [81]

2.6.2. Rheological Classification of Fluids

Fluids can be classified by their ability to exhibit Newtonian and Non-Newtonian behaviour, this depends on whether they can be described as materials that obey Newton's law of viscosity or not. Newtonian fluids demonstrate constant viscosity is linearly dependent on the velocity gradient and independent of shear rate and the shear stress. This ability enables it to display uniform resistance to flow which is independent of any flow condition[82]. Non-Newtonian fluids can be categorized into two, which can either be time-independent (behavioral plot shown in Fig. 18) or time-dependent (plot shown in Fig. 19), this categories are well explained below.

Time independent Non-Newtonian fluids [83]

- Bingham-plastic: This kind of fluid resists a small shear stress but flow easily under larger shear stresses.
- Pseudoplastic: A large number of non-Newtonian fluids fall into this class. Viscosity decreases with increasing velocity gradient. Pseudoplastic fluids are also called as Shear thinning fluids. At low shear rates, $\dot{\gamma}$ the shear thinning fluid is more viscous than the Newtonian fluid, and at high shear rates it becomes less viscous.
- Dilatant fluids: for this variant of fluids viscosity increases with increasing velocity gradient. Dilatant fluids are also called as shear thickening fluids.

Time dependent Non-Newtonian fluids [83]

- Thixotropic fluids: are fluids in which the dynamic viscosity decreases with the time for which shearing forces are applied.
- Rheopectic fluids: are those fluids in which dynamic viscosity increases with the time for which shearing forces are applied.

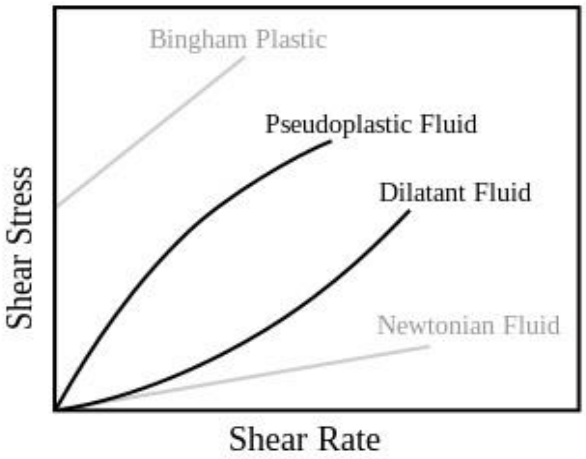

Fig. 18. Shear stress-rate response for time independent Non-Newtonian and Newtonian fluids [84]

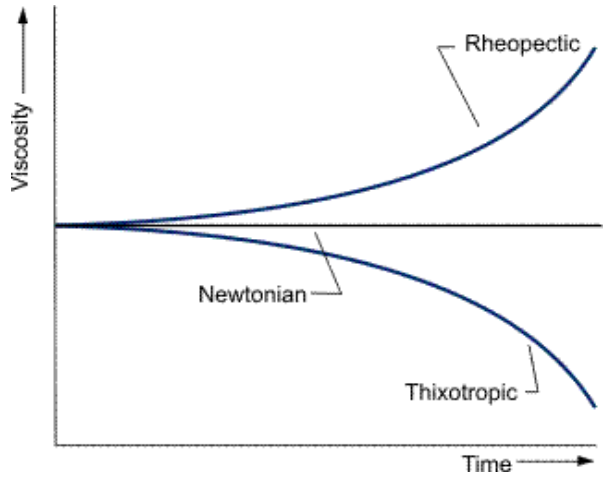

Fig. 19. Viscosity-time response for time dependent Non-Newtonian and Newtonian fluids [85]

There is another category of fluids that does not fall in the Newtonian and Non-Newtonian classification, they are called the Viscoelastic fluids. They are similar to Newtonian fluids but if there is a sudden change in shear they behave like plastic in response which makes them spring back to the initial state when the shear force is released[83, 86].

2.6.3. Rheometry

This is the use of experimental procedures for determining the rheological characteristics of materials. This technique helps in obtaining the qualitative and quantitative connection between the material's deformation and stresses and their derivatives such as viscosity, modulus, compliance, yield shear stress, relaxation times, etc. In rheometry, the material to be tested is placed in the rheometer and subjected to well-defined stress or strain. If the experiment is strain-controlled, the strain or strain rate is set and the stress response gets measured and recorded. In stress-controlled rheometers the stress is well-defined as a constant and the strain rate response is recorded [87]. There are three main types of rheometers: capillary, torque, and rotational, each of them serves a different purpose, they are explained as follow:

Capillary rheometer

This rheometer is one of the oldest rheometer types, it works on the principle of Hagen-Poiseuille equation which expresses the physical law governing the pressure drop, Δp caused by an incompressible and Newtonian fluid in laminar flow through a long cylindrical pipe of constant cross section (radius R, length L) at a constant volumetric flow rate, Q by obtaining its shear viscosity, μ. It is shown mathematically in Eq.10.

$$\mu = \frac{\Delta p\, \pi R^4}{8QL} \tag{10}$$

Capillary rheometers can measure the changes in the material's shear viscosity at different temperatures and pressures, they can also be used for Non-Newtonian fluids [87, 88].

Torque rheometer

There are essentially small extruders or mixers used in the polymer industries. They use a special motor to measure the torque of mixing rotors or screws, this indicates how hard it is to mix the material. Then the machine torque, is then correlated to the viscosity of the material being tested[88].

Rotational rheometer

This type of rheometer works using a motor, torque-sensing mechanism and a means of applying force along the rotor axis. Its operation is based on fixing or controlling one of these parameters such as stress, strain or oscillation and recording the response of the other parameters. Rotational rheometers can be functional under different operating modes, which could either be controlled rate, controlled deformation or controlled stress. There are three different types of stress-sensor geometry/configuration: cone and plate, parallel plate, or concentric cylinder [88, 89].

- *Cone and plate*: In this configuration, the liquid is placed on a horizontal plate and a very shallow cone supported by a torsion bar is placed on the plate is placed over it as illustrated in Fig. 20. The angle between the surface of the cone and the plate is of the order of 1 degree. The plate is rotated and the torsion bar measures the force that the fluid applies to the cone. Because of the constant shear along the complete gap, they are suitable for homogenous fluids [90].

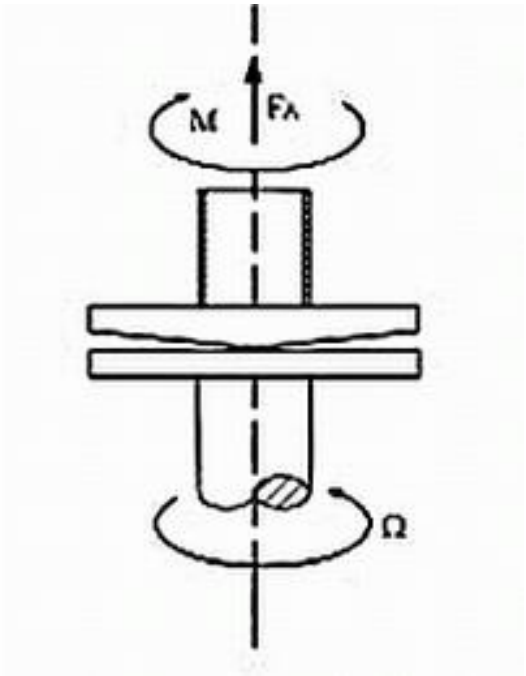

Fig. 20. Cone and plate sensor configuration [89]

- *Parallel plate*: In this kind of sensor system, one plate moves and the other parallel plate is stationary as shown in Fig. 21. Laminar flow of layers occurs when a constant torque is applied to the fluid by upper plate, the rate of strain or angular deflection is measured. The set-back for this method is the variability in the shear rate across the sample. The shear strain at the edges are greater than those at the centre. Therefore, this method suitable for investigating fluids that are independent of shear rate, which are Newtonian fluids.

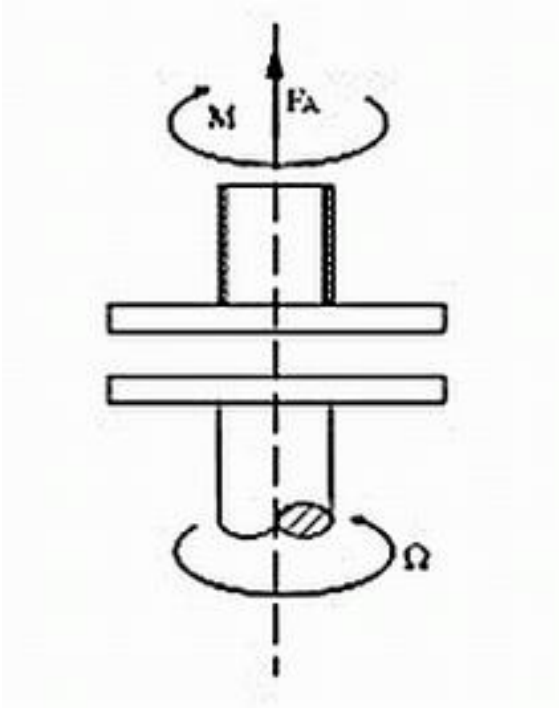

Fig. 21. Parallel plate sensor configuration [89]

- *Concentric cylinder*: As implied by the name, there are two coaxial cylinders, with a known uniform gap between them. This type of configuration can be in two types of assembly, either Double-Gap or Cup-and-Bob. The fluid to be measured is placed in the annulus of one cylinder. One cylinder rotates independently of the other or together in the same or opposite direction. Depending on the choice of rotating cylinder, there are two categories which are:

    1. Searle system: Outer cylinder fixed, inner cylinder rotating.
    2. Couette system: Inner cylinder suspended, outer cylinder rotating.

  This rotation introduces shear forces within the liquid held in the annulus between the coaxial cylinders. These forces are opposed by the viscous forces within the fluid which leads to a shear stress which is measured as torque of one of the coaxial cylinders. Measurement of this torque, along with the knowledge of the speed of rotation, enables the

calculation of the viscosity of the liquid in the gap, a way of calculating is described by the Margules equation (Eq. 11), which is applicable to only Newtonian fluids [91, 92].

$$\mu = \frac{M}{4\pi h\Omega} \cdot \left(\frac{1}{R_b^2} - \frac{1}{R_c^2}\right) \tag{11}$$

Where, μ is the dynamic viscosity; h, the length of the bob in contact with the fluid; M, the torque on the bob or cup; Ω, the angular velocity of the rotating member; R_c, radius of the cup and R_b, the radius of the bob.

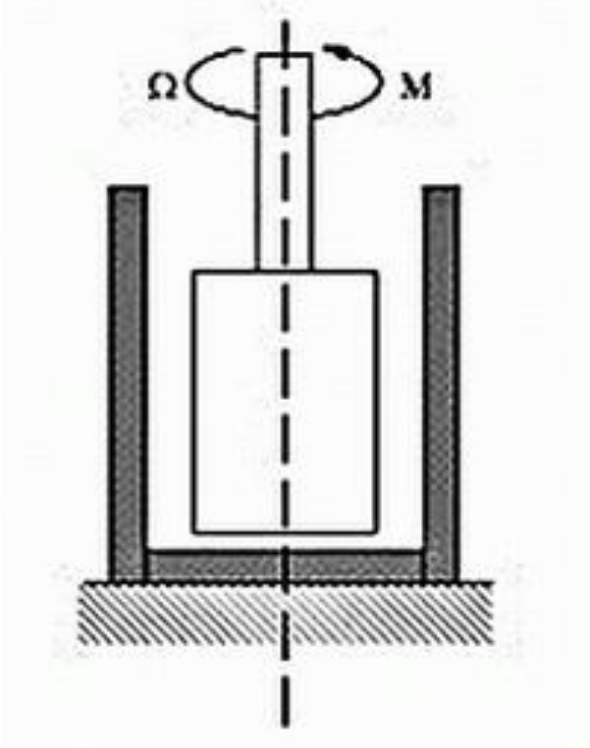

Fig. 22. Typical concentric cylindrical sensor configuration [89]

2.6.4. Rheological Models

These are flow models which are mathematical equation that depicts the rheological data, such as plot of viscosity against shear rate or shear rate against shear stress. From this diagrams, these models can produce suitable and concise behaviour describing the experimental data by solving explicitly the parameters of the rheological model with the appropriate number of equations

simultaneously. If the sample fluids response to applied stress are simplistic in nature, such that it does not contain any colloidal particles, long chain molecules, etc., the model for the fluid is usually well defined by the Newton model, where the applied stress is directly proportional to the rate of deformation of a volumetric element of the fluid. So when the correlation between the rate of deformation and the stress is more complex. These categories of fluids are characterized by other rheological models. Rheological models may be grouped under the categories[93, 94]:

- *Empirical models*: As the name implies, there are models that are deduced from experimental data, such as the Power law model.
- *Theoretical models*: These type of models are derived from essential concepts and it provides valuable guidelines on understanding the role of structure, such as the Krieger–Dougherty model. It specifies the factors that influence a rheological parameter.
- *Structural models*: These kind of models are derived from evaluations of the structure of the sample fluid and kinetics of changes in it. It is sometimes used together with experimental data to estimate values of parameters that characterize its rheological behavior. A typical example of this kind of model is Casson model.

2.6.5. Applications of Rheology

The relevance of rheology is applicable to an ample number of fields such as engineering, physiology, geophysics and pharmaceutics. In geophysics, rheology is used in the study of flow of molten lava, debris flows and solid earth materials which exhibit flow over extended time scales. Earth materials that demonstrate viscous characteristics are known as rheids. In physiology, there is an aspect called haemorheology, which studies the flow properties of blood and its elements. This study help determine the rheological properties limit for proper tissue perfusion with blood. In engineering and related disciplines, polymers are the raw materials of the rubber and plastic

industries and they are of high importance to the textile, petroleum, automobile, paper, and pharmaceutical industries. The knowledge of its viscoelastic properties determine the mechanical behaviour and strength of the products of these industries [95].

2.7. Gas turbine

2.7.1. Theory

The gas turbine is an internal combustion engine that uses air as the working fluid. The engine uses the chemical energy from fuel and transforms it to mechanical energy using the gaseous energy of the working fluid (air) to drive the engine and propeller, which, in turn, propel the airplane or the land based prime movers [96] .

Essentially, a gas turbine is made up of a compressor which draws in and compresses the working fluid (usually air); a combustor to add fuel to heat the compressed air; and a turbine to extract power from the hot air flow. The gas turbine, an internal combustion engine employing a continuous combustion, has the ability to be simultaneously used in the aviation and power generation industry, their configurations are similar for these purposes except for minor changes which is schematically illustrated in Fig. 23. There are different name by which the gas turbine can be called. For example, in the electrical power generation and marine applications it is generally called a gas turbine, combustion turbine, a turboshaft engine or gas turbine engine. For aviation applications it is usually called a jet engine, and various other names depending on the particular engine configuration or application, such as: jet turbine engine; turbojet; turbofan; fanjet; and turboprop or prop jet (when it is driven by a propeller) [97].

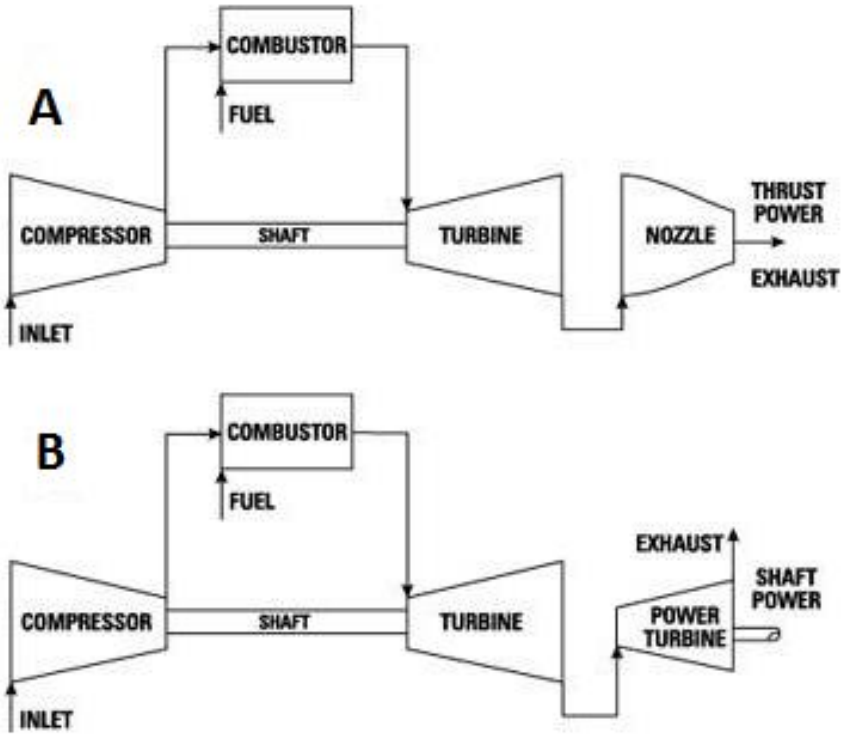

Fig. 23 Schematic for a) an aircraft jet engine; and b) a land-based gas turbine [97]

2.7.2. Fuel flexibility

As the name implies, it is expected that the gas turbine be powered by natural gas alone. However, due to considerations of cost, market flexibility and availability, other forms of energy sources are considered as fuel. These other fuels generally have characteristics and constituents that increase emissions, reduce turbine efficiency and consequently turbine lifespan. For an alternate fuel to be used in a gas turbine, several modifications have to be made to the conventional gas turbine most especially the combustor chamber. Prior to modification of the combustor, it is important to determine the fuel's Lower Wobbe Indices Wo_i which is stated below in Eq.12.

$$Wo_i = LHV_{vol}\sqrt{\frac{\rho_{Air}}{\rho_{Fuel}}} \tag{12}$$

The Wobbe index is a function of the lower heating value (LHV) of the fuel, it indicates that fuels characterized by the same Wobbe number will cause the same pressure loss in the fuel piping system when same amount of heat is released in the combustor. Therefore, the lower the Wobbe index, the larger the cross-section areas of the fuel delivery system and vice versa [98, 99].

There are various non-traditional fuels for gas turbines that capitalizes on the universal combustion system, robust design and distinctive proficiencies of the gas turbine to accommodate the use of different kinds of fuel. The non –traditional gas turbine fuel can be classed as follows [100];

- Oils: This categories includes refineries residuals and crude oil. In order to use these fuels, they are heated to reduce its viscosity to accepted level that will ease gas turbine combustion.
- Syngas and Synfuels: This class comprises of carbon fuels such as coal, lignite, tar sand, shale oil and heavy refinery bottoms. These class of fuels poses high environmental pollution. So, it is recommended that its exhaust should be subjected to carbon capture in a carbon constrained economy.
- Bio-liquid fuels: These are carbon neutral fuels. There are several kinds of biofuel and biofuel feed stock. This class of fuel ensures additional carbon is not introduced into the existing environment unlike fossil fuels which exposes carbon-based fuels that have been sequestered for millions of years.
- Process by-product fuels: combustible by-product from petrochemical plants can be used independently or mixed with natural gas to fuel gas turbines. This is an efficient utilization of supposed waste product to generate electricity.

2.7.3. Lower Heating Value of Fuel

The LHV (lower heating value) of a fuel is the amount of heat released by combusting a specified quantity of fuel initially at 25°C and returning the temperature of the combustion products to 150°C, the value obtained from this calculation assumes the latent heat of vaporization of water in the reaction products is not recovered. This parameter is obtainable empirically using the bomb calorimeter. However, relationship between the LHV and the elemental composition of fuels can be predicted using the Boie and Verbandsformel model [101] .

$$LHV\left(\frac{kJ}{kg_{fuel}}\right) = 35160C + 94438H - 11090O + 6280N + 10465S \quad (Boie) \tag{13}$$

$$LHV\left(\frac{kJ}{kg_{fuel}}\right) = 33900C + 121400\left(H - \frac{O}{8}\right) + 10500S - 2440W \quad (Verbandsformel) \tag{14}$$

Where, H, C, N, O,S and W denotes the mass fractions of Hydrogen, Carbon, Nitrogen, Oxygen, Sulphur and water respectively in the fuel. The difference between these two models is that the Boie model assumes that the oxygen content of the fuel is free while Verbandsformel treats all the oxygen content as being bonded with the hydrogen to form water and the remaining hydrogen is available for combustion [102].

CHAPTER 3

Methodology

3.1. Materials

The liquid fuels used in this study which consist of three different Crude oil and a fuel oil was provided by Abu Dhabi National Oil Company (ADNOC) from different oilfields located in Abu Dhabi, United Arab Emirates (UAE). The sources of the crude oil samples was identified and tagged with letters A, B and C, while the fuel oil is not tagged with letters. The experimental work involves the characterization of the liquid fuels via evaluating of density, pour point, Asphaltene percentage content, moisture content, pH value and rheological properties. The rheological characterization addressed the liquid fuels' behaviour such as steady flow, thixotropy and yield shear stress measurement.

3.2. Experimental Set-up

3.2.1. Density Measurement

The density of the liquid fuels was measured using the Anton Paar Density Meter DMA 5000M and DMA HP (shown in Fig. 24) in accordance with the ISO 12185:1996 standard [103]. The density meter DMA 5000M unit consists of a U-shaped oscillating tube and a system for electronic

excitation, frequency counting and LCD display. It has the capacity of measuring densities of sample between the temperatures of 20 – 90^{o}C at atmospheric pressure which was done at an increment of 10^{o}C. This equipment was calibrated with the ultra-pure water at 20^{o}C with density of 0.99820 gcm^{-3} to ensure the precision of the equipment. The temperature was controlled to ± 0.01°C during the measurement using a built in Peltier instrument. By measuring the damping of the U-tube's oscillations caused by the dynamic viscosity of the filled-in sample, the instrument automatically corrects the viscosity related errors. The above equipment allows density to be measured with an accuracy of ±0.000005 gcm^{-3}.

The liquid fuel was injected into the density meter with a syringe till there was no bubble observed on the display screen. This was done in triplicates for each sample at a particular temperature of measurement to ensure reproducibility of result and precision of the density meter. Upon completion of measuring of density of a specific liquid fuel, the U-tube cell is flushed with toluene to dissolve and cleanse the previously filled crude oil. This is followed by the injection of acetone to dry up the remnant fluid in the tube before another sample is introduced into the density meter DMA 5000M for measurement.

The Anton Paar DMA HP is the density measuring equipment for determining density at high temperature and Pressure with temperature ranges between -10 ^{o}C and 200 ^{o}C and pressure ranges between 0 and 700 bar. The introduction of sample in this equipment is rather different from Density meter DMA 5000M, the sample has to be preheated using the heating block peripheral, so as to reduce the viscosity before introducing into the equipment. The density of the liquid fuels was measured by the density meter DMA HP at a temperature between 100 – 200^{o}C at an increment of 10^{o}C and atmospheric pressure, this equipment was calibrated with the n-Hexadecane (which boils at 250^{o}C) to ensure the precision of the equipment.

Fig. 24. Density meter

3.2.2. Pour Point Measurement

Pour point of a petroleum specimen is the lowest temperature under defined conditions where sample fluid shows no flow characteristics. Measurement of this property was done in accordance with the American Standard for Testing and Material, ASTM D 97- 04 [104]. The Scavini petroleum testing apparatus for measuring Pour Point and Cloud Point illustrated in Fig. 25, was utilized in accomplishing the pour point temperature of the liquid fuels, this apparatus has

Fig. 25. Pour point measuring apparatus

four baths with target temperature of 0, -18, -33 and -51^{o}C. The sample was poured in the test jar to the marked level, lowered into the jacket. When the specimen has not ceased to flow when its temperature has reached 27°C, the test jar is transferred to the next lower temperature bath in accordance with the standard's schedule. The pour point was observed by checking if the liquid will flow when tilted horizontally for 5 seconds at every 3 ^{o}C drop in temperature. Once no motion is observed when the jar is tilted horizontally for 5 seconds, the temperature of observation was recorded. For standard reporting of the pour point as recommended by ASTM D97-04, 3^{o}C is added to the observation temperature[104].

3.2.3. Asphaltene Content Measurement

Determination of the mass percent of asphaltenes in liquid fuel can be defined by their insolubility in n-Heptane, this experiment was carried out in accordance with the ASTM D3279-12 standard[105]. The liquid fuels were heated to reduce the viscosity, then 3 grams of the sample was measured and transferred into the Erlenmeyer flask as described by the experimental set-up in Fig. 26, the mass of the Sample (designated 'B'). N-Heptane 99% grade is added in ratio of 100mL to 1g as stipulated by the standard, which means 300 mL of N-heptane is added to the sample, and the mixture is heated and stirred under a reflux condenser for 30 min. After that, the sample is left for 60 min to cool down to ambient temperature. A gooch crucible having a filter paper (Whatman Glass-Microfibre - 47mm diameter with 1.5 µm particle retention) is heated at 110 ^{o}C for 30 min, after which it is placed in the desiccator for (30 min) and final weight is recorded (designated as 'A').

The sample is then filtered using the filtering crucible with the filter pad in the suction flask under gentle vacuum, the supernatant liquid is filtered first followed by the insolubles. The precipitates was washed with three portions of n-Heptane of 10mL each. The crucible, filter pad and precipitate was placed in the 110^{o}C oven for a period of 30 minutes, after which it was removed and allowed to cool in a desiccator, then weighed to the nearest 0.1mg, this mass was designated 'C'. The mass percent of asphaltenes existing in the liquid fuels is calculated as percentage weight in the original sample by the formula in Eq. (5).

Fig. 26. Liquid fuel-solvent reflux heating set-up

3.2.4. Moisture Content Measurement

Moisture content of the liquid fuels was measured using the Mitsubishi Chemical Analytech moisture meter KF-21 equipped with a BNC detection electrode described in Fig. 27. This meter carries out volumetric titration following the principle of Karl Fischer reaction based on the ASTM D4377-11 standard [59]. The solvent used during the analysis was a mixture of Methanol, 2-(Methylamino) pyridine and sulphur dioxide. Upon the supply of the dehydrated solvent into the titration flask, the sample to be analyzed is injected and dissolved in the solvent, and the moisture is extracted, the moisture volume is determined by the titration with Karl Fischer reagent which

contains Iodine, Sulphur dioxide and base (2-methylamino-pyridine). The water reacts with iodine and sulphur dioxide in base and alcohol.

$$H_2O + I_2 + SO_2 + CH_3OH + 3RN \rightarrow 2RN \cdot HI + RN \cdot HSO_4CH_3 \qquad (15)$$

Fig. 27. Potentiometric Karl-Fischer moisture meter

As implied by Eq. (15), the stoichiometric ratio of H_2O to I_2, which is 1:1. Therefore, moisture milligram in 1ml of Karl Fischer reagent (factor) is preliminary determined with water or standard water solution, the moisture content (mg) is calculated from the titration content (ml) of Karl Fischer reagent required. The moisture content, M_c is evaluated using the formula in Eq. (16).

$$M_c(\text{mg}) = \text{Titration volume of Karl Fischer(ml)} \times \text{Factor } (\frac{\text{mg}H_2O}{\text{ml}}) \qquad (16)$$

In order to evaluate the percentage moisture content in the liquid fuels, the mass of the sample introduced into the equipment must be determined injection as shown in Eqs. (17).

$$\text{Moisture content}, \% = \frac{\text{M}_c(\text{mg})}{\text{Mass of sample analyzed(mg)}} \times 100 \qquad (17)$$

3.2.5. pH Measurement

The degree of acidity and alkalinity of the liquid fuel was measured using the Thermo-scientific Orion Dual Star pH Meter, illustrated in Fig. 28. This equipment was calibrated using the US buffer set 4.01, 7.00 and 10.01 prior to use to ascertain the precision of its functionality. The pH electrode and Automatic Temperature Controller (ATC) probe was rinsed with distilled water, then dried with lint-free tissue and inserted into the sample for measurement. Prior to measurement the samples were homogenized by stirring using the magnetic stirrer.

Fig. 28. pH meter

3.2.6. Rheological Properties

The rheological properties investigated are the viscosity, steady flow behaviour, yield shear stress and thixotropic properties at different temperatures ranging from 20^{o}C to 200^{o}C with an increment of 10^{o}C for viscosity measurement and 20^{o}C increment for other measurements. These test was performed using Thermo-Scientific Haake RheoStress 6000 Rheometer shown in Fig. 29. A

temperature controller and heat exchanger works with the RheoStress equipment to regulate the temperature applied to the rheometer set-up. The rheometer operates using several test modes such as the controlled stress (CS) and controlled rate (CR) mode. The drive shaft of the RheoStress 6000 is centered by an air bearing to ensure an almost frictionless transmission of the applied stress to the test fluid. The rheometer measuring geometry is a hollow cylinder rotor and a double gap coaxial cylinder.

Fig. 29. Thermo-Scientific rheometer

The computer controlled rheometer was switched between both CS and CR modes, where CS ode e specifically applied in yield shear stress measurement because of its ability to apply very low inertia and gradually ramp-up the stress applied to samples in order to detect the point at which yield occurs. The CR mode was used for other measurements such as steady flow behaviour and thixotropy, since the parameters to be determined are not based on early detection of very low

values [80, 106]. 3 ml of the sample is measured by a syringe and injected into the annulus clearance in the beaker (cup), which is a double gap coaxial cylinder shown in Fig. 30. Before the commencement of measurement the Rheometer is set to the measuring temperature and allowed sufficient long heating period so that the inner part of the beaker which is not temperature controlled equilibrates to the set-temperature, this was done for 360 seconds. The Haake data manager software was used to control the test routines and data evaluation.

Fig. 30. Double gap concentric cylindrical cup and rotating spindle

3.3. Gas turbine modelling

The concept of modelling the gas turbine to be fuelled by liquid fuel was carried out by using the advanced power plant library of the IPSEpro^{TM} process simulator software. This software was designed to model a wide range of thermal systems. This makes it possible to design and analyze any power plants such as combined-cycle plants, cogeneration plants and conventional plants. Operating parameters of units in this software can be fixed or estimated. Whenever it is estimated,

upon convergence an appropriate value that thermodynamically agrees with the functionality of the specific unit will be obtained.

In order for the liquid fuel to be modelled using the aforementioned software, it must be specified using its major elemental components which are: Carbon, Nitrogen, Hydrogen, Oxygen and Sulphur. Also, the inlet air for combustion must be specified. A simple gas turbine was modelled to determine the effect of variation in the elemental component of the liquid fuel while the operation conditions of the units and the flow characteristics of the fuel and air source were kept constant (shown in Table 1 and

Table 2). The gas turbine configuration comprises of the; air compressor, liquid fuel combustor, turbine and generator unit as illustrated in Fig. 31.

Table 1. Gas turbine unit operation specification

Unit	Unit Specification	
Generator	Electrical Efficiency	98%
	Mechanical Efficiency	97%
Turbine	Isentropic Efficiency	91%
	Mechanical Efficiency	98%
Compressor	Pressure Ratio	13
	Mechanical Efficiency	98%
	Isentropic Efficiency	87%

Table 2. Inlet fuel and air flow parameters

Stream	Flow Parameters	
Fuel Source	Mass Flow Rate	1kg/s
	Temperature	15^{o}C
Air source	Nitrogen (kg/kg)	0.76
	Oxygen (kg/kg)	0.24
	Temperature	26.7^{o}C

Pressure	1.013 bar
Humidity	61.30%
Altitude	13m

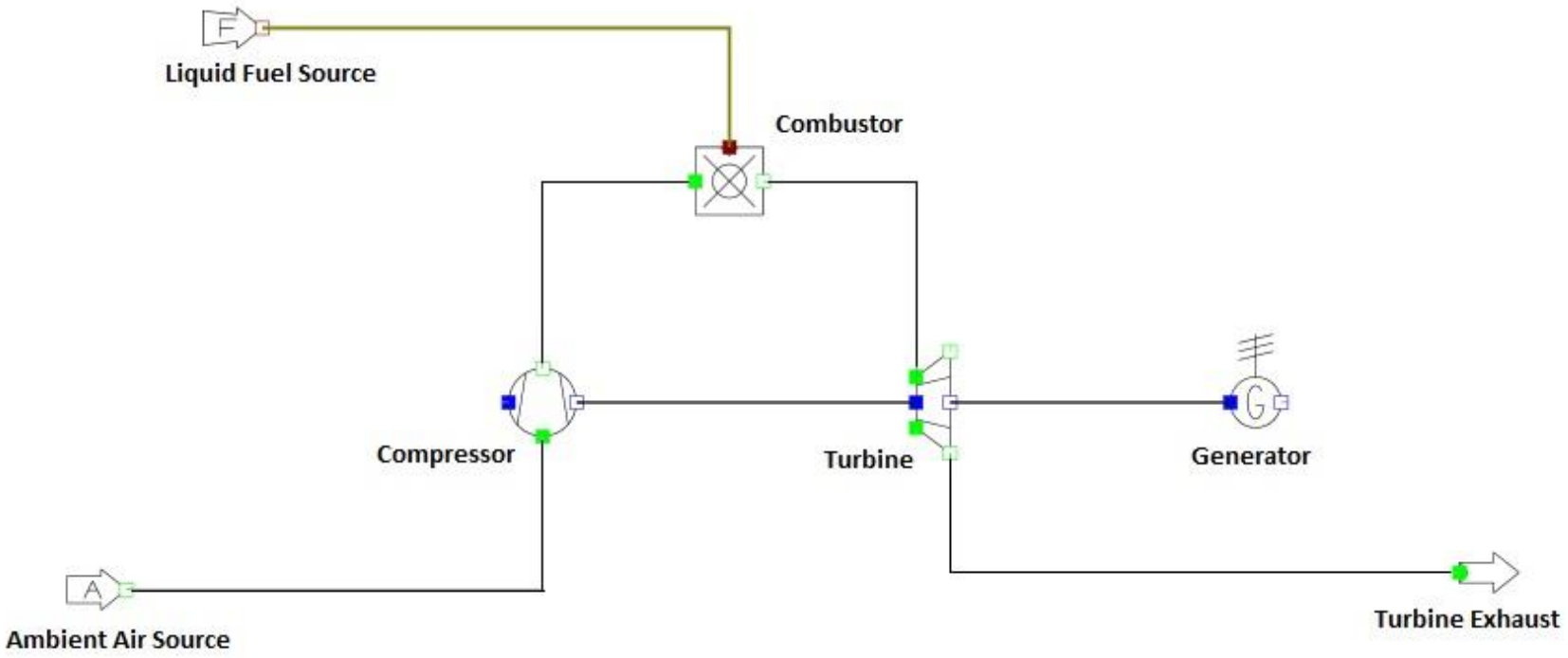

Fig. 31 Process flow diagram of a simple liquid fuel powered gas turbine model

CHAPTER 4

Results and Discussions

4.1. Temperature effect on the density of the liquid fuels.

The density of three crude oil and fuel was investigated oil at different temperatures, with the objective of determining the sensitivity of the liquid fuels' density with respect to temperature change. Table 3 reports the variation of the density of the liquid fuels as the temperature increases.

As the temperature of measurement increases the volatile components vaporize and evacuates from the liquid fuel, the less volatile components left behind after heating have their chemical structure or bonds of the heavy components broken, therefore reducing the agglomeration of higher molecular weight fractions of the liquid fuels such as resins, asphaltenes and waxes. These factors account for the reduction of the density as temperature[107]. However, the fashion of reduction is different for each sample. The data obtained from the density measurement is shown in Fig. 32, the correlation that best fits the relationship between the temperatures, T is in ^{o}C and densities, ρ in gcm^{-3} of Crude oil A, B, C and fuel oil are respectively shown in Eqs. 18-26 and goodness of fit (R^2-value) shown in Fig. 32

$$\rho_{crude\ A} = -0.0007T + 0.8373 \quad (20 \leq T \leq 90^{\circ}C) \tag{18}$$
$$= -0.0002T + 0.7890 \quad (100 \leq T \leq 150^{\circ}C) \tag{19}$$
$$= -0.0004T + 0.8093 \quad (160 \leq T \leq 200^{\circ}C) \tag{20}$$

$$\rho_{crude\ B} = -0.0007T + 0.8328 \quad (20 \leq T \leq 90^{\circ}C) \tag{21}$$
$$= -0.0003T + 0.7957 \quad (100 \leq T \leq 200^{\circ}C) \tag{22}$$

$$\rho_{crude\ C} = -0.0007T + 0.8429 \quad (20 \leq T \leq 90^{\circ}C) \tag{23}$$
$$= -0.0005T + 0.8230 \quad (100 \leq T \leq 150^{\circ}C) \tag{24}$$
$$= -0.0003T + 0.7835 \quad (160 \leq T \leq 200^{\circ}C) \tag{25}$$

$$\rho_{fuel\ oil} = -0.0006T + 0.957 \quad (20 \leq T \leq 200^{\circ}C) \tag{26}$$

Since density indicates the heaviness or lightness of a matter, it is observed from the values in Table 3, that the Fuel oil is heavier than all crude oils. This is so because the fuel oil which are sometimes residual oil from distillation process or a mixture of residual and distillate fuel oil contains mostly heavy and long chain hydrocarbons which falls in the range of C_{20} to C_{50} and above. Other attributes that contribute to its comparatively higher density are the tendencies of fuel oil to have higher Conradson carbon residue and asphaltene content [13, 108].

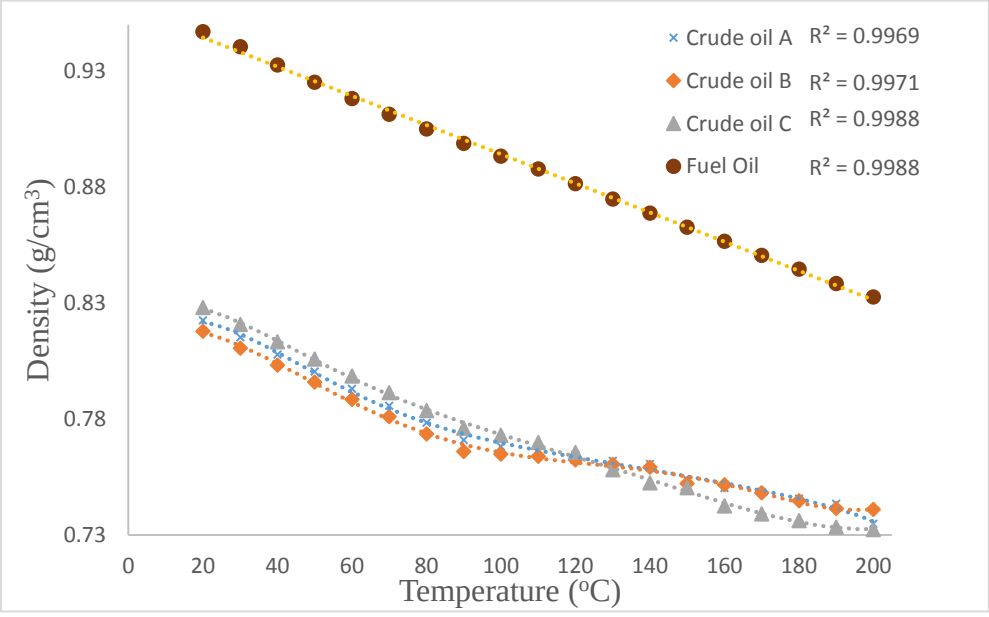

Fig. 32. Density measurements of the liquid fuels at different temperatures.

Table 3 Data of the density of the liquid fuels at different temperatures

	Density (g/cm^3)			
Temperature (°C)	Crude A	Crude B	Crude C	Fuel oil
20	0.82249	0.81781	0.82799	0.94702
30	0.81528	0.81058	0.82069	0.94047
40	0.80783	0.80322	0.81329	0.93265
50	0.80045	0.79585	0.80589	0.92515
60	0.79305	0.78852	0.79847	0.91814
70	0.78565	0.78102	0.79135	0.91143
80	0.77840	0.77350	0.78358	0.90510
90	0.77094	0.76597	0.77608	0.89881
100	0.76817	0.76489	0.77292	0.89333
110	0.76671	0.76393	0.76977	0.88785
120	0.76458	0.76237	0.76548	0.88148
130	0.76195	0.76041	0.75809	0.87487
140	0.76057	0.75915	0.75240	0.86873
150	0.75387	0.75216	0.75039	0.86273
160	0.75018	0.75154	0.74254	0.85656
170	0.74857	0.74819	0.73900	0.85053
180	0.74569	0.74466	0.73612	0.84464
190	0.74351	0.74145	0.73340	0.83840
200	0.73473	0.74095	0.73233	0.83258

Crude oil and fuel oils naturally contain traces of metal contaminants, treatment of this fuel is recommended prior to combustion in gas turbines. This should be done to minimize or inhibit the deleterious effect that can be contributed by these constituents such as pollution and compromise of equipment integrity. Density of the fuel affects the treatment phase because it is more difficult to treat fuels when its density is close to that of water [109]. The density values obtained at lower temperatures suggests that treatment should be carried out by heating to reduce the density. The fashion of density reduction are seen in Table 3.

4.2. Pour point determination

As temperature reduces, wax crystals in the liquid fuel precipitate and interact with each other to form large structures of flocculated wax crystal. This large structure of flocculated wax crystals do not only impede flow but also set up elastic deformation to an extent when subjected to shear stress, this makes the liquid fuels semi-solid at low temperature[110]. Also, pour point measurement shows the aromaticity or paraffinity of crude oil and its fractions, so a lower pour point indicates that the paraffin content is low[111]. For paraffinic crude oils, pour points are usually between −12°C and −15°C, which are determined by the activity of the dewaxing unit while the pour points of naphthenic crude oils, which can have very low wax content, may be much lower, ranging from −30 °C to −50 °C [112].

Table 4 reports the measured pour point of the samples. It is observed that the fuel oil has a higher pour point than the Crude oils indicating high paraffin or wax content, the range of the crude oil's pour point is between -27 and -21^{o}C. This implies that the liquid fuels can be categorized as intermediates or naphthenic crude oil with their paraffinic tendencies increasing as pour point temperature reduces.

Table 4 Pour point of the liquid fuels

Sample	Pour point (^{o}C)
Crude oil A	-27
Crude oil B	-21
Crude oil C	-24
Fuel Oil	12

The significantly high pour point of the fuel oil indicates it is a paraffin-based oil. Therefore, there is need for high temperature storage, heat tracing of pipe lines, suction heaters with higher capacity to create and maintain the operating temperature if this fuel should be used in a gas turbine [109].

4.3. Determination of mass percentage asphaltene content

In order to evaluate the asphaltene percentage content of the liquid fuels, the ASTM D3279-12 standard was followed, where the normal-heptane insoluble precipitate is defined as the asphaltene content of the liquid fuels. Table 5 reports the values of the n-heptane insoluble asphaltene in percentage mass. It is observed that the fuel oil has a relatively higher asphaltene content compared to the crude oil, this accounts for its high viscosity at room temperature compared to the crude oils while the crude oil with lesser viscosity exhibits lower asphaltene content.

The noticeable high content of asphaltenes in the fuel oil is due to the fact that fuel oils are mostly residual fuels -dirty fractions- obtained from the atmospheric distillation column, which contains heavy constituents such as heteroatoms (Oxygen, Sulphur and Nitrogen) and organometallic compound (Nickel and Vanadium) in high proportion [113, 114]. The higher the quantity of asphaltene in liquid fuels, the difficult it is to ignite. High content of this impurity makes the fuel burn slowly and consequently contributing to deposit formation in the combustion chamber and exhaust system of the gas turbine [115].

Table 5 Asphaltenes content (%NHI) in Liquid Fuels

Sample	Asphaltene Content (% NHI)
Crude oil A	0.1938
Crude oil B	0.2934
Crude oil C	0.2714
Fuel Oil	2.8213

4.4. Determination of moisture content and pH values

The accurate measurement of moisture content in crude oil, which is a crucial quality determining parameter constitutes an important role in the extraction, processing and utility of crude oil and its derivatives. The measurement of the water content in the liquid fuel was carried out, based on the

volumetric titration proposed by the Karl Fischer reaction, which is reported in Table 6. It can be observed that Crude oil B has higher percentage water content by weight and the fuel oil having the lowest water content, this implies that the more the water content, the lesser the liquid fuels' quality based on water content. The widely accepted water content in crude oil should be below 0.5% by weight to prevent accumulation or corrosion during transportation[116], this criteria was met by all the liquid fuels.

The pH value signifies the hydrogen ion concentration of a solution, in this case liquid fuels. Solutions with a high concentration of hydrogen ions have a low pH and solutions with a low concentrations of H^+ ions have a high pH. The presence of water in the samples makes it possible to measure the apparent pH values which is reported in Table 7. It is observed that the liquid fuels are acidic in varying degrees. It can be proposed that this characteristic can be attributed to the variation in the rock formation from which these sample were extracted and the dissolved substances in samples.

Table 6 Mosture content of the liquid fuels,

Sample	Moisture Content (%)
Crude oil A	0.104
Crude oil B	0.126
Crude oil C	0.100
Fuel Oil	0.057

Table 7 pH values of the liquid fuels

Sample	pH values
Crude oil A	2.720
Crude oil B	4.373
Crude oil C	3.167
Fuel Oil	6.046

4.5. Rheological measurements

The rheological properties of the liquid fuels is of high importance in evaluating the flow behaviour of liquid samples. Temperature effect on viscosity, thixotropy and yield shear stress measurement was investigated in this study.

4.5.1. Effect of temperature on dynamic viscosity

The viscosity properties of fluids provide important information about the deformation and flowability properties. In this study, this property was measured using the Haake RheoStress 6000 rotational rheometer. The RheoStress 6000 allows the application of shear force to the specimen being analyzed. The viscosity of the sample was analyzed using the Controlled Rate (CR) mode of the RheoStress 6000 by the applying shear rate of 239.9s^{-1} for a period of 120 seconds under natural logarithm distribution of the analyzed data. Fig. 33 and Fig. 35 displays the trend by which viscosity changes with increasing temperature. Since, the dynamic viscosity decreases exponentially with increasing temperature, it can be described using Arrhenius relationship in Eqs. 27 or 28.

$$\mu = Ae^{Ev/RT} \tag{27}$$

Or

$$\ln \mu = \ln A + \frac{E_v}{RT} \tag{28}$$

Ev , is the energy barrier that must be overcome before flow can occur. The activation energy of the flow, Ev, can be pictured as the energy required to create a hole in the liquid, large enough for a molecule to switch places with a neighboring molecule[117]. At elevated temperature, molecules require less energy as observed in Fig. 36 and Fig. 37 to create holes in the liquid, allowing them

to move, this consequently reduces viscosity at higher temperature. The activation energy, E_v/R for Crude oil A, B, C and fuel oil is 1246.1, 1201.3, 1309.5 and 4809.8 mPa.s.K respectively.

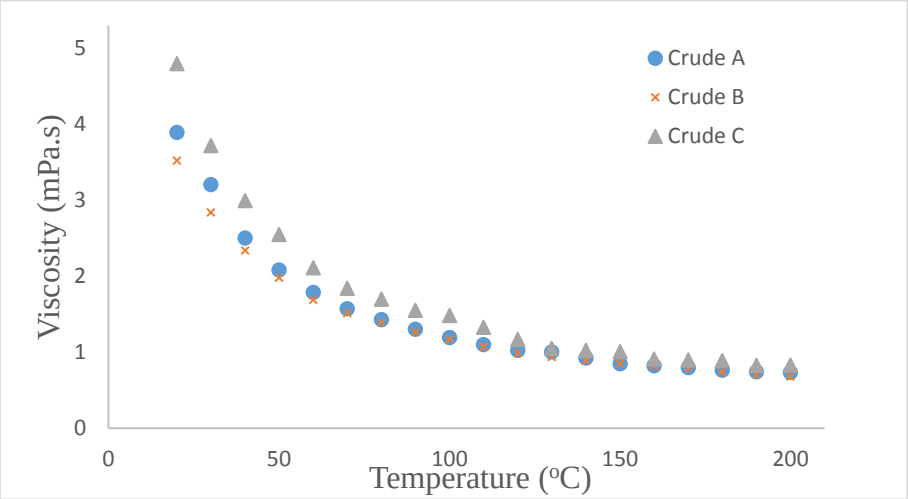

Fig. 33 Plot of viscosity against temperature for the crude oils

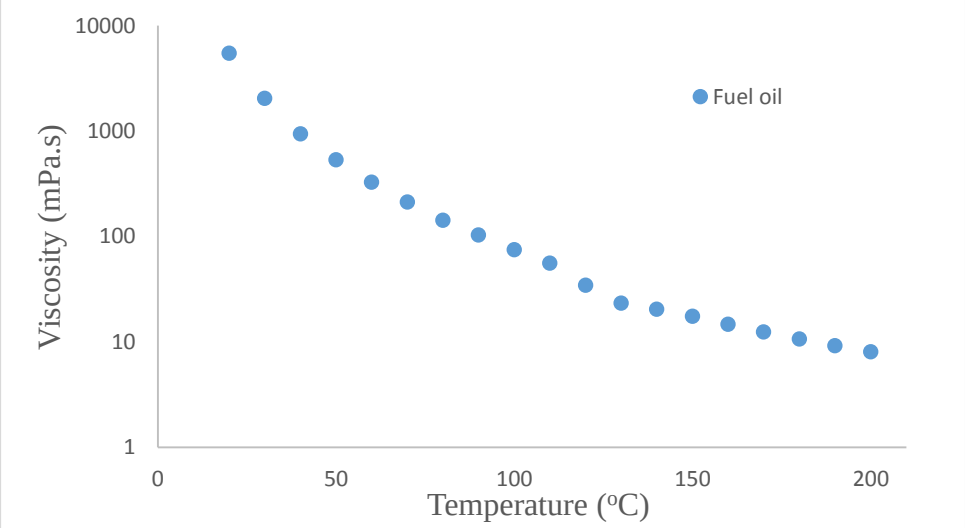

Fig. 34 Plot of viscosity against temperature for the fuel oil

Viscosity has a high effect on the atomization process of liquid fuel in the gas turbine combustion chamber. This negatively affects the ignition characteristics of the fuel, if it is very viscous. Lower viscosity spells the need for lower fuel/air ratio and high mass flow rate through the atomizer for efficient utilization of liquid fuel. For a more efficient method of improving low-temperature ignition, it is important to heat the fuel prior to atomization or use a lower viscosity fuel [118].

Reducing the viscosity of liquid fuels increases its flowability properties, one of the ways this can be done is by applying heat. Temperature increase weakens the bonds of heavy components such as wax and asphaltenes, which consequently reduces the viscosity of the fuels[119] . The flow behaviour curve as observed in Fig. 38-Fig. 41 that the viscosity-shear stress curve, shows that flow properties is well affected by the change in temperature. In order to determine the extent of viscosity reduction as shown in

Table 8, [106] the degree of viscosity reduction (DVR) was evaluated using Eq. (29):

$$\mathrm{DVR}\% = \frac{(\mu_c - \mu_r)}{\mu_r} \times 100 \qquad (29)$$

Where μ_r, is the reference viscosity in Pa at 239.9s^{-1} shear rate at 20^{o}C and μ_c in Pa, is the corresponding viscosity at 239.9s^{-1} shear rate and corresponding temperature.

Table 8 reports the DVR% over temperature rate 20 to 200^{o}C at an increment of 10^{o}C. This data in

Table 8 indicates that the heavier and more paraffinic fuel oil can attain a higher DVR% of 99.853%, which is a high viscosity reduction percentage compared to the crude oils.

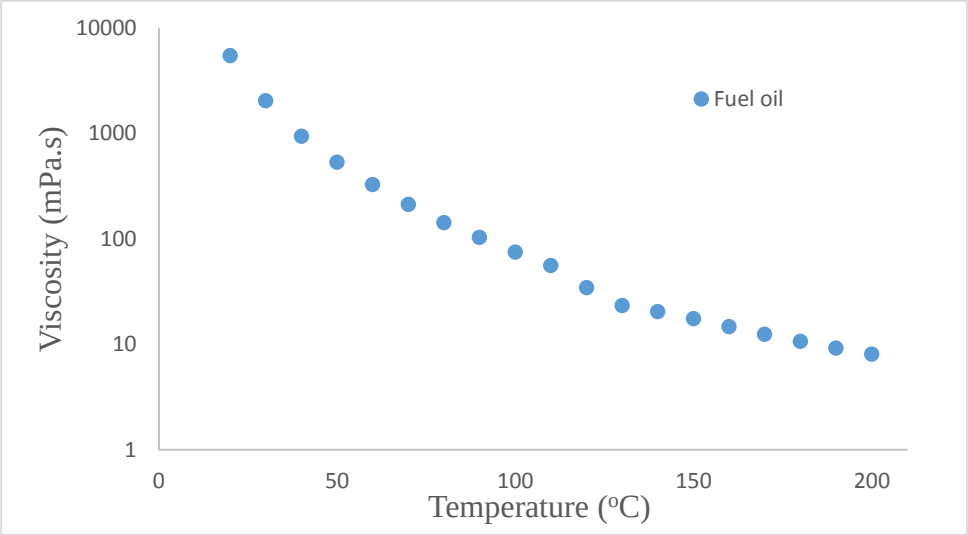

Fig. 35 Plot of viscosity against temperature for the fuel oil

Table 8 DVR% of liquid fuels versus temperature

	DVR (%)			
Temperature (°C)	Crude oil A	Crude oil B	Crude oil C	Fuel Oil
20	0	0	0	0
30	17.722	19.326	22.512	62.697
40	35.795	33.636	37.581	82.853
50	46.509	43.744	46.851	90.238
60	54.150	52.063	56.003	94.022
70	59.704	57.023	61.635	96.117
80	63.289	60.477	64.627	97.404
90	66.550	64.149	67.738	98.109
100	69.399	66.733	69.065	98.631
110	71.744	69.610	72.314	98.980
120	73.695	72.023	75.661	99.371
130	74.215	73.462	78.147	99.574
140	76.258	74.888	78.650	99.626
150	78.258	75.765	79.047	99.679
160	78.853	76.795	81.050	99.731
170	79.595	77.495	81.266	99.773

180	80.413	79.095	81.478	99.805
190	80.989	79.851	82.766	99.832
200	81.151	80.762	82.691	99.853

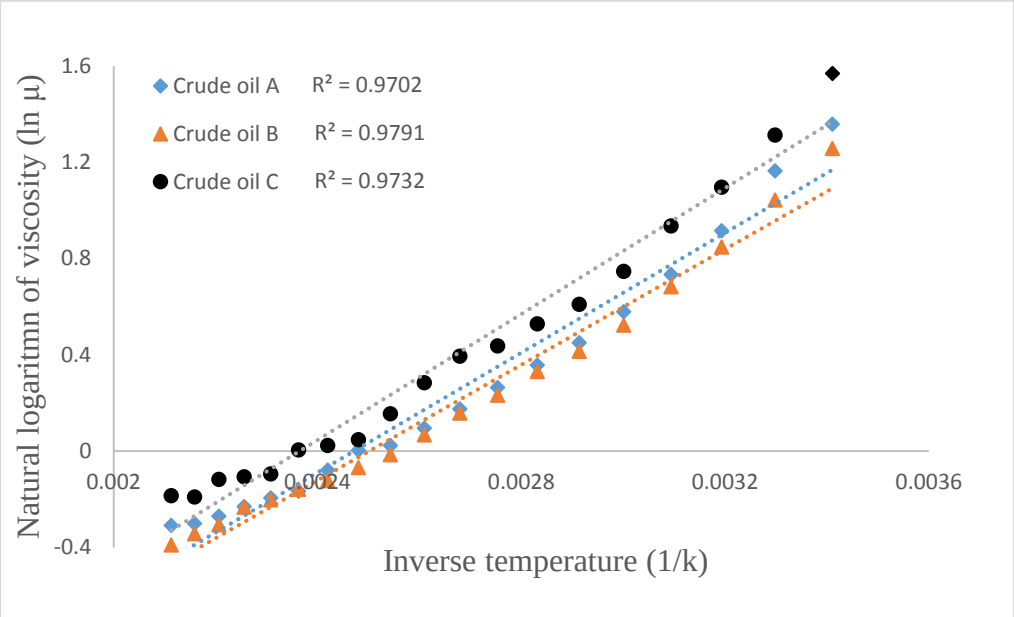

Fig. 36 Effect of temperature on the viscosity of the crude oils

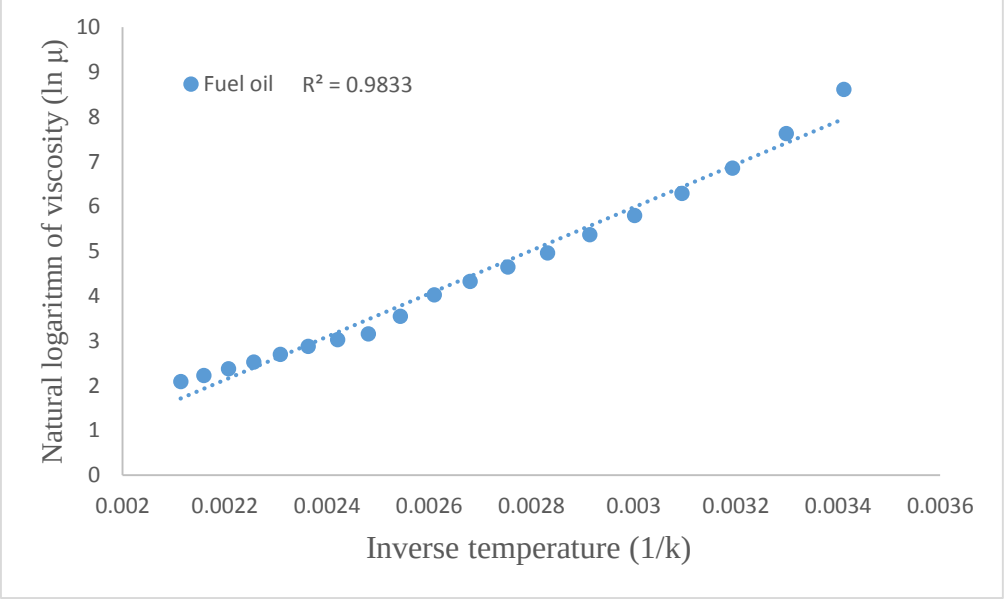

Fig. 37 Effect of temperature on the viscosity of the fuel oil

4.5.2. Steady flow behaviour

The time-independent flow behaviour of the liquid fuels was investigated as a function of the relationship between viscosity and shear rate using the Controlled rate (CR) mode of the RheoStress 6000 Rheometer by the stepwise application of shear rate from $0.1s^{-1}$ to $1000s^{-1}$ for a period of 120 seconds under natural logarithm distribution of the analyzed data. Prior to commencement of each measurement, all samples were at rest at their measuring temperature for 360 seconds after loading, in order to allow induced stress to be absorbed and temperature equilibrated through the liquid fuels.

Steady flow behaviour measurements were carried out at temperature range 20 – 200^{o}C with an increment of 20^{o}C. These experiments were carried out in triplicates for each sample, the average value of the results obtained from the experiments is plotted in. It is observed in Fig. 38-Fig. 40 that the crude exhibits quasi-Newtonian behaviour at lower temperatures and gradually becomes Newtonian as temperature increases. As for the fuel oil behaviour in Fig. 41, it is observed that it exhibits non-Newtonian shear-thinning behaviour at lower temperature regimes, at temperatures above 40^{o}C it shows almost Newtonian characteristics. This clearly demonstrates that at low shear rates, viscosity differences are greater than when shear rates are high. Temperature increase will not allow the higher molecular weight fractions of the crude oil, such as waxes, resins and asphaltenes to cluster and form aggregates. This eventually affects the interaction bonds between the particles and consequently reduces oil viscosity. This effect can also be observed in Fig. 33 and Fig. 35 which shows a significant reduction in viscosity over the experiment temperatures. This effect can be credited to the high impact of temperature on chemical structure and viscosity of crude oils and fuel oil components such as asphaltene and wax[119].

Steady flow of the liquid fuel samples into the combustor chamber of the gas turbine are assured as temperature increases. It is observed in Fig. 38 - Fig. 41 that the rate of change of viscosity with increasing shear rate is constant as temperature rises. This characteristic will ensure proper atomization of all the liquid fuels analyzed as it is injected in the combustor.

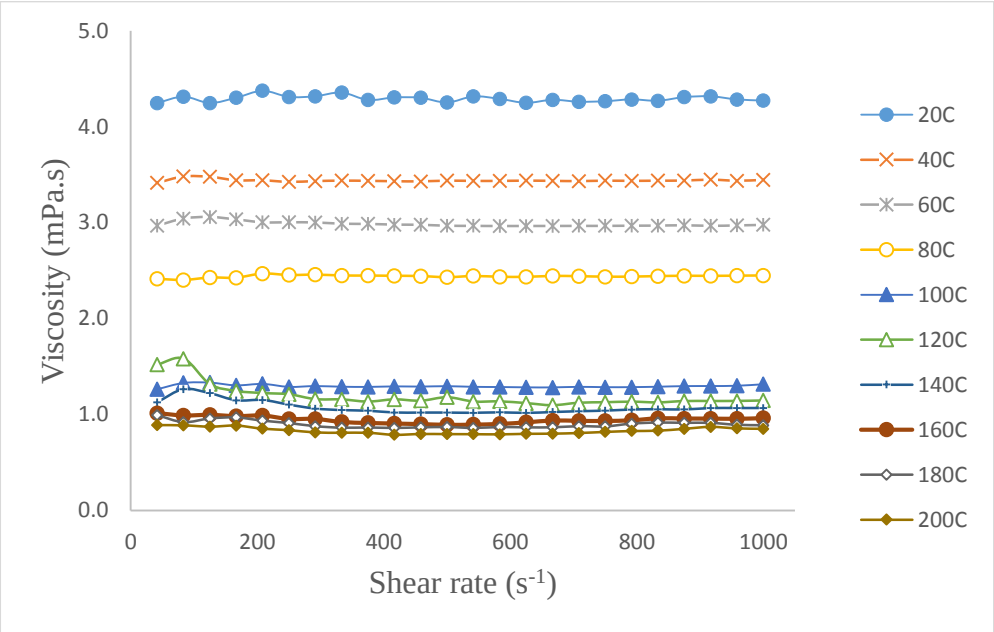

Fig. 38 Effect of temperature on viscosity of crude oil A

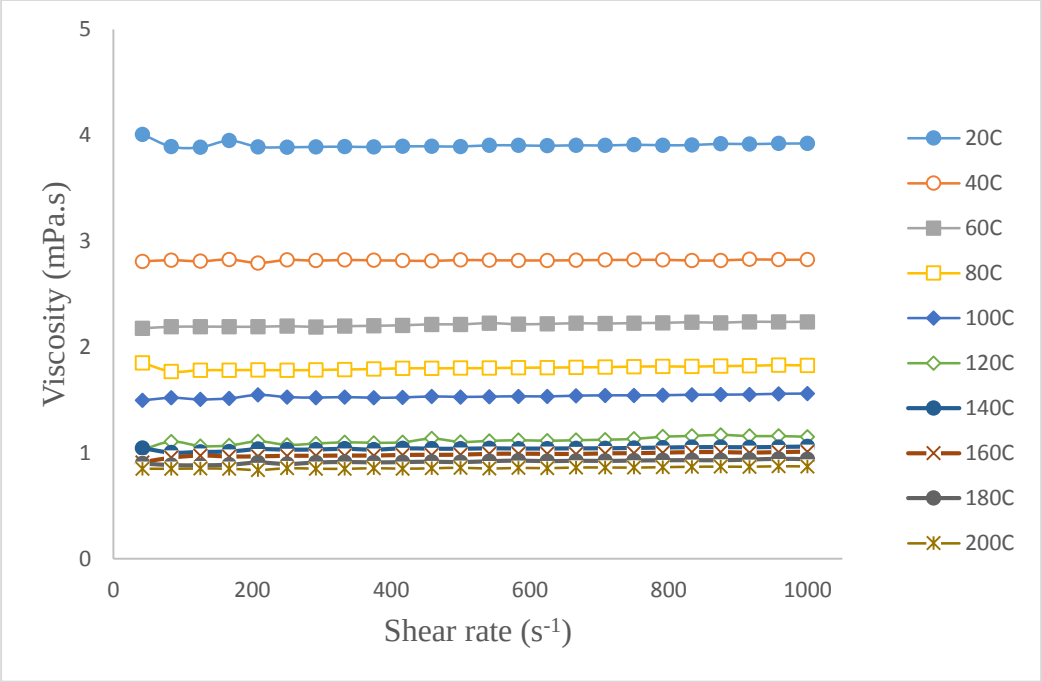

Fig. 39 Effect of temperature on viscosity of crude oil B

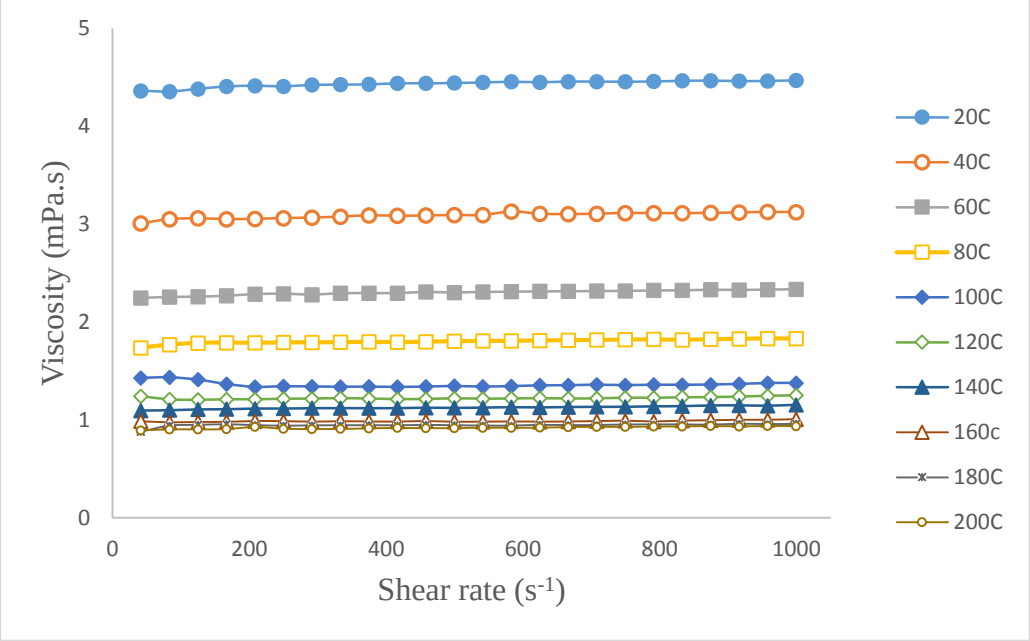

Fig. 40 Effect of temperature on viscosity of crude oil C

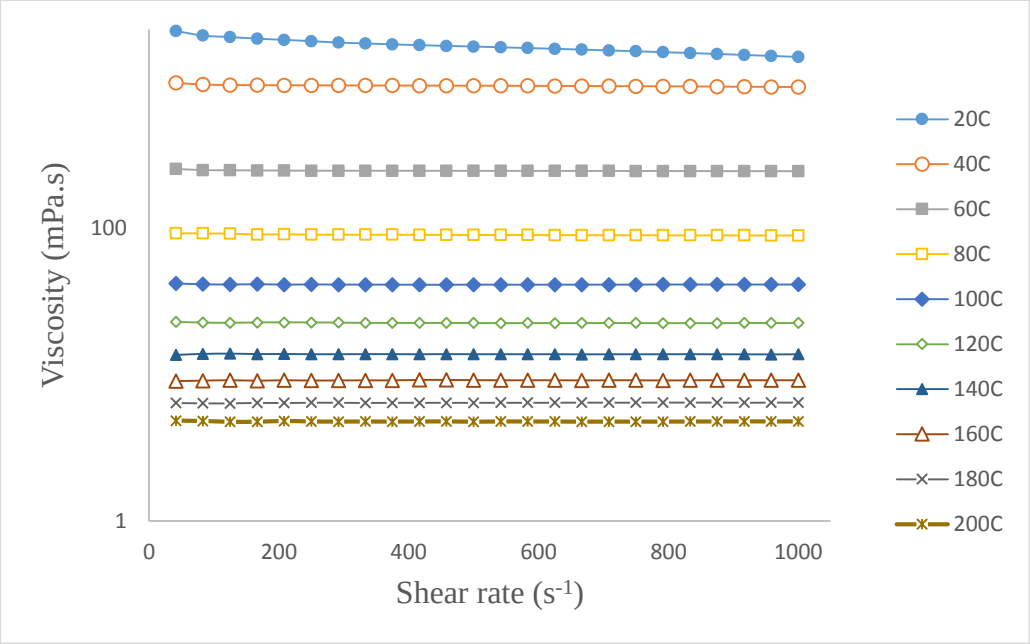

Fig. 41 Effect of temperature on viscosity of Fuel oil

4.5.3. Thixotropy behaviour

All liquids with microstructure composition have the ability or tendency to exhibit thixotropy, because thixotropy only indicates the finite time taken to move from any one state of microstructure to another and back again, whether from different states of flow or to and from rest. In order to determine the thixotropy properties of the fuel oil, the thixotropic material is placed into the rheometer and constant shear rate is applied, the measured shear stress will increase with time, but it will eventually steady out to a constant value. Switching off the shear and allowing the material to rest for a long time, and switching the shear on again, the measured shear stress will be initially higher, but it will then again decrease and end up at the same value as that which was seen after the original long-term shearing[120].

Measurement of the thixotropy behaviour of the fuel oils was carried out using the RheoStress 6000 under the Controlled Rate mode. Shear rate was increased gradually from 1 to 800s^{-1} so as to obtain the up-curve rheogram, a plot of shear stress against the shear rate. In order to obtain the

down-curve part of the rheogram, steady reduction of shear rate from 800 to 1 s^{-1} was assigned, it took 120 seconds for each part of the rheogram.

The three crude oil exhibited non-thixotropic properties, because the up-curve rheogram follows the same pattern as the down-curve rheogram as shown by their response at 40^{o}C in Fig. 42, while the fuel oil displayed a thixotropic response as the down-curve rheogram and up-curve rheogram pattern are different as illustrated by the response of fuel oil at 40^{o}C in Fig. 43. The deviation of the down-curve from the up-curve rheogram was higher at low temperature regimes and this reduced as temperatures increases as quantified by the hysteresis area. This hysteresis area values shown in Table 9 is the area that is within the bounded region and it is approximated using the Simpson's 1/3 rule of approximating integrals illustrated in Eq.30:

$$I = \int_{a}^{b} f(x)dx \tag{30}$$

Where, $f(x)$ is the integrand, a is the lower limit of integration and b is the upper limit of integration.

Table 9 Hysteresis area at different temperatures for Fuel oil

Temperature (°C)	Area (Pa/s)
40	29170
60	625.1
80	286.6
100	57.85
120	26.03
140	-0.4067
160	-0.6646
180	-3.419
200	-5.617

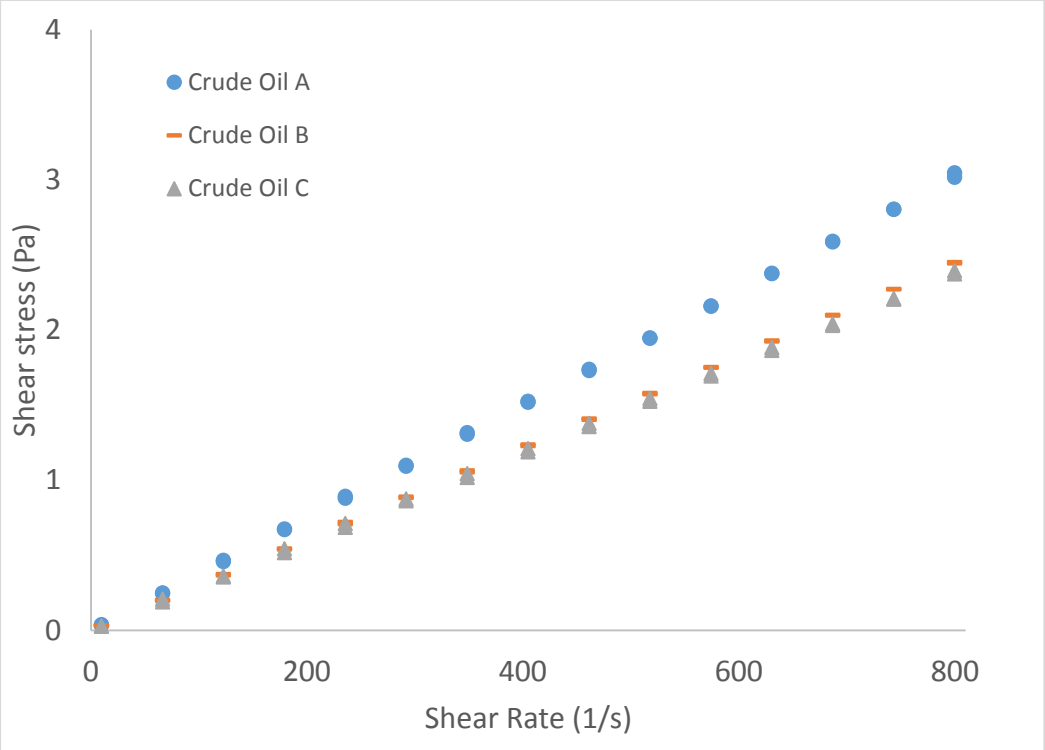

Fig. 42. Thixotropic behaviour of Crude oils at 40°C

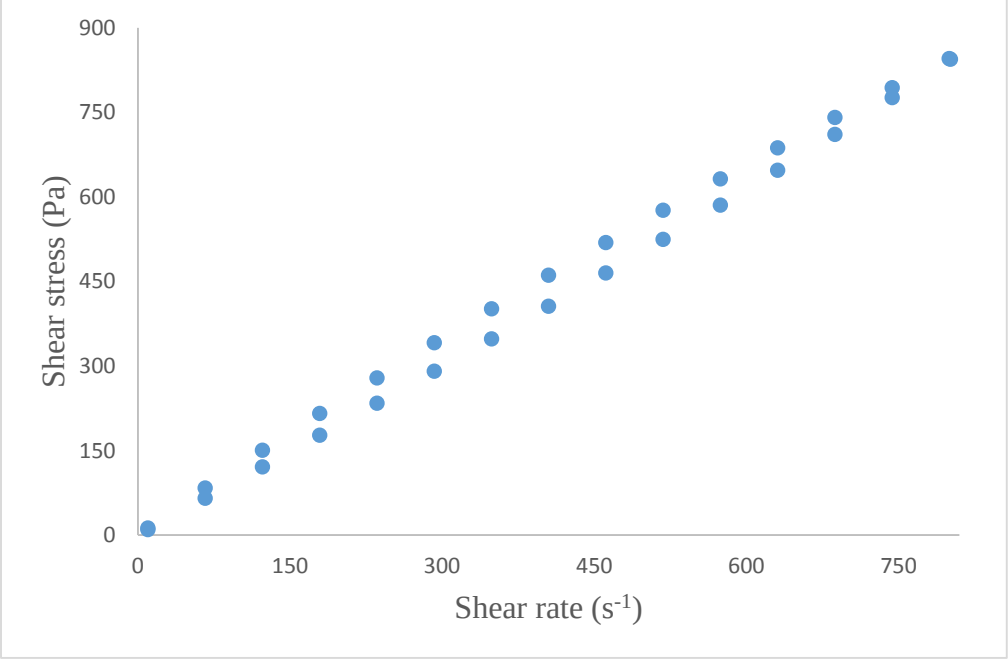

Fig. 43 Thixotropic behaviour of Fuel oil at 40°C

4.5.4. Yield shear stress Measurement

Yield shear stress is the unique parameter of any substance that expresses the stress level above which the stress applied will lead to continuous and unlimited deformation which makes the substance to flow. The substance will deform with finite rigidity under conditions below the stress level. This threshold that dictate the flowing tendencies of substances is called apparent yield shear stress, τ_o [121, 122].

The measurements of the yield shear stress for the liquid fuel samples was executed at various temperatures using Haake RheoStress 6000 under controlled stress mode. The rheometers under controlled stress mode uses a more direct procedure for measurements of the yield shear stress. The shear stress applied to the sample is gradually increased until the yield shear stress is attained without shear flow. In each test measurements of the yield shear stress, the shear stress applied to the sample was continuously ramped from 0.1 to 4.0 Pa within a period of 120s in order to plot the shear stress–shear rate curve. Modelling analysis was carried out digitally by the rheometer using the Bingham model to determine the apparent yield shear stress for each sample at different temperatures, the results obtained results is tabulated in Table 10, and as temperature increases it is observed that the value of apparent yields stress is reduced.

The rheograms illustrated from Fig. 44 - Fig. 47 indicates the changes in the shear rate as shear stress is ramped-up from 0 to 4Pa. For every 20^{o}C increase in temperature, the rate of shear observed increases as shear stress is ramped up, the increase in temperature reduces the internal friction that inhibits the liquid-like motion of the crude oil samples. With regards to the fuel oil, it exhibited a relatively constant shear rate over the shear stress range at 20-40^{o}C, at this temperature the fuel oil acts like a semi-solid, the fuel oil started displaying linear relationship between shear stress and shear rate at 60^{o}C.

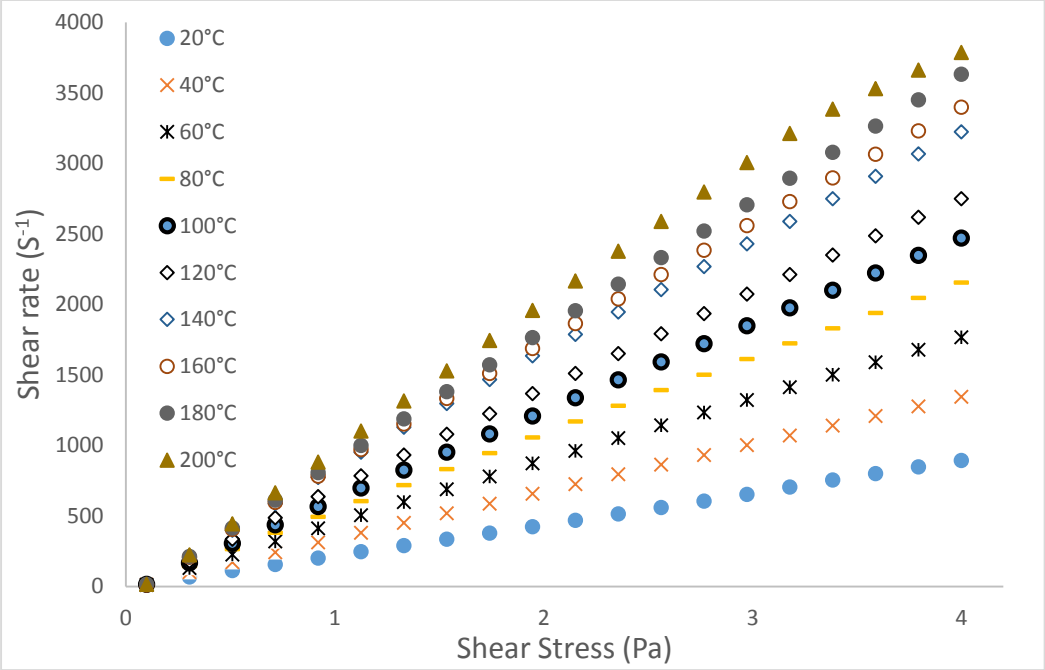

Fig. 44. Rheogram behaviour for Crude oil A

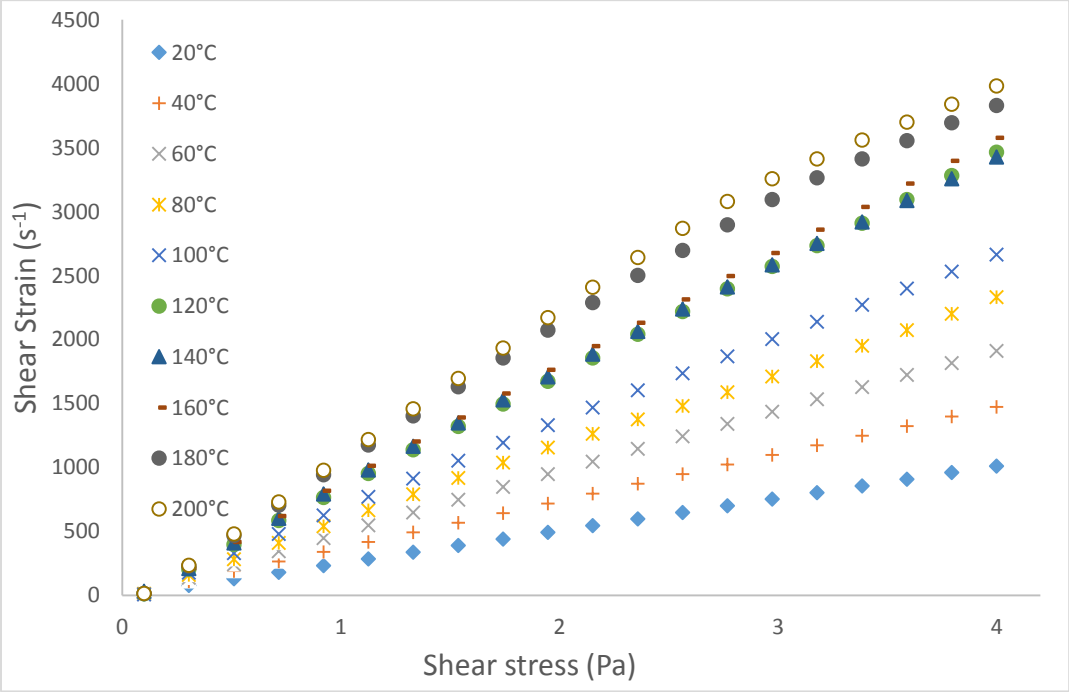

Fig. 45. Rheogram behaviour for Crude oil B

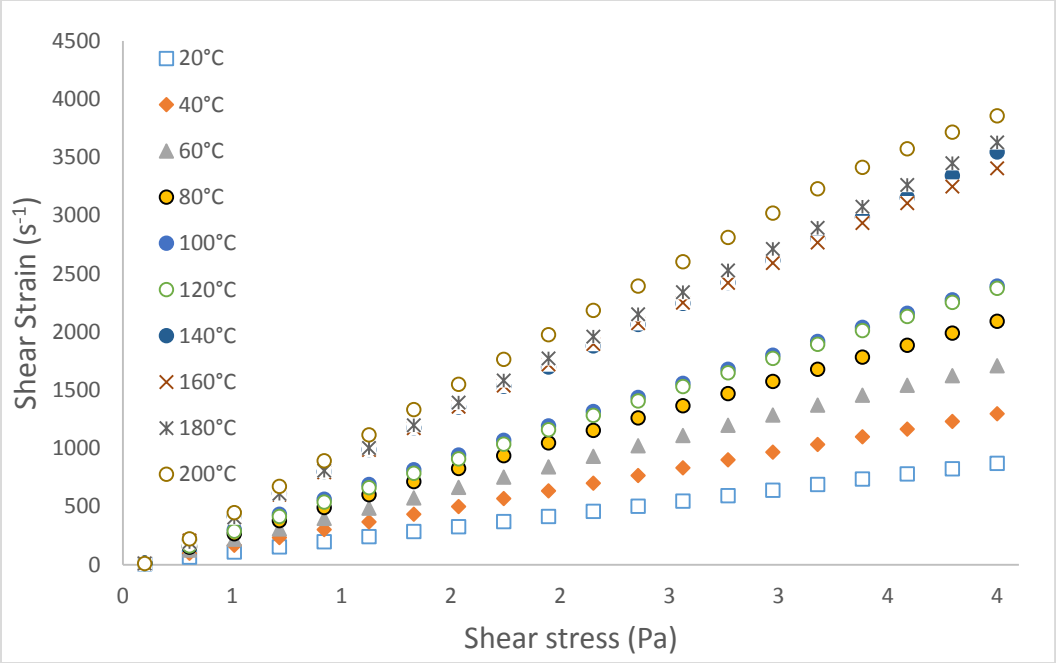

Fig. 46. Rheogram behaviour for Crude oil C

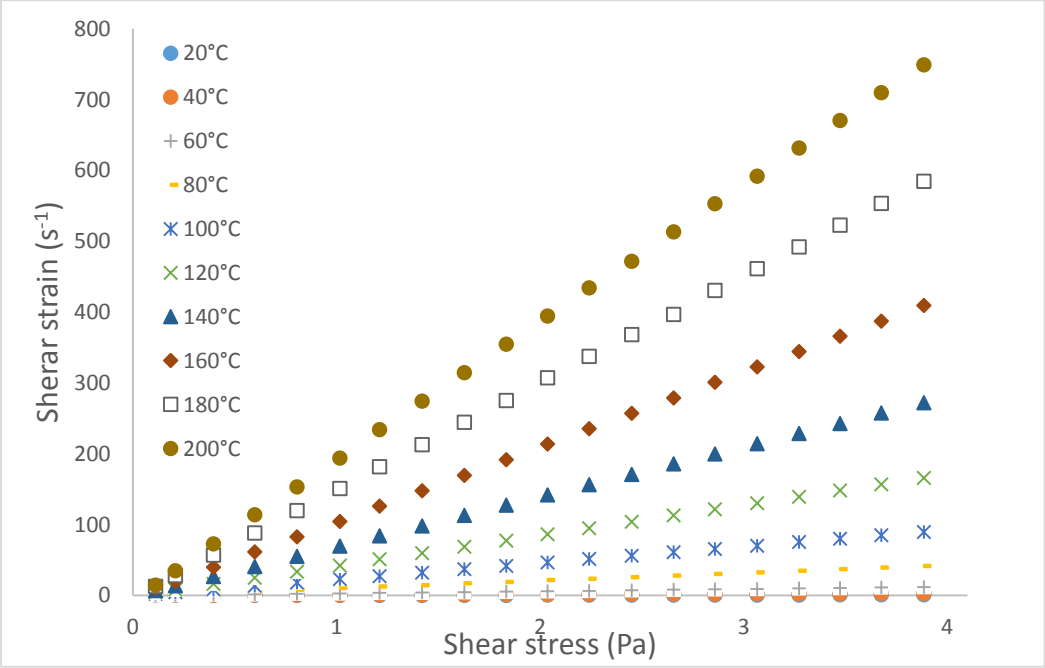

Fig. 47. Rheogram behaviour for Fuel oil

Table 10: Apparent yield shear stress measurement

Temperature (°C)	Yield shear stress (Pa)			
	Crude oil A	Crude oil B	Crude oil C	Fuel Oil
20	1.969	1.995	1.932	2.001
40	1.906	1.937	1.792	1.983
60	1.882	1.880	1.782	1.939
80	1.851	1.875	1.732	1.869
100	1.793	1.830	1.716	1.819
120	1.778	1.826	1.669	1.805
140	1.696	1.818	1.642	1.707
160	1.624	1.816	1.468	1.605
180	1.587	1.803	1.462	1.541
200	1.573	1.802	1.440	1.540

Pumping the liquid fuel samples for combustion into the gas turbine at higher temperature will be a smoother process. Since, the pressure required to initiate continuous flow is lower at higher temperatures as a result of the reduced yield stress level as indicated in Table 10.

4.6. Rheological Model

Flow behaviour of the liquid fuel samples was analyzed over a wide range of shear rates at temperature range of 20 – 200^{o}C with increment of 20^{o}C. The experiment was carried out under the controlled rate (CR) mode, as the shear rate was varied from 0 to 100Pa, the corresponding shear stress was obtained. The results recorded was modelled to ascertain which specific rheological model fits the measurement as the temperature increases. The rheological model investigated are Newton, Herschel-Bulkley, Casson models as described in Eqs. (31) – (33). Where τ is the applied shear stress in Pa and $\dot{\gamma}$ is the corresponding shear rate in s^{-1} in Eqs.(31) – (33), the τ_o in Eqs.(32) and (33) is the apparent yield shear stress in Pa, k and n in Eq. (32) are consistency index; where k is in Pa.s^{n} and η in Eqs. (31) and (33) represents the apparent viscosity in Pa.s. The standard deviation coefficient (R^2) was used for the estimation of relationship that exist

between the calculated and experimental values. The values obtained from the modelling analysis are reported in Table 11 - Table 14.

$$\tau = \eta\dot{\gamma} \tag{31}$$

$$\tau = \tau_o + k\dot{\gamma}^n \tag{32}$$

$$\tau = (\tau_o^n + (\dot{\gamma}\eta)^n)^{1/n} \tag{33}$$

It can be observed in Table 11 that the Newton model characterizes flow behaviour of crude A well over the range of temperature tested. Crude oil B has similar R^2 value at 20 and 40^{o}C for all the model used, at temperatures above 40^{o}C, its flow behaviour is in tandem with Herschel-Bulkley model. Crude oil C has similar R^2 value at 20^{o}C for all the model used, at temperatures above 20^{o}C, its flow behaviour fits more with Herschel-Bulkley model. Regarding the fuel oil, at 20 and 40^{o}C it fits more with Herschel-Bulkley model, at temperatures above 40^{o}C, it exhibited similar R^2 value for all the model used.

Using measurements obtained at 20^{o}C for all the liquid fuels, it is observed that crude oils exhibited quasi-Newtonian behaviour as illustrated in Fig. 48, though according to the agreement between the experimental values and those predicted by the models and the non-Newtonian behaviour of the fuel oil in Fig. 49.

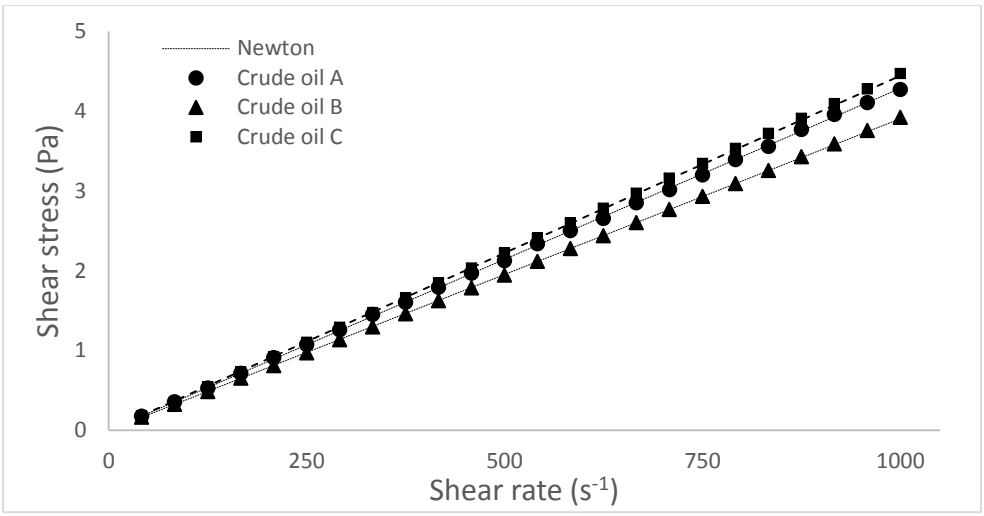

Fig. 48. Model sensitivity analysis for Crude oils at 20ºC

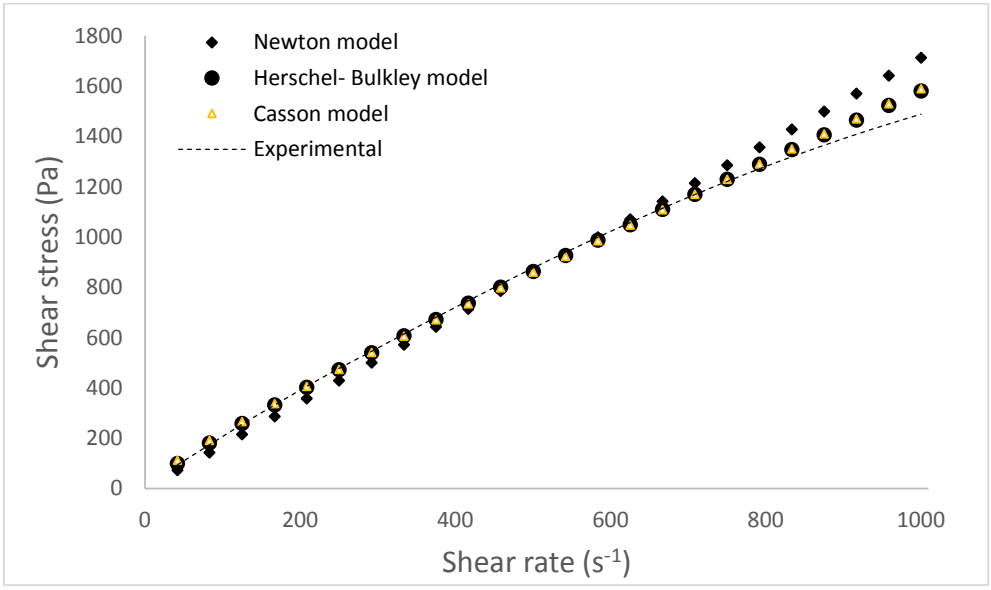

Fig. 49. Model sensitivity analysis for Fuel oil at 20ºC

Table 11: Modelling analysis of Crude oil A at different temperatures

		Crude oil A									
Model		20°C	40 °C	60 °C	80 °C	100 °C	120 °C	140 °C	160 °C	180 °C	200 °C
Newton	η	0.00428	0.00344	0.00297	0.00244	0.00129	0.00114	0.00105	0.00094	0.00088	0.00082
	R^2	1.00000	1.00000	1.00000	1.00000	1.00000	1.00000	1.00000	1.00000	1.00000	1.00000
Herschel-Bulkley	τ_o	0	0	0	0	0	0	0	0	0	0
	k	0.00437	0.00342	0.00315	0.00238	0.00135	0.00180	0.00126	0.00111	0.00106	0.00101
	n	0.99710	1.00090	0.99082	1.00402	0.99314	0.92810	0.97020	0.97322	0.97023	0.96589
	R^2	0.99989	0.99999	0.99998	0.99999	0.99986	0.99888	0.99858	0.99857	0.99851	0.99764
Casson	τ_o	0.07794	0.07796	0.07791	0.07796	0.03697	0.02915	0.02258	0	0	0
	η	0.00417	0.00337	0.00292	0.00245	0.00133	0.00110	0.00104	0.00090	0.00084	0.00076
	n	1.04833	1.06207	1.05719	1.08875	1.06567	1.00899	1.02488	0.97323	0.97429	0.96585
	R^2	0.99994	0.99999	0.99999	0.99999	0.99987	0.99915	0.99884	0.99879	0.99882	0.99798

Table 12: Modelling analysis of Crude oil B at different temperature

`		Crude oil B									
Model		20 °C	40 °C	60 °C	80 °C	100 °C	120 °C	140 °C	160 °C	180 °C	200 °C
Newton	η	0.00390	0.00282	0.00221	0.00180	0.00153	0.00111	0.00104	0.00098	0.00092	0.00086
	R^2	0.99999	1.00000	0.99998	0.99996	0.99994	0.99955	0.99995	0.99991	0.99990	0.99992
Herschel-Bulkley	τ_o	0	0	0	0	0	0	0	0	0	0
	k	0.00385	0.00279	0.00198	0.00165	0.00142	0.00089	0.00096	0.00081	0.00080	0.00082
	n	1.00232	1.00158	1.01746	1.01411	1.01237	1.03568	1.01343	1.03139	1.02166	1.00799
	R^2	0.99999	1.00000	1.00000	0.99999	0.99997	0.99974	0.99997	0.99998	0.99996	0.99994
Casson	τ_o	0	0	0	0	0	0	0	0	0	0
	η	0.00390	0.00282	0.00221	0.00180	0.00153	0.00111	0.00104	0.00098	0.00092	0.00086
	n	0.50013	0.50000	0.50000	0.69030	0.50006	0.77993	0.67815	0.69386	0.57161	0.89563
	R^2	0.99999	1.00000	0.99998	0.99996	0.99994	0.99955	0.99995	0.99991	0.99990	0.99992

Table 13: Modelling analysis of Crude oil C at different temperature

Model		Crude oil C									
		20 °C	40 °C	60 °C	80 °C	100 °C	120 °C	140 °C	160 °C	180 °C	200 °C
Newton	η	0.00444	0.00309	0.00231	0.00181	0.00136	0.00122	0.00113	0.00099	0.00095	0.00092
	R^2	1.00000	0.99998	0.99998	0.99997	0.99984	0.99985	0.99991	0.99988	0.99995	0.99992
Herschel-Bulkley	τ_o	0	0	0	0	0	0	0	0	0	0
	k	0.00422	0.00284	0.00208	0.00165	0.00131	0.00116	0.00103	0.00096	0.00088	0.00082
	n	1.00827	1.01361	1.01634	1.01488	1.00566	1.00806	1.01430	1.005271	1.01212	1.01859
	R^2	1.00000	0.99999	1.00000	0.99999	0.99987	0.99988	0.99995	0.99989	0.99997	0.99997
Casson	τ_o	0	0	0	0	0.00046	0	0	0	0	0
	η	0.00444	0.00309	0.00231	0.00181	0.00134	0.00122	0.00113	0.00099	0.00095	0.00092
	n	0.50255	0.50000	0.50003	0.50000	0.64826	0.61771	0.74537	0.63473	0.81255	0.57701
	R^2	1.00000	0.99998	0.99998	0.99997	0.99982	0.99985	0.99991	0.99988	0.99995	0.99992

Table 14: Modelling analysis of Fuel oil at different temperature

		Fuel Oil									
Model		20 °C	40 °C	60 °C	80 °C	100 °C	120 °C	140 °C	160 °C	180 °C	200 °C
Newton	η	1.71172	0.94470	0.24711	0.09019	0.04119	0.02255	0.01377	0.00914	0.00642	0.00477
	R^2	0.99611	0.99994	1.00000	0.99999	1.00000	1.00000	1.00000	0.99999	1.00000	0.99999
Herschel-Bulkley	τ_o	0	1.03485	0	0	0	0.00046	0	0	0	0
	k	3.80840	0.99659	0.25757	0.09647	0.04162	0.02316	0.01395	0.00902	0.00623	0.00478
	n	0.87259	0.99072	0.99340	0.98926	0.99827	0.99572	0.99790	1.00204	1.00499	0.99964
	R^2	0.99870	0.99996	1.00000	1.00000	0.99999	1.00000	1.00000	0.99999	1.00000	0.99999
Casson	τ_o	0.89925	0.04360	0.00321	0.00385	0.00022	0	0	0	0	0
	η	1.10030	0.92428	0.24457	0.08851	0.04092	0.02242	0.01377	0.00914	0.00642	0.00475
	n	0.30175	0.50003	0.50010	0.49997	0.50016	0.50001	0.50000	0.50000	0.92330	0.50000
	R^2	0.99818	0.99995	1.00000	1.00000	0.99999	1.00000	1.00000	0.99999	1.00000	0.99999

4.7. Turbine model analysis

In order for the turbine to be modelled using a liquid fuel, Murban crude oil was used as the fuel of choice. This was chosen because of the availability of the elemental composition of sulphur and nitrogen content (mass percent), this values were gotten from the most recent assay of Murban crude oil available on the TOTAL website [123]. The unavailability of the carbon and hydrogen content in the assay necessitated the used of compositional ranges available in literature, which stipulates that the mass percent of hydrogen and carbon content of crude oil are in the range of 83-87% for carbon and 11-16% hydrogen [13]. Therefore, the carbon-to-hydrogen ratio was used to establish the stoichiometry. This ratio was used in creating scenarios of the variations of carbon and hydrogen content of the sample.

In furtherance, the modelling was carried out to evaluate the power generation of the gas turbine by carrying out sensitivity analysis of carbon, hydrogen and sulphur. As seen in Table 15 that the power generated are dependent on the model used in determining the liquid fuel's lower heating value (LHV) ,in this case Boie and Verbandsformel were used.

Table 15. Sensitivity analysis results

Murban-oil	Element				Power Generated (kW)	
	C/H ratio	Nitrogen	Sulphur	Oxygen	Boie	Verbandsformel
Carbon-Hydrogen sensitivity	6.8	0.242%	0.743%	0.800%	11441.7	12299.5
	7.0	0.242%	0.743%	0.800%	11696.9	12579.3
	7.2	0.242%	0.743%	0.800%	11952.1	12859.0
Sulphur sensitivity	5.2	0.242%	0.743%	0.200%	12529.6	13797.8
	5.2	0.242%	0.843%	0.200%	12535.2	13805.1
	5.2	0.242%	0.943%	0.200%	12540.9	13812.3

It is observed from the values in the table above that if the carbon-hydrogen ratio, sulphur and nitrogen content is kept constant and the amount of the carbon-hydrogen ratio is increased, the amount of power generated increases by about 2.2% for every 0.2 increase in carbon-hydrogen ratio. Regarding the sulphur sensitivity analysis, the quantity of power generated increases by 0.045% for every 0.1% increase in sulphur component of the crude oil.

Lower heating value of the liquid fuel shown in Table 16, which is a function of the elemental composition of the fuel was obtained upon convergence of the simulation using the Boie model. The obtained LHV was used in computing the turbine power generation efficiency of the simple gas turbine using the Eq.34.

$$\eta, \% = \frac{power\ generated,\ kW}{Lower\ Heating\ Value_{fuel}, \frac{kJ}{kg} \times mass\ flow\ rate, kg/s} \times 100 \tag{34}$$

Table 16. Lower heating value of liquid fuel

	LHV, kJ/kg		
Carbon- Hydrogen sensitivity	40061.8	40974.5	41887.2
Sulphur sensitivity	43829.9	43851.2	43872.5

Table 17. Turbine power generation efficiency

	Generation efficiency, η (%)		
Carbon-Hydrogen sensitivity	31.551	29.996	28.534
Sulphur sensitivity	28.725	28.711	28.698

The efficiency obtained from the different permutations of elemental composition used in the simulation of the simple cycle gas turbine falls within the performance range of existing gas

turbine. For example, the Siemens gas turbine SGT-400 which operates on liquid and gaseous fuel interchangeably has an electrical efficiency of 35.4% [124].

It can be inferred from the values in Table 17, that a variation in the carbon content in the liquid fuel has more effect on improving the efficiency of the plant compared to hydrogen and sulphur.

The quality and quantity of the exhaust was monitored. This is important because it helps determine the volume of pollutant released, abatement method and reuse of heat generated. As described in Fig. 50 and Fig. 51, the major component of the exhausts are carbon dioxide, sulphur dioxide, nitrogen, water and oxygen but nitrogen was not displayed in the figure because of high deviation from other data points. The mass percent for each component is different for all of the sensitivity analysis done. The temperature of the exhaust shown in

Table 18 is very high, this sensible heat can be utilized for other purposes such as sludge drying in waste water plants, desalination, etc.

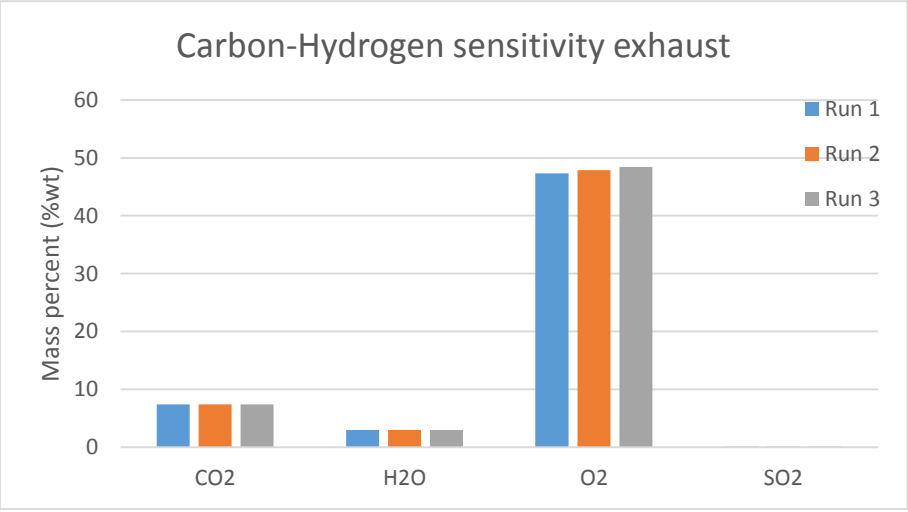

Fig. 50. Mass percent of exhaust from carbon sensitivity analysis

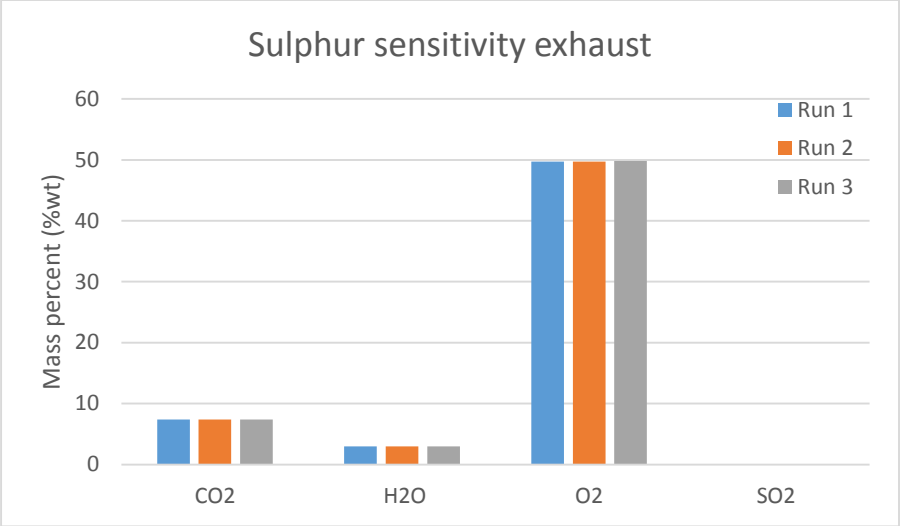

Fig. 51. Mass percent of exhaust from sulphur sensitivity analysis

Table 18. Gas turbine exhaust temperature

	Exhaust Temperature, ^{o}C		
Carbon sensitivity	611.252	611.675	612.080
Sulphur sensitivity	605.919	605.899	605.878

CHAPTER 5

Conclusions and Recommendations

5.1. Conclusions

This study has systematically characterized three crude oils and a fuel oil from the emirates of Abu Dhabi in the UAE. The following conclusions have been drawn:

It was observed that the density of the three crude oils exhibited linear relationship with temperature with changing linear relationship over specific temperature range, while the fuel oil demonstrated a linear model with temperature over the entire temperature range measured.

From the pour point value obtained it can be deduced that the liquid fuels are more paraffinic than naphthenic oils. The increasing order of their paraffinity is Crude oil A < Crude oil C < Crude oil B < fuel oil. It is observed that the percentage asphaltene content (%NHI) follows similar fashion as paraffinity of the liquid fuels, so it can be proposed that there is direct relationship between asphaltene content and pour point of the fuels. The samples measured are acidic in nature, with a decreasing order of acidity; Crude oil A > Crude oil C > Crude oil B > fuel oil.

A large span of temperature was investigated in the course of this study to observe temperature effect on rheological properties. Viscosity of the liquid fuels decreased significantly with

temperature from 3.895 to 0.734 mPa.s for Crude A, 3.522 to 0.678 mPa.s for Crude B, 4.800 to 0.831mPa.s for crude C and 5497.333 to 8.081 mPa.s for fuel oil when temperature changes from 20 to 200^{o}C. The yield shear stress also reduced over the same range of temperature. Only the fuel oil demonstrated thixotropic tendency, with thixotropic area ranging from 29170 to -5.617 Pa.s^{-1}.

The rheological properties of the liquid fuels clearly established by the $\tau = f(\dot{\gamma})$ rheograms exhibited that the liquid fuels possess different attributes in terms of fit to the rheological models proposed as temperature increases. Conclusively, the crude oils can be categorized as Newtonian and quasi-Newtonian in nature and the fuel oil as Non-Newtonian at lower temperature regimes and gradually become quasi-Newtonian as temperature rises.

Data suggests that Lower Zakum (Crude oil A) is the most suitable among the tested oils based on it Newtonian behavior over wide range of temperature measured and the results acquired from the determination of activation energy, pour point, asphaltene content and moisture content.

The liquid fuels can be used directly as fuel after proper pre-treatment measure have been carried out to eliminate or reduce the amount of contaminants that would hinder its utility. The naphthenic tendencies of the crude oils makes it a reliable fuel in terms of transportation and pumpibility as it is less waxy compared to the asphaltenic fuel oil which has to be pre-heated or blended with less waxy and viscous oil before use.

From the simulation of the simple gas turbine on IPSEpro^{TM}, it can be observed that increase in the C/H ratio has a significant effect on power generation. In spite of the fact that the constituent of the exhaust are environmentally unfriendly, they produce sensible heat that can be useful for other purposes.

5.2. Recommendations

Based on the results of present work, the following future research directions are recommended:

- During combustion it would be important to determine the deleterious effect of the liquid fuel constituent on the component of the gas turbine. Hence an investigation into the heavy metal content is suggested.

- For more impeccable gas turbine modelling, the quantity of elemental component such as C, H, N,O and S should be experimentally investigated.

- The density and viscosity of the liquid fuels should be evaluated at higher pressures other than atmospheric pressure.

- `The viscoelastic behaviors of the liquid fuels such as the complex modulus (G^*), loss modulus (G'') and storage modulus (G') should be investigated.

Bibliography

[1] "Middle East and North Africa (MENA) Renewables Status Report," 2013.

[2] (Accessed on: 15th March,2015). *Generation Game: O&G project site power report*, 2013. Available: http://www.arabianoilandgas.com/article-10885-generation-game-og-project-site-power-report/2/

[3] (Accessed on: 15th March,2015). *Nuclear Power in the United Arab Emirates*, 2014. Available: http://www.world-nuclear.org/info/Country-Profiles/Countries-T-Z/United-Arab-Emirates/

[4] Rahman, S. (Accessed on: 15th March,2015). *UAE power capacity outpaces demand*, 2012. Available: http://gulfnews.com/business/economy/uae-power-capacity-outpaces-demand-1.1068506

[5] USA Department of Energy. Energy Information Administration, E. (Accessed on: 14th January,2015). Available: http://www.eia.gov/cfapps/ipdbproject/IEDIndex3.cfm

[6] (Accessed on: 29th January,2015). *Oil and Gas*, 2014. Available: http://www.uaeinteract.com/business/oilandgas.asp

[7] Butt, G., "Oil and Gas in the UAE," in *United Arab Emirates: A New Perspective*, ed: Trident Press, 2001.

[8] Fernandez-Lima, F. A., C. Becker, A. M. McKenna, R. P. Rodgers, A. G. Marshall, and D. H. Russell, "Petroleum Crude Oil Characterization by IMS-MS and FTICR MS," *Analytical Chemistry*, vol. 81, 2009.

[9] Ruberto, R. G., D. M. Jewell, R. K. Jensen, and D. C. Cronauer, "Characterization of Synthetic Liquid Fuels," ed: Gulf Research & Development Company, 1974.

[10] Zoschak, R. G. and L. L. Stavinoha, "Review Of Physical And Chemical Methods For Characterization Of Fuels," ed: U.S. Army Fuels and Lubricants Research Laboratory, Southwest Research Institute, San Antonio, Texas, 1981.

[11] Behrenbruch, P. and T. Dedigama, "Classification and characterisation of crude oils based on distillation properties," *Journal of Petroleum Science and Engineering*, vol. 57, pp. 166-180, 5// 2007.

[12] Chang, A.-F., K. Pashikanti, and Y. A. Liu, "Characterization, Physical and Thermodynamic Properties of Oil Fractions," in *Refinery Engineering*, ed: Wiley-VCH Verlag GmbH & Co. KGaA, 2012, pp. 1-55.

[13] American Petroleum Institute , P. H. T. G., "Crude oil Category : Category Assessment Document," U. E. P. A. (EPA), Ed., ed: High Production Volume (HPV) Chemical Challenge Program, 2011.

[14] Leontaritis, K. J., "PARA-based (paraffin-aromatic-resin-asphaltene) reservoir oil characterizations," in *SPE international symposium on oilfield chemistry*, Houston TX,, 1997, pp. 421-440.

[15] Lundanes, E. and T. Greibrokk, "Separation of fuels, heavy fractions, and crude oils into compound classes: A review," *Journal of High Resolution Chromatography,* vol. 17, pp. 197-202, 1994.

[16] Suatoni, J. C. and R. E. Swab, "Rapid Hydrocarbon Group-Type Analysis by High Performance Liquid Chromatography," *Journal of Chromatographic Science,* vol. 13, pp. 361-366, August 1, 1975 1975.

[17] Bollet, C., J. C. Escalier, C. Souteyrand, M. Caude, and R. Rosset, "Rapid separation of heavy petroleum products by high-performance liquid chromatography," *Journal of Chromatography A,* vol. 206, pp. 289-300, 2/20/ 1981.

[18] Dark, W. A., "Crude Oil Hydrocarbon Group Separation Quantitation," *Journal of Liquid Chromatography,* vol. 5, pp. 1645-1652, 1982/01/01 1982.

[19] Ali, M. A. and W. A. Nofa, "Application Of High Performance Liquid Chromatography For Hydrocarbon Group Type Analysis Of Crude Oils," *Fuel Science and Technology International,* vol. 12, pp. 21-33, 1994/01/01 1994.

[20] Speight, J. G., *The Chemistry and Technology of Petroleum*: M. Dekker, 1991.

[21] Aske, N., H. Kallevik, and J. Sjöblom, "Determination of Saturate, Aromatic, Resin, and Asphaltenic (SARA) Components in Crude Oils by Means of Infrared and Near-Infrared Spectroscopy," *Energy & Fuels,* vol. 15, pp. 1304-1312, 2001/09/01 2001.

[22] Musser, B. J. and P. K. Kilpatrick, "Molecular Characterization of Wax Isolated from a Variety of Crude Oils," *Energy & Fuels,* vol. 12, pp. 715-725, 1998/07/01 1998.

[23] Lee, R. F., "Agents Which Promote and Stabilize Water-in-Oil Emulsions," *Spill Science & Technology Bulletin,* vol. 5, pp. 117-126, 5// 1999.

[24] Zaki, N., P.-C. Schoriing, and I. Rahimian, "Effect Of Asphaltene And Resins On The Stability Of Water-In-Waxy Oil Emulsions," *Petroleum Science and Technology,* vol. 18, pp. 945-963, 2000/08/01 2000.

[25] Andersen, S. I. and J. G. Speight, "Petroleum Resins: Separation, Character, And Role In Petroleum," *Petroleum Science and Technology,* vol. 19, pp. 1-34, 2001/03/26 2001.

[26] Iwsiak.T, A. V. Kemp-Jones, and O. P. Strausz. (Accessed on). *Properties Of Asphaltenes From Various Alberta Crude Oils*

[27] Pineda-Flores, G. and A. M. Mesta-Howard, "Petroleum asphaltenes: generated problematic and possible biodegradation mechanisms," *Rev Latinoam Microbiol*, vol. 43, pp. 143-50, Jul-Sep 2001.

[28] Gasthauer, E., M. Mazé, J. P. Marchand, and J. Amouroux, "Characterization of asphalt fume composition by GC/MS and effect of temperature," *Fuel*, vol. 87, pp. 1428-1434, 6// 2008.

[29] Hackett, D., L. Noda, S. Grissom, M. C. Moore, and J. Winter, "Pacific Basin Heavy Oil Refining Capacity," *The School of Public Policy: SPP Research Papers*, vol. 6, 2013.

[30] (Accessed on: 7th, February,2015). *Sweet vs. Sour Crude Oil*, 2013. Available: http://www.petroleum.co.uk/sweet-vs-sour

[31] Maatschappij, K. N. P., *The Petroleum handbook*: Elsevier, 1983.

[32] ASTM, "Standard Test Method for Density, Relative Density, or API Gravity of Crude Petroleum and Liquid Petroleum Products by Hydrometer Method,," in *ASTM D1298-12b*, ed. ASTM International, West Conshohocken, PA, 2012.

[33] (Accessed on: 8th, February,2015). *Volume Conversion: ASTM/API/IP TABLE 5A/B*. Available: http://www.globalsecurity.org/military/library/policy/army/fm/10-67-1/APPI.HTML

[34] ASTM, "Standard Test Method for Density, Relative Density, and API Gravity of Liquids by Digital Density Meter," in *ASTM D4052-11*, ed. ASTM International, West Conshohocken, PA,, 2011.

[35] ASTM, "Standard Test Method for Density and Relative Density (Specific Gravity) of Viscous Materials by Bingham Pycnometer," in *ASTM D1480-12*, ed. ASTM International, West Conshohocken, PA, 2012.

[36] Koleske, J. V., *Paint and Coating Testing Manual*, 14th ed. Philadelphia, PA: ASTM International, 1995.

[37] ASTM, "Standard Test Method for Density and Relative Density (Specific Gravity) of Viscous Materials by Lipkin Bicapillary Pycnometer," in *ASTM D1481-12*, ed. ASTM International, West Conshohocken, PA, 2012.

[38] (Accessed on: 12th January, 2015). *Relative density*. Available: en.wikipedia.org

[39] Mudgal, P. S., "Characterization Of West Texas Intermediate Crude Oil, And The Development Of True Boiling Point, Density, And Viscocity Curves For The Oil With The Help Of ASTM Standard.," MASTER OF ENGINEERING, Petroleum Engineering, Dalhousie University, Halifax, Nova Scotia, 2014.

[40] Lane, J. L. and K. O. Henderson. Viscosity Measurement: So Easy, Yet So Difficult [Online]. Available: http://www.astm.org/SNEWS/JUNE_2004/lanhen_jun04.html

[41] ASTM, "Standard Test Method for Dynamic Viscosity and Density of Liquids by Stabinger Viscometer (and the Calculation of Kinematic Viscosity)," in *ASTM D7042-14*,, ed. ASTM International, West Conshohocken, PA, 2014.

[42] Anton-Paar. (Accessed on: 9th, February,2015). *Introduction to the Principle of the Stabinger Viscometer™*. Available: http://www.viscopedia.com/methods/measuring-principles/

[43] ASTM, "Standard Test Method for Kinematic Viscosity of Transparent and Opaque Liquids (and Calculation of Dynamic Viscosity)," in *ASTM D445-14a*, ed. ASTM International, West Conshohocken, PA, 2014.

[44] (Accessed on: 12th January, 2015). *Glass capillary viscometer*. Available: http://www.hoskin.ca/catalog/index.php?main_page=index&cPath=2_418_907_914

[45] ASTM, "Standard Test Method for Low-Temperature Viscosity of Lubricants Measured by Brookfield Viscometer,," in *ASTM D2983-09*, ed. ASTM International, West Conshohocken, PA, 2009.

[46] (Accessed on: 9th, February,2015). *Brookfield Viscosity, Brookfield Viscometers, Measurements & Specifications: Brookfield Viscosity Explained*, 2013. Available: http://www.rheologyschool.com/advice/brookfield-viscosity-explained

[47] ASTM_Committee_D-2_on_Petroleum_Products_Lubricants, *The Significance of Tests of Petroleum Products: A Report*: American Society for Testing Materials, 1949.

[48] ASTM, "Standard Test Method for No Flow Point and Pour Point of Petroleum Products," in *ASTM D7346-14*, ed. West Conshohocken, PA, 2014.

[49] (Accessed on: 10th, February,2015). *ASTM D7346 Is Now Approved as a Pour Point Test Method for Petroleum Products* 2012. Available: http://news.thomasnet.com/companystory/astm-d7346-is-now-approved-as-a-pour-point-test-method-for-petroleum-products-621839

[50] BIS, "Foam Concentrate For Producing Mechanical Foam For Fire Fighting—Specification," in *IS 4989 : 2006*, ed. New Delhi, India: Bureau Of Indian Standards, 2006.

[51] (Accessed on: 11th, February,2015). *Background Knowledge Pour Point*, 2014. Available: http://www.psl-systemtechnik.de/pour_point_tester_knowledge.html?&L=1

[52] ASTM, "Standard Test Method for Pour Point of Crude Oils," in *ASTM D5853-11*, ed. ASTM International, West Conshohocken, PA, 2011.

[53] ASTM, "Standard Test Method for Pour Point of Petroleum Products (Robotic Tilt Method)," in *ASTM D6892-03*, ed. ASTM International, West Conshohocken, PA, 2014.

[54] Kim, H.-K., K.-B. Chung, and M.-N. Kim, "Measurement of the asphaltene and resin content of crude oils," *Journal of Ind. & Eng. Chemistry*, vol. 2, pp. 72-78, 1996.

[55] ASTM, " Standard Test Method for n-Heptane Insolubles," in *ASTM D3279-12*, ed. ASTM International, West Conshohocken, PA, 2012.

[56] ASTM, "Standard Test Method for Determination of Asphaltenes (Heptane Insolubles) in Crude Petroleum and Petroleum Products," in *ASTM D6560-12*, ed. West Conshohocken, PA, 2012.

[57] Drews, A. W., *Manual on Hydrocarbon Analysis*, 6th ed. West Conshohocken, PA: ASTM International, 1998.

[58] ASTM, "Standard Test Method for Water in Crude Oil by Distillation," in *ASTM D4006-11(2012)e1*, ed. ASTM International, West Conshohocken, PA, 2012.

[59] ASTM and International, "ASTM D4377-00(2011), Standard Test Method for Water in Crude Oils by Potentiometric Karl Fischer Titration," ed. West Conshohocken, PA, 2011.

[60] (Accessed on: 19th February,2015). *Karl Fischer Volumetric Titration*. Available: http://www.wako-chem.co.jp/english/labchem/product/analytical/aquamicron/index.htm

[61] ASTM, "Standard Test Method for Water in Crude Oils by Coulometric Karl Fischer Titration," in *ASTM D4928-12*, ed. ASTM International, West Conshohocken, PA, 2012.

[62] (Accessed on: 11th February,2015). *Karl Fischer Method of Moisture Detection: The Karl Fischer Method*, 2014. Available: http://www.cscscientific.com/moisture/karl-fischer

[63] (Accessed on: 11th February,2015). *Coulometric Titrator*, 2011. Available: http://www.grscientific.com/coulometric-titrator/

[64] Bruttel, P. and R. Schlink, *Water Determination by Karl Fischer Titration*. Herisau, Switzerland: Metrohm Ltd., 2003.

[65] ASTM, "Standard Test Method for Water and Sediment in Crude Oil by the Centrifuge Method (Laboratory Procedure)," in *ASTM D4007-11e1*, ed. ASTM International, West Conshohocken, PA, 2011, 2011.

[66] Kamarudin, N. H., "Optimization Of Chromium, Nickel And Vanadium Analysis In Crude Oil Using Graphite Furnace Atomic Absorption Spectroscopy," Master of Science Chemistry, Universiti Teknologi Malaysia, Malaysia, 2013.

[67] Von E. Doering, H., *Manual on Requirements Handling and Quality Control of Gas Turbinefuel*: ASTM International.

[68] Goldmeer, J., "Gas turbine fuel evaluation process: A case study on the application of Arabian Super Light Crude Oil for use in GE 7F-class Dry Low NOx (DLN) combustion systems," in *PowerGen International* Orlando, Florida, 2014.

[69] Colombo, M. and R. Rüetschi, *Chemistry and Corrosion Aspects in Gas Turbine Power Plant*. Baden, Switzerland: Alstom.

[70] Welch, M. and B. M. Igoe, "Combustion, Fuels and Emissions for Industrial Gas Turbines," in *Turbomachinery Symposium*, Houston, Texas, 2012.

[71] Bornsteln, N., H. Roth, and R. Pike, "VANADIUM CORROSION STUDIES," O. o. N. Research, Ed., ed. Arlington, Virginia United Technologies Research Center, 1993.

[72] OSHA, "OSHA Technical Manual (OTM), Section IV: Chapter 2," D. o. L. United State, Ed., ed. Washington DC: Occupational Safety & Health Administration, 1999.

[73] Johansson, P. and A. Larsson, "Heavy Crude Oil as a Fuel for the SGT-500 Gas Turbine " in *Fórum de Turbomáquinas Petrobras*, Rio de Janeiro, Brazil, 2011.

[74] Kaplan, H. J. and K. E. Majchrzak, "Liquid Fuel Treatment Systems," Schenectady, NY

[75] Motyka, A. L., "An Introduction to Rheology with an Emphasis on Application to Dispersions," *Journal of Chemical Education,* vol. 73, p. 374, 1996/04/01 1996.

[76] Schowalter, W. R., *Mechanics of non-Newtonian fluids*. Oxford: Pergamon Press, 1978.

[77] Barnes, H. A., J. F. Hutton, and K. Walters, *An Introduction to Rheology*: Elsevier, 1989.

[78] Schlumberger. (Accessed on: 19th February,2015). *Drilling fluids*. Available: http://www.glossary.oilfield.slb.com/en/Terms/s/shear_rate.aspx

[79] (Accessed on: 19th February,2015). *Shear rate*. Available: http://en.wikipedia.org/wiki/Shear_rate

[80] Semancik, J. R. (Accessed on: 14th February,2015). *Yield Stress Measurements Using Controlled Stress Rheometry*. Available: http://tainstruments.co.jp/application/pdf/Rheology_Library/Application_Briefs/RH058.PDF

[81] Rheotec. (Accessed on: 19th february,2015). *Introduction to rheology*. Available: http://www.dongjins.com/service/file/Introduction%20to%20rheology.pdf

[82] Ibarz, A., E. Castell-Perez, and G. V. Barbosa-Canovas, "Newtonian and Non-Newtonian Flow," in *Food Engineering*. vol. 2, ed: Encyclopaedia of Life Support Systems (EOLSS)

[83] (Accessed on: 19th February,2015). *Newtonian and non-Newtonian Fluids*, 2014. Available: http://www.msubbu.in/ln/fm/Unit-I/NonNewtonian.htm

[84] (Accessed on: 19th February,2015). *Visco-elastic: Wikis*. Available: http://www.thefullwiki.org/Visco-elastic

[85] Richardson, S. M., "Non-Newtonian Fluids," *Thermopedia*, 2011.

[86] (Accessed on: 19th February,2015). *Fluid Mechanics and Properties of Fluids*. Available: http://www.efm.leeds.ac.uk/CIVE/CIVE1400/PDF/Notes/section1.pdf

[87] Winter, H. H., Ed., *Rheometry with Capillary Rheometers* (Encyclopedia of Life Support Systems (EOLSS) UNESCO- Publishers Co Ltd, 2008, p.^pp. Pages.

[88] Sherman, L. M. (2004) Rheometers: Which Type Is Right for You? *Plastics Technology*.

[89] Hochstein, B. (Accessed on). *Rotational Rheometry*, 2012. Available: http://www.mvm.kit.edu/english/697_786.php

[90] McDonagh, B. (Accessed on: 19th February,2015). *Rheometers – How do they Compare?* , 2010. Available: http://www.atascientific.com.au/blog/2010/11/12/rheometers-compare/

[91] Margules, M., *Ueber die Bestimmung des Reibungs und Gleitungscoefficienten aus ebenen Bewegungen einer Fluessigkeit* vol. 83: Wien Sitzungsberger, Abt, 1881.

[92] Ritwik, "Measuring The Viscous Flow Behaviour Of Molten Metals Under Shear," Doctor of Philosophy, Brunel Centre for Advanced Solidification Technology, Brunel University, United Kingdom, 2012.

[93] Versan Kok, M., "Determination of Rheological Models for Drilling Fluids (A Statistical Approach)," *Energy Sources*, vol. 26, pp. 153-165, 2004/02/01 2004.

[94] Rao, A., *Rheology of Fluid and Semisolid Foods: Principles and Applications: Principles and Applications*: Springer, 2010.

[95] Hasan, S. W., "Rheology of heavy crude oil and viscosity reduction for pipeline transportation," Masters, Mechanical and Industrial Engineering, Concordia University, Canada, 2007.

[96] (Accessed on: 4th March,2015). *Fundamentals Of Gas Turbine Engines*. Available: http://www.cast-safety.org/pdf/3_engine_fundamentals.pdf

[97] Langston, L. S. and G. Opdyke, "Introduction to Gas Turbines for Non-Engineers," *Global Gas Turbine News,* vol. 37, 1997.

[98] Clark, J. S. and S. M. DeCorso, *Stationary Gas Turbine Alternative Fuels*: American Society for Testing and Materials, 1983.

[99] Lieuwen, T. C. and V. Yang, *Gas Turbine Emissions*: Cambridge University Press, 2013.

[100] Rahm, S., J. Goldmeer, M. Molière, and A. Eranki, "Addressing Gas Turbine Fuel Flexibility," presented at the POWER-GEN Middle East conference, Manama, Bahrain, 2009.

[101] Boundy, B., S. W. Diegel, L. Wright, and S. C. Davis, *BIOMASS ENERGY DATA BOOK*, Fourth ed., 2011.

[102] Ringen, S., J. Lanum, and F. P. Miknis, "Calculating heating values from elemental compositions of fossil fuels," *Fuel,* vol. 58, pp. 69-71, 1// 1979.

[103] InternationalOrganizationforStandardization, "Determinationof Density; Oscillating U-tube Method," in *Crude Petroleum and Petroleum Products* vol. ISO 12185:1996, ed. Geneva, Switzerland, 1996.

[104] ASTM and International, "ASTM D97-12, Standard Test Method for Pour Point of Petroleum Products, ," ed. West Conshohocken, PA, 2012.

[105] ASTM and International, "ASTM D3279-12, Standard Test Method for n-Heptane Insolubles," ed. West Conshohocken, PA, 2012.

[106] Hasan, S. W., M. T. Ghannam, and N. Esmail, "Heavy crude oil viscosity reduction and rheology for pipeline transportation," *Fuel,* vol. 89, pp. 1095-1100, 5// 2010.

[107] Ghannam, M. T., S. W. Hasan, B. Abu-Jdayil, and N. Esmail, "Rheological properties of heavy & light crude oil mixtures for improving flowability," *Journal of Petroleum Science and Engineering,* vol. 81, pp. 122-128, 1// 2012.

[108] ABS, "Notes on Heavy Fuel Oil," A. B. o. Shipping, Ed., ed. Houston, TX, 1984.

[109] Soares, C., *Gas Turbines: A Handbook of Air, Land and Sea Applications*: Elsevier Science, 2014.

[110] Li, C., Q. Yang, and M. Lin, "Effects of stress and oscillatory frequency on the structural properties of Daqing gelled crude oil at different temperatures," *Journal of Petroleum Science and Engineering,* vol. 65, pp. 167-170, 4// 2009.

[111] Fahim, M. A., T. A. Alsahhaf, and A. Elkilani, "Chapter 2 - Refinery Feedstocks and Products," in *Fundamentals of Petroleum Refining*, M. A. Fahim, T. A. Alsahhaf, and A. Elkilani, Eds., ed Amsterdam: Elsevier, 2010, pp. 11-31.

[112] Onojake, M. C., L. C. Osuji, and N. C. Oforka, "Preliminary hydrocarbon analysis of crude oils from Umutu/Bomu fields, south west Niger Delta Nigeria," *Egyptian Journal of Petroleum,* vol. 22, pp. 217-224, 12// 2013.

[113] Speight, J. G., *The Chemistry and Technology of Petroleum, Fifth Edition*: CRC Press, 2014.

[114] Couper, J. R., O. T. Beasley, and W. R. Penney, *The Chemical Process Industries Infrastructure: Function and Economics*: Taylor & Francis, 2000.

[115] Woodyard, D., *Pounder's Marine Diesel Engines and Gas Turbines*: Elsevier Science, 2009.

[116] Jahn, F., M. Cook, and M. Graham, "Chapter 11 Surface Facilities," in *Developments in Petroleum Science*. vol. Volume 55, M. C. Frank Jahn and G. Mark, Eds., ed: Elsevier, 2008, pp. 265-310.

[117] Eyring, H., "Viscosity, Plasticity, and Diffusion as Examples of Absolute Reaction Rates," *The Journal of Chemical Physics*, vol. 4, pp. 283-291, 1936.

[118] Naegeli, D. W. and L. G. Dodge, "Effects Of Fuel Properties An Atomization On Ignition In A T63 Gas Turbine Combustor," N. Naval Air Propulsion Center Trenton, Ed., ed: U.S. Army Belvoir Research, Development and Engineering Center, 1987.

[119] Khan, M. R., "Rheological Properties of Heavy Oils and Heavy Oil Emulsions," *Energy Sources*, vol. 18, pp. 385-391, 1996/06/01 1996.

[120] Barnes, H. A., "Thixotropy—a review," *Journal of Non-Newtonian Fluid Mechanics*, vol. 70, pp. 1-33, 5// 1997.

[121] Cheng, D. C. H., "Yield stress: A time-dependent property and how to measure it," *Rheologica Acta*, vol. 25, pp. 542-554, 1986/09/01 1986.

[122] Schramm, G., *A Practical Approach to Rheology and Rheometry*. Karlsruhe, Germany, 1994.

[123] (Accessed on: 14th March,2015). *Crude Assays -Murban*. Available: http://www.totsa.com/pub/crude/index2.php?expand=5&iback=5&rub=11

[124] Siemens. (Accessed on: 15th March,2015). *Gas Turbine SGT-400*. Available: http://www.energy.siemens.com/mx/en/fossil-power-generation/gas-turbines/sgt-400.htm

Appendix

Table 19. Detailed experimental value of pH measurement

	pH measurement			
Sample	Run 1	Run 2	Run3	Average
Crude oil A	2.713(23.9°C)	2.708(23.9°C)	2.743(23.9°C)	2.720
Crude oil B	4.267(23.6°C)	4.470(23.6°C)	4.381(23.6°C)	4.373
Crude oil C	3.193(26.2°C)	3.163(26.1°C)	3.146(26.1°C)	3.167
Fuel Oil	6.038(23.7°C)	6.048(23.7°C)	6.053(23.7°C)	6.046

Table 20. Detailed experimental value of pour point measurement

	Pour point measurement						
	Beaker 1		Beaker 2		Beaker 3		Average Pour point (°C)
Sample	Reading (°C)	Normalized Reading (°C)	Reading (°C)	Normalized Reading (°C)	Reading (°C)	Normalized Reading (°C)	
Crude oil A	-30	-27	-30	-27	-30	-27	-27
Crude oil B	-24	-21	-24	-21	-24	-21	-21
Crude oil C	-27	-24	-27	-24	-27	-24	-24
Fuel oil	9	12	9	12	9	12	12

Table 21. Detailed experimental value of asphaltene content measurement

	Asphaltene content measurement			
Sample	Run 1	Run 2	Run3	Average
Crude oil A	0.1936	0.1922	0.1956	0.1938
Crude oil B	0.2898	0.2956)	0.2948	0.2934
Crude oil C	0.2699	0.2708	0.2735	0.2714
Fuel Oil	2.8401	2.7868	2.8370	2.8213

Table 22. Detailed experimental value of moisture content measurement

	Moisture content measurement			
Sample	Run 1	Run 2	Run3	Average
Crude oil A	0.099	0.103	0.11	0.104
Crude oil B	0.129	0.121	0.128	0.126
Crude oil C	0.107	0.092	0.101	0.100
Fuel Oil	0.054	0.051	0.0660	0.057

Table 23 Values of arrhenius relationship of viscosity with temperature

	Arrhenius relationship of viscosity with temperature.			
	Natural logarithm of Viscosity			
Inverse of Temperature (1/K)	Crude oil A	Crude oil B	Crude oil C	Fuel oil
0.00341	1.35978	1.25903	1.56869	8.61202
0.00330	1.16471	1.04427	1.31363	7.62592
0.00319	0.91669	0.84901	1.09739	6.84868
0.00310	0.73413	0.68377	0.93662	6.28538
0.00300	0.57998	0.52374	0.74764	5.79494
0.00292	0.45086	0.41453	0.61067	5.36348
0.00283	0.35767	0.33074	0.52945	4.96074
0.00275	0.26467	0.23323	0.43739	4.64375
0.00268	0.17563	0.15843	0.39541	4.32126
0.00261	0.09592	0.06797	0.28443	4.02684
0.00254	0.02437	-0.01478	0.15558	3.54347
0.00248	0.00439	-0.06757	0.04784	3.15373
0.00242	-0.07814	-0.12281	0.02456	3.02383
0.00236	-0.16613	-0.15833	0.00582	2.86998
0.00231	-0.19391	-0.20179	-0.09468	2.69463
0.00226	-0.22962	-0.23239	-0.10614	2.52386
0.00221	-0.27054	-0.30616	-0.11751	2.37087
0.00216	-0.30038	-0.34301	-0.18959	2.22101
0.00211	-0.30893	-0.38925	-0.18529	2.08956

Table 24. Detailed experimental value of density measurement

Temp. (°C)	Density(g/cm^3)															
	Crude oil A				Crude oil B				Crude oil C				Fuel Oil			
	Run 1	Run 2	Run 3	Average	Run 1	Run 2	Run 3	Average	Run 1	Run 2	Run 3	Average	Run 1	Run 2	Run 3	Average
20	0.82248	0.82249	0.82251	0.82249	0.81782	0.81780	0.81780	0.81781	0.82795	0.82800	0.82802	0.82799	0.94699	0.94703	0.94704	0.94702
30	0.81530	0.81528	0.81527	0.81528	0.81059	0.81058	0.81058	0.81058	0.82059	0.82074	0.82074	0.82069	0.94056	0.94044	0.94042	0.94047
40	0.80785	0.80782	0.80783	0.80783	0.80323	0.80322	0.80321	0.80322	0.81330	0.81328	0.81329	0.81329	0.93275	0.93260	0.93259	0.93265
50	0.80045	0.80045	0.80045	0.80045	0.79584	0.79586	0.79586	0.79585	0.80590	0.80589	0.80589	0.80589	0.92526	0.92510	0.92510	0.92515
60	0.79306	0.79305	0.79305	0.79305	0.78847	0.78849	0.78859	0.78852	0.79848	0.79846	0.79846	0.79847	0.91818	0.91812	0.91812	0.91814
70	0.78566	0.78564	0.78565	0.78565	0.78105	0.78101	0.78101	0.78102	0.79105	0.79118	0.79183	0.79135	0.91143	0.91142	0.91143	0.91143
80	0.77840	0.77839	0.77840	0.77840	0.77356	0.77347	0.77347	0.77350	0.78355	0.78359	0.78359	0.78358	0.90510	0.90509	0.90510	0.90510
90	0.77093	0.77095	0.77096	0.77094	0.76612	0.76611	0.76610	0.76597	0.77609	0.77608	0.77608	0.77608	0.89882	0.89880	0.89881	0.89881
100	0.76750	0.76850	0.76850	0.76817	0.76492	0.76486	0.76490	0.76489	0.77332	0.77291	0.77254	0.77292	0.89333	0.89332	0.89334	0.89333
110	0.76663	0.76663	0.76687	0.76671	0.76392	0.76395	0.76393	0.76393	0.77055	0.76975	0.76900	0.76977	0.88784	0.88784	0.88787	0.88785
120	0.76436	0.76482	0.76456	0.76458	0.76228	0.76236	0.76246	0.76237	0.76543	0.76551	0.76551	0.76548	0.88149	0.88147	0.88148	0.88148
130	0.76196	0.76194	0.76195	0.76195	0.76039	0.76042	0.76041	0.76041	0.75808	0.75805	0.75813	0.75809	0.87480	0.87495	0.87487	0.87487
140	0.76066	0.76055	0.76051	0.76057	0.75929	0.75923	0.75892	0.75915	0.75250	0.75232	0.75237	0.75240	0.86874	0.86872	0.86872	0.86873
150	0.75397	0.75394	0.75371	0.75387	0.75233	0.75209	0.75207	0.75216	0.75053	0.75033	0.75030	0.75039	0.86274	0.86272	0.86272	0.86273
160	0.75019	0.75012	0.75022	0.75018	0.75169	0.75150	0.75142	0.75154	0.74270	0.74265	0.74226	0.74254	0.85657	0.85656	0.85655	0.85656
170	0.74882	0.74851	0.74839	0.74857	0.74809	0.74821	0.74827	0.74819	0.73886	0.73914	0.73900	0.73900	0.85054	0.85053	0.85052	0.85053
180	0.74569	0.74567	0.74572	0.74569	0.74415	0.74411	0.74571	0.74466	0.73625	0.73639	0.73572	0.73612	0.84465	0.84463	0.84463	0.84464
190	0.74333	0.74352	0.74367	0.74351	0.74131	0.74163	0.74142	0.74145	0.73360	0.73323	0.73336	0.73340	0.83833	0.83844	0.83842	0.83840
200	0.73834	0.73405	0.73181	0.73473	0.74094	0.74096	0.74094	0.74095	0.73237	0.73255	0.73207	0.73233	0.83258	0.83259	0.83258	0.83258

Table 25. Detailed experimental value of viscosity measurement

Temp. (°C)	Viscosity(mPa.s)															
	Crude oil A				Crude oil B				Crude oil C				Fuel Oil			
	Run 1	Run 2	Run 3	Average	Run 1	Run 2	Run 3	Average	Run 1	Run 2	Run 3	Average	Run 1	Run 2	Run 3	Average
20	3.9390	3.8740	3.8730	3.8953	3.5710	3.4650	3.5300	3.5220	4.7510	4.8380	4.8120	4.8003	5718.0000	5673.0000	5101.0000	5497.3333
30	3.1760	3.2460	3.1930	3.2050	2.8690	2.8440	2.8110	2.8413	3.6950	3.8140	3.6500	3.7197	2063.0000	2024.0000	2065.0000	2050.6667
40	2.4940	2.5420	2.4670	2.5010	2.3310	2.3440	2.3370	2.3373	3.0320	2.9430	3.0140	2.9963	907.6000	940.3000	980.0000	942.6333
50	2.0480	2.1230	2.0800	2.0837	1.9780	1.9690	1.9970	1.9813	2.5750	2.5320	2.5470	2.5513	503.5000	538.7000	567.8000	536.6667
60	1.7820	1.8060	1.7700	1.7860	1.7140	1.6840	1.6670	1.6883	2.1000	2.1340	2.1020	2.1120	314.5000	328.8000	342.6000	328.6333
70	1.5870	1.5500	1.5720	1.5697	1.5390	1.5030	1.4990	1.5137	1.8480	1.8650	1.8120	1.8417	205.9000	211.8000	222.7000	213.4667
80	1.4700	1.4170	1.4030	1.4300	1.4260	1.3640	1.3860	1.3920	1.7160	1.7150	1.6630	1.6980	137.7000	142.9000	147.5000	142.7000
90	1.3130	1.2760	1.3200	1.3030	1.2940	1.2710	1.2230	1.2627	1.4890	1.5830	1.5740	1.5487	97.2000	106.3000	108.3000	103.9333
100	1.2100	1.1680	1.1980	1.1920	1.1640	1.1650	1.1860	1.1717	1.4830	1.4890	1.4830	1.4850	73.8300	75.3500	76.6700	75.2833
110	1.1150	1.0720	1.1150	1.1007	1.0840	1.0660	1.0610	1.0703	1.3420	1.3330	1.3120	1.3290	55.0900	56.0900	57.0700	56.0833
120	1.0080	1.0190	1.0470	1.0247	0.9657	1.0450	0.9453	0.9853	1.1970	1.1730	1.1350	1.1683	32.3800	34.5400	36.8400	34.5867
130	0.9972	1.0090	1.0070	1.0044	0.9385	0.9367	0.9288	0.9347	1.0880	1.0320	1.0270	1.0490	22.0500	23.5800	24.6400	23.4233
140	0.9219	0.9312	0.9214	0.9248	0.8866	0.8724	0.8943	0.8844	1.0430	1.0400	0.9916	1.0249	19.9600	20.4600	21.2900	20.5700
150	0.8644	0.8287	0.8477	0.8469	0.8319	0.8487	0.8801	0.8536	0.9999	0.9936	1.0240	1.0058	17.1600	17.6400	18.1100	17.6367
160	0.8131	0.8439	0.8142	0.8237	0.7955	0.8675	0.7888	0.8173	0.9031	0.9163	0.9096	0.9097	14.6400	14.6900	15.0700	14.8000
170	0.8022	0.8088	0.7735	0.7948	0.7892	0.8276	0.7611	0.7926	0.8998	0.8990	0.8991	0.8993	12.2800	12.4400	12.7100	12.4767
180	0.7294	0.8113	0.7482	0.7630	0.7643	0.7234	0.7211	0.7363	0.8908	0.8851	0.8915	0.8891	10.5100	10.7200	10.8900	10.7067
190	0.7541	0.7389	0.7286	0.7405	0.7196	0.7030	0.7063	0.7096	0.8077	0.8265	0.8477	0.8273	9.1120	9.1950	9.3430	9.2167
200	0.7156	0.7529	0.7342	0.7342	0.6882	0.6799	0.6646	0.6776	0.8309	0.8310	0.8307	0.8309	7.9570	8.1220	8.1650	8.0813

Table 26. Steady flow behaviour of Crude oil A

Steady Flow Behaviour - Crude oil A										
˝Shear rate, $\dot{\gamma}$ (1/s)	Shear stress, τ (Pa)									
	20°C	40°C	60°C	80°C	100°C	120°C	140°C	160°C	180°C	200°C
41.76180	0.17731	0.14253	0.12398	0.10078	0.05270	0.06343	0.04711	0.04235	0.04145	0.03714
83.42403	0.35971	0.29044	0.25381	0.20038	0.11083	0.13196	0.10546	0.08256	0.07670	0.07399
125.08339	0.53102	0.43501	0.38264	0.30350	0.16662	0.16455	0.15281	0.12456	0.11984	0.10926
166.75205	0.71724	0.57372	0.50572	0.40444	0.21731	0.20746	0.19142	0.16386	0.16152	0.14744
208.40778	0.91147	0.71701	0.62588	0.51436	0.27476	0.25480	0.23991	0.20607	0.19492	0.17758
250.08073	1.07780	0.85609	0.75103	0.61337	0.32188	0.30242	0.27572	0.23860	0.22756	0.20941
291.73892	1.25925	1.00125	0.87569	0.71675	0.37795	0.33816	0.30960	0.27831	0.25598	0.23734
333.40070	1.45210	1.14575	0.99636	0.81610	0.42962	0.38532	0.34859	0.30757	0.28722	0.27016
375.06659	1.60411	1.28816	1.12007	0.91775	0.48257	0.42515	0.38960	0.34230	0.32396	0.30367
416.71289	1.79341	1.42949	1.24148	1.01877	0.53849	0.48182	0.42521	0.37776	0.35798	0.32889
458.38791	1.97124	1.57174	1.36476	1.11920	0.59136	0.52364	0.46741	0.41286	0.39654	0.36555
500.06967	2.12557	1.71834	1.48392	1.21514	0.64732	0.58946	0.50981	0.44678	0.43437	0.39812
541.69513	2.33721	1.86007	1.60677	1.32303	0.69736	0.61451	0.55107	0.48501	0.46539	0.43095
583.35571	2.50191	2.00309	1.72947	1.42024	0.74984	0.66244	0.59613	0.52662	0.50672	0.46304
625.04401	2.65448	2.14805	1.85325	1.52105	0.80133	0.69845	0.63534	0.57407	0.54082	0.49957
666.69763	2.85270	2.28950	1.97689	1.62892	0.85425	0.73054	0.68339	0.62530	0.57704	0.53402
708.37152	3.01680	2.43069	2.10102	1.72869	0.91203	0.79426	0.73232	0.66163	0.62165	0.57201
750.05072	3.19822	2.57730	2.22456	1.82657	0.96279	0.84489	0.77986	0.69989	0.65624	0.61410
791.66901	3.39088	2.71875	2.34976	1.92876	1.01672	0.89659	0.83227	0.74411	0.71584	0.65560
833.36249	3.55775	2.86354	2.47416	2.03454	1.07390	0.93750	0.87880	0.80037	0.76291	0.69304
875.01282	3.76877	3.00780	2.60076	2.13936	1.13329	0.99649	0.92047	0.83814	0.79815	0.74437
916.67999	3.95613	3.16001	2.71956	2.24025	1.18796	1.04433	0.97771	0.87764	0.83630	0.79863
958.37512	4.10470	3.29277	2.84708	2.34400	1.24486	1.09264	1.02235	0.91542	0.85470	0.81985
999.99817	4.27088	3.44464	2.97660	2.44804	1.31501	1.14495	1.06716	0.96198	0.88759	0.85095

Table 27. Steady flow behaviour of Crude oil B

Steady Flow Behaviour - Crude oil B										
˝ Shear rate, $\dot{\gamma}$ (1/s)	Shear stress, τ (Pa)									
	20°C	40°C	60°C	80°C	100°C	120°C	140°C	160°C	180°C	200°C
41.76279	0.16744	0.11730	0.09090	0.07733	0.06247	0.04310	0.04365	0.03807	0.03764	0.03555
83.42413	0.32480	0.23534	0.18279	0.14749	0.12676	0.09245	0.08374	0.07968	0.07389	0.07090
125.08872	0.48616	0.35152	0.27426	0.22273	0.18819	0.13333	0.12636	0.12191	0.11064	0.10672
166.71137	0.65519	0.47152	0.36544	0.29713	0.25250	0.17854	0.16913	0.16104	0.14833	0.14180
208.41144	0.81090	0.58237	0.45662	0.37161	0.32256	0.23135	0.21589	0.20152	0.18953	0.17484
250.07568	0.97211	0.70603	0.54934	0.44536	0.38183	0.26927	0.25800	0.24311	0.22413	0.21378
291.73706	1.13517	0.82164	0.63892	0.52029	0.44397	0.31775	0.30126	0.28373	0.26533	0.24825
333.39761	1.29790	0.94111	0.73229	0.59611	0.50892	0.36706	0.34646	0.32494	0.30494	0.28324
375.06064	1.45884	1.05735	0.82529	0.67208	0.57023	0.41111	0.38694	0.36546	0.34159	0.32092
416.72357	1.62337	1.17390	0.91891	0.74996	0.63472	0.45899	0.43477	0.40845	0.38082	0.35470
458.38821	1.78594	1.28963	1.01499	0.82461	0.70263	0.52078	0.47679	0.44977	0.42052	0.39171
500.04984	1.94741	1.41132	1.10703	0.90027	0.76423	0.55258	0.51995	0.49148	0.45678	0.42992
541.70874	2.11596	1.52747	1.20539	0.97560	0.82937	0.60366	0.56523	0.53658	0.49947	0.46151
583.36975	2.27814	1.64426	1.29201	1.05283	0.89513	0.65379	0.60757	0.57863	0.54094	0.50074
625.03235	2.43854	1.76136	1.38621	1.12882	0.95817	0.69751	0.65109	0.61910	0.57647	0.53490
666.69751	2.60437	1.88041	1.48287	1.20567	1.02675	0.74728	0.69556	0.65959	0.61739	0.57459
708.36096	2.76546	1.99947	1.57340	1.28269	1.09311	0.79759	0.73948	0.70494	0.65491	0.61061
750.01996	2.93328	2.11783	1.66933	1.36153	1.15746	0.84969	0.78550	0.74766	0.69581	0.64586
791.69183	3.09271	2.23576	1.76347	1.43910	1.22271	0.91374	0.83181	0.79310	0.73671	0.68492
833.35016	3.25674	2.34840	1.86149	1.51309	1.29076	0.96748	0.87873	0.83898	0.77616	0.72411
875.00427	3.43008	2.46620	1.95046	1.59269	1.35628	1.02485	0.92283	0.88098	0.81459	0.76137
916.66620	3.59057	2.59256	2.05166	1.67131	1.42269	1.06335	0.96596	0.91850	0.85853	0.79677
958.33484	3.75877	2.70723	2.14320	1.75321	1.49304	1.11169	1.01269	0.96505	0.90478	0.83694
999.99133	3.92261	2.82506	2.23793	1.82727	1.55980	1.15317	1.06003	1.01091	0.94045	0.87203

Table 28. Steady flow behaviour of Crude oil C

Steady Flow Behaviour - Crude oil C										
Shear rate, $\dot{\gamma}$ (1/s)	Shear stress, τ (Pa)									
	20°C	40°C	60°C	80°C	100°C	120°C	140°C	160°C	180°C	200°C
41.76231	0.18227	0.12562	0.09382	0.07257	0.05973	0.05199	0.04585	0.04123	0.03677	0.03737
83.42446	0.36336	0.25461	0.18826	0.14769	0.11986	0.10096	0.09189	0.08146	0.07873	0.07548
125.08637	0.54830	0.38281	0.28268	0.22357	0.17666	0.15085	0.13871	0.12256	0.11903	0.11317
166.75058	0.73503	0.50899	0.37842	0.29866	0.22799	0.20198	0.18528	0.16363	0.15967	0.15131
208.41151	0.92032	0.63681	0.47651	0.37284	0.27893	0.25257	0.23291	0.20618	0.19776	0.19356
250.07553	1.10275	0.76590	0.57289	0.44831	0.33616	0.30425	0.27951	0.24709	0.23580	0.22780
291.73691	1.29074	0.89504	0.66561	0.52315	0.39170	0.35562	0.32702	0.28689	0.27614	0.26497
333.39902	1.47593	1.02621	0.76533	0.59867	0.44644	0.40780	0.37407	0.32913	0.31588	0.30308
375.06024	1.66157	1.15933	0.86157	0.67441	0.50291	0.45710	0.42050	0.36942	0.35555	0.34310
416.72214	1.85048	1.28612	0.95755	0.74841	0.55740	0.50586	0.46757	0.40989	0.39472	0.38301
458.38422	2.03571	1.41609	1.05803	0.82525	0.61487	0.55661	0.51599	0.45341	0.43597	0.42032
500.04871	2.22231	1.54724	1.15198	0.90264	0.67343	0.61100	0.56223	0.49122	0.47394	0.45879
541.70917	2.41055	1.67597	1.25102	0.97935	0.72652	0.65950	0.61059	0.53255	0.51160	0.49905
583.37183	2.59976	1.82629	1.34869	1.05541	0.78538	0.71171	0.65969	0.57451	0.55059	0.53716
625.03503	2.78292	1.94215	1.44681	1.13345	0.84584	0.76429	0.70601	0.61452	0.59471	0.57602
666.69440	2.97248	2.06912	1.54418	1.21007	0.90363	0.81312	0.75507	0.65656	0.63263	0.61858
708.35742	3.15866	2.20128	1.64252	1.28804	0.96339	0.86510	0.80370	0.70067	0.67314	0.65861
750.02509	3.34312	2.33614	1.74024	1.36660	1.01718	0.92079	0.85144	0.74456	0.71669	0.69742
791.68347	3.53125	2.46504	1.84025	1.44404	1.07697	0.97137	0.90219	0.78012	0.75710	0.73861
833.34161	3.72205	2.59436	1.93870	1.51662	1.13298	1.02692	0.95152	0.82817	0.79693	0.77802
875.00934	3.91005	2.72649	2.04040	1.59758	1.19202	1.08024	1.00477	0.87300	0.83501	0.82138
916.67902	4.09233	2.86045	2.13590	1.67721	1.25451	1.13665	1.05355	0.91873	0.88273	0.85653
958.34381	4.27947	2.99508	2.23658	1.75718	1.32011	1.19582	1.09836	0.96127	0.91992	0.89959
1000.00159	4.47200	3.12510	2.33708	1.83220	1.37864	1.25428	1.15485	1.00845	0.96156	0.93743

Table 29. Steady flow behaviour of Fuel oil

Steady Flow Behaviour - Fuel oil										
˝ Shear rate, $\dot{\gamma}$ (1/s)	Shear stress, τ (Pa)									
	20°C	40°C	60°C	80°C	100°C	120°C	140°C	160°C	180°C	200°C
41.90595	93.72583	41.37469	10.63434	3.86530	1.75635	0.95569	0.56977	0.37642	0.26705	0.20218
83.23758	173.28598	80.43292	20.87088	7.70893	3.46081	1.89279	1.15452	0.75844	0.53063	0.40162
125.08947	254.49052	119.75090	31.20823	11.50285	5.16250	2.83013	1.73868	1.14467	0.79426	0.59467
166.98862	331.30795	159.07355	41.53409	15.16297	6.92162	3.78966	2.30242	1.51486	1.06952	0.79308
208.42369	405.72278	198.46513	51.74837	19.01395	8.58578	4.74224	2.88114	1.90576	1.33227	1.00375
250.10968	477.08569	237.83772	62.01969	22.67180	10.33660	5.68424	3.44468	2.27617	1.60807	1.19393
291.96478	544.67957	277.15265	72.31173	26.45446	12.02699	6.61525	4.01823	2.65972	1.87468	1.39153
333.64825	613.88818	316.49146	82.59604	30.19369	13.73037	7.53491	4.59887	3.04690	2.13627	1.59171
375.23227	680.66736	355.79062	92.87266	33.97667	15.44327	8.47056	5.17442	3.42567	2.40766	1.78875
416.91354	746.79053	395.02466	103.13010	37.71330	17.12869	9.40805	5.73569	3.83587	2.67618	1.99040
458.55231	812.16901	434.13031	113.42341	41.45133	18.82828	10.34174	6.32575	4.21905	2.94337	2.19147
500.24420	876.54132	473.14331	123.67869	45.14106	20.59282	11.27979	6.88609	4.58301	3.21061	2.37999
541.95038	938.56152	511.98138	133.91840	48.87935	22.27701	12.19396	7.46356	4.95579	3.48105	2.58866
583.62470	998.96631	550.68054	144.18942	52.59877	23.99137	13.14616	8.03161	5.33502	3.74697	2.78639
625.30243	1057.44714	589.21924	154.43567	56.30064	25.72647	14.07875	8.60920	5.71834	4.01869	2.98261
667.00275	1114.06335	627.55524	164.64491	60.00517	27.44142	15.02489	9.16480	6.08577	4.29652	3.17574
708.68939	1168.64087	665.74567	174.95764	63.71536	29.16953	15.96699	9.75121	6.47781	4.55941	3.37642
750.35571	1221.20520	703.71747	185.09460	67.44773	30.91473	16.90529	10.32185	6.85968	4.83094	3.57589
792.07990	1271.28198	741.42053	195.29111	71.10281	32.68741	17.81932	10.89819	7.21938	5.10656	3.77428
833.79315	1319.39490	778.86176	205.46753	74.82230	34.37972	18.76903	11.48716	7.61859	5.36921	3.97861
875.45929	1365.04834	816.07062	215.63011	78.51919	36.10218	19.69270	12.03597	8.00933	5.64455	4.18067
917.03290	1408.58704	852.87500	225.75070	82.25409	37.83167	20.67855	12.61154	8.38465	5.89414	4.38516
958.81836	1449.75244	889.46289	235.91631	85.90128	39.54681	21.60983	13.16285	8.76770	6.17770	4.58059
1000.45831	1488.98572	925.84387	246.04715	89.61676	41.26867	22.55926	13.77189	9.14450	6.44135	4.78730

Table 30. Yield shear stress Measurement of Crude oil A

Yield shear stress Measurement – Crude oil A										
	Shear rate (1/s)									
Shear Stress (Pa)	20°C	40°C	60°C	80°C	100°C	120°C	140°C	160°C	180°C	200°C
0.100	11.867	11.953	10.667	3.947	14.466	15.882	11.714	10.857	15.792	13.928
0.305	66.510	101.157	130.209	144.284	164.853	179.051	206.181	208.626	212.922	223.250
0.511	111.424	171.987	226.108	265.450	303.426	335.838	398.904	404.967	414.459	443.872
0.716	156.591	242.621	319.855	381.277	434.980	487.147	586.781	595.701	611.099	664.077
0.921	201.009	312.360	412.992	494.206	566.243	636.599	772.787	782.991	806.861	882.075
1.126	245.533	380.822	505.506	605.168	696.149	784.936	951.973	970.167	999.693	1101.464
1.332	290.626	450.072	597.203	719.125	824.751	931.311	1128.469	1151.527	1187.826	1315.721
1.537	335.124	519.908	688.595	832.014	951.775	1078.358	1296.684	1333.567	1381.436	1528.305
1.742	378.476	588.001	779.919	944.945	1081.232	1223.727	1466.892	1509.783	1573.026	1743.842
1.947	423.379	657.327	872.000	1056.778	1208.303	1367.439	1634.960	1688.425	1763.919	1957.026
2.153	468.043	726.204	962.415	1169.506	1337.042	1511.210	1787.635	1864.146	1954.679	2167.559
2.358	513.360	795.724	1052.891	1281.073	1464.659	1652.440	1946.956	2039.063	2143.962	2378.469
2.563	558.935	864.110	1143.530	1391.816	1591.398	1792.941	2105.399	2211.570	2331.599	2589.550
2.768	605.409	932.974	1233.690	1502.411	1720.333	1934.304	2269.481	2385.378	2520.539	2798.189
2.974	653.717	1001.643	1322.500	1613.631	1847.465	2074.261	2430.261	2558.908	2707.612	3006.442
3.179	704.374	1070.764	1412.515	1722.962	1974.021	2212.545	2589.368	2728.528	2894.098	3212.724
3.384	754.228	1139.954	1501.144	1829.863	2099.376	2351.163	2750.299	2896.699	3078.667	3386.028
3.589	801.239	1208.564	1590.812	1938.642	2221.632	2486.725	2908.881	3065.910	3264.428	3530.887
3.795	847.027	1276.890	1678.116	2047.437	2346.374	2617.395	3068.075	3232.012	3452.089	3662.292
4.000	893.028	1344.931	1766.756	2155.396	2470.029	2750.103	3224.677	3399.557	3632.535	3787.882

Table 31. Yield shear stress Measurement of Crude oil B

	Yield shear stress Measurement - Crude oil B									
	Shear rate (1/s)									
Shear Stress (Pa)	20°C	40°C	60°C	80°C	100°C	120°C	140°C	160°C	180°C	200°C
0.100	8.480	12.194	10.805	13.178	9.436	12.285	33.213	13.715	15.030	15.318
0.305	77.269	110.556	139.359	161.585	178.907	206.600	210.468	214.379	230.864	236.604
0.511	130.251	189.772	243.557	282.343	331.551	397.919	409.787	418.794	468.360	481.641
0.716	180.726	266.217	347.006	411.692	480.964	586.099	603.746	620.393	706.513	730.857
0.921	233.101	341.858	447.833	540.726	626.945	766.805	794.037	818.490	944.615	977.908
1.126	286.118	417.254	548.406	666.955	771.129	953.079	981.674	1012.934	1176.795	1218.570
1.332	338.297	493.509	647.811	791.439	913.431	1139.786	1165.157	1203.035	1403.649	1458.300
1.537	390.769	568.564	749.591	917.443	1054.389	1320.014	1348.094	1391.771	1630.404	1696.463
1.742	441.048	644.678	849.271	1038.993	1194.355	1496.824	1529.944	1579.035	1856.482	1934.560
1.947	494.477	718.379	948.672	1155.634	1332.062	1673.028	1708.917	1763.924	2074.189	2172.683
2.153	546.217	795.880	1046.937	1264.015	1469.013	1856.657	1887.200	1948.536	2288.494	2408.900
2.358	597.610	872.527	1146.966	1376.306	1603.716	2042.091	2064.596	2132.536	2501.453	2641.837
2.563	649.399	947.866	1244.728	1481.283	1736.682	2219.880	2238.065	2313.087	2697.579	2869.632
2.768	701.351	1024.606	1341.395	1589.269	1870.122	2397.055	2412.739	2495.406	2896.851	3079.021
2.974	752.843	1098.056	1436.972	1710.107	2003.861	2571.138	2584.358	2677.060	3094.775	3257.452
3.179	804.586	1173.250	1533.015	1831.702	2137.919	2733.923	2752.307	2858.078	3264.847	3412.365
3.384	856.560	1248.912	1628.195	1951.822	2270.865	2910.386	2919.057	3037.559	3412.005	3558.984
3.589	908.370	1324.085	1723.449	2075.119	2400.296	3095.406	3087.807	3219.023	3553.770	3699.150
3.795	960.070	1399.145	1817.179	2201.551	2530.624	3282.214	3256.929	3396.335	3694.899	3840.525
4.000	1011.780	1473.349	1911.917	2331.267	2663.564	3465.526	3426.960	3576.033	3830.552	3981.558

Table 32. Yield shear stress Measurement of Crude oil C

Yield shear stress Measurement - Crude oil C										
	Shear rate (1/s)									
Shear Stress (Pa)	20°C	40°C	60°C	80°C	100°C	120°C	140°C	160°C	180°C	200°C
0.100	8.939	11.806	12.743	12.600	11.197	11.901	14.655	12.431	11.298	11.389
0.305	65.402	97.945	126.169	149.862	165.797	161.398	210.601	209.741	194.727	223.421
0.511	109.459	166.397	218.520	266.977	301.230	289.407	415.916	409.206	406.640	448.528
0.716	153.260	234.236	308.564	379.658	433.239	413.928	612.937	602.505	610.352	673.457
0.921	197.081	301.022	398.202	491.767	562.237	539.338	800.798	794.883	809.482	894.799
1.126	240.925	368.233	487.223	603.336	689.767	663.111	990.558	985.912	1004.102	1116.740
1.332	284.523	434.651	575.829	715.175	817.837	786.918	1176.733	1173.599	1199.274	1332.775
1.537	328.363	501.407	664.457	826.379	944.058	910.149	1355.091	1359.101	1393.135	1551.915
1.742	371.876	567.974	752.834	936.562	1070.442	1036.174	1534.236	1539.884	1584.121	1764.446
1.947	415.394	634.443	842.131	1046.327	1194.197	1161.072	1699.548	1721.153	1773.696	1977.010
2.153	459.236	700.740	932.740	1154.797	1317.181	1284.828	1881.489	1897.925	1959.588	2185.544
2.358	503.228	767.439	1022.788	1261.221	1439.260	1407.862	2065.917	2074.844	2152.606	2394.417
2.563	547.437	834.171	1111.072	1367.790	1560.225	1531.531	2245.280	2250.724	2341.243	2604.339
2.768	592.742	900.423	1198.619	1472.230	1680.177	1650.728	2426.286	2421.835	2529.143	2812.227
2.974	640.645	966.636	1285.625	1576.708	1800.615	1772.887	2615.622	2593.232	2714.226	3020.496
3.179	690.560	1033.009	1372.369	1680.490	1919.641	1894.541	2804.333	2768.127	2894.469	3229.698
3.384	736.967	1098.965	1458.022	1783.671	2039.177	2013.065	2986.608	2936.486	3075.695	3415.198
3.589	781.648	1164.790	1541.899	1886.787	2160.467	2133.301	3154.945	3106.043	3262.997	3572.961
3.795	826.139	1230.642	1625.846	1989.952	2277.022	2253.548	3343.562	3249.986	3449.263	3718.087
4.000	870.803	1296.442	1709.601	2092.454	2394.609	2375.170	3548.112	3407.442	3630.282	3858.616

Table 33. Yield shear stress Measurement of fuel oil

Yield shear stress Measurement - Fuel oil										
	Shear rate (1/s)									
Shear Stress (Pa)	20°C	40°C	60°C	80°C	100°C	120°C	140°C	160°C	180°C	200°C
0.111295	0.0192	0.08744	0.323639	1.143417	2.374014	4.330594	7.033308	10.091703	12.93807	14.45542
0.208844	0.035522	0.160852	0.627597	2.199355	4.563148	8.447989	13.87725	19.992702	28.162331	34.775608
0.396535	0.07016	0.295165	1.175172	4.170685	9.013448	16.362621	26.79353	39.869949	56.944893	72.919106
0.598944	0.109037	0.446824	1.786893	6.285592	13.704646	25.159855	40.99574	61.673431	88.380402	113.85444
0.805949	0.150827	0.594706	2.401554	8.514842	18.134613	33.842636	55.50756	82.912628	119.96426	153.4642
1.017153	0.200712	0.749153	3.019103	10.69954	23.067009	42.358452	69.63422	104.55289	150.86668	194.01189
1.212152	0.250978	0.898433	3.630244	12.70802	27.413183	51.116199	84.24931	126.3017	181.96668	234.10408
1.421051	0.307854	1.051229	4.235657	14.87595	32.344345	59.910519	98.4532	148.10857	213.17844	274.41281
1.628548	0.364439	1.202644	4.828466	17.29189	37.063808	68.715889	112.9216	169.68701	244.67107	314.45908
1.834741	0.419041	1.35381	5.421639	19.24722	41.952724	77.518066	127.5181	191.85249	275.39807	354.65643
2.038132	0.475355	1.503154	6.050505	21.68023	46.776371	86.466316	141.9223	213.74225	307.22296	394.69742
2.241088	0.528127	1.653218	6.725819	23.82576	51.608631	95.172195	156.603	235.41075	337.43042	434.4245
2.451148	0.585474	1.805042	7.460816	26.17495	56.231968	104.16107	171.1664	257.15219	368.33044	471.77292
2.656055	0.646785	1.957406	8.154901	28.24936	61.159309	113.03378	185.6362	278.89078	396.94043	513.44019
2.859852	0.708377	2.115454	8.770329	30.59864	65.853271	121.76656	199.9253	301.03748	430.70242	553.04999
3.067035	0.774923	2.272275	9.328768	32.76537	70.357224	130.46872	214.166	322.57089	461.18869	591.99445
3.273442	0.850904	2.439484	9.957339	34.98589	75.445496	139.26726	228.7407	344.3187	491.96729	631.53479
3.474324	0.930008	2.611219	10.736954	37.22789	80.32428	148.17656	242.9449	366.03967	523.04761	670.73737
3.676981	1.010076	2.788784	11.452223	39.46655	84.999352	156.86818	257.6667	387.5116	553.60095	709.81232
3.885766	1.09116	2.964716	11.995554	41.65469	89.791374	165.95923	272.2297	409.31461	584.55151	749.07233